NTNU – Trondheim
Norwegian University of
Science and Technology

TBM Tunnelling at the Stillwater Mine

Leon Nikolay Røren Eide

NORWEGIAN UNIVERSITY OF SCIENCE AND TECHNOLOGY
DEPARTMENT OF CIVIL AND TRANSPORT ENGINEERING

Report Title:	Date: 24.06.2014		
TBM Tunnelling at the Stillwater Mine	Number of pages (incl. appendices): 183		
	Master Thesis	x	Project Work	

Name:
Leon Nikolay Røren Eide

Professor in charge/supervisor:
Prof. Amund Bruland

Other external professional contacts/supervisors:
Sindre Log

Abstract:

When considering the use of TBM as an alternative to conventional Drill & Blast tunnelling, it is of great importance to be able to give thorough and realistic performance predictions. Errors in prediction could be fatal for hard rock TBM projects, as these have a high geological risk and also demands high investment costs. This thesis is meant to provide field data to be used in the work of updating the NTNU prediction model. The effect of RPM on the rock breaking and TBM performance, as well as the effect of the rock mass fracturing have in particular been investigated. As a final purpose of this thesis laboratory testing has been performed to find the Drilling Rate Index™ and the Cutter Life Index™ of rock material. The field study of this thesis has been done at the Stillwater Mine in Montana, USA.

The findings of the RPM trials conducted seem to support the notion that running the TBM at a lower RPM gives a higher basic penetration in millimeter per cutterhead revolution, and that the rock breaking process is more efficient. The effect on the rock breaking process may be explained by how the loading rate between cutter and rock surface is influenced by the speed the cutterhead rotates with. Through analyzing shift logs from the TBM in areas of high rock fracturing it has also been found that lowering the RPM will give a higher basic penetration. In this case it is however not certain if this is due to how the rock break off the surface, or if it is caused by the fact that the penetration rate in areas of high rock fracturing is limited by the muck removal capacity of the TBM conveyor.

Through analysis of collected core sample data from probe drilling ahead of the TBM, it has been found that the rock mass fracturing has a strong correlation with the TBM penetration rate. It was also found that the rock mass fracturing highly influences the applicable thrust force of the TBM and thusly has an indirect effect on the TBM performance. More work should be done at the Stillwater Mine regarding geological back mapping, in order to further assess the importance of the rock mass fracturing factor k_s.

A full laboratory testing of rock samples from the tunnel at the Stillwater Mine has been performed. Rock material in the form of both rock chips from the tunnel face and core samples from probe drilling have been tested. It was in the course of this testing observed that the Sievers' J test results are greatly different in rock chips compared with core samples. This is most likely caused by difference in mineralogy in the samples, and the fact that rock chips contain micro fractures from the rock breaking process. More work on assessing this difference should nonetheless be done.

_____

Abstract

When considering the use of TBM as an alternative to conventional Drill & Blast tunnelling, it is of great importance to be able to give thorough and realistic performance predictions. Errors in prediction could be fatal for hard rock TBM projects, as these have a high geological risk and also demands high investment costs. This thesis is meant to provide field data to be used in the work of updating the NTNU prediction model. The effect of RPM on the rock breaking and TBM performance, as well as the effect of the rock mass fracturing have in particular been investigated. As a final purpose of this thesis laboratory testing has been performed to find the Drilling Rate Index™ and the Cutter Life Index™ of rock material. The field study of this thesis has been done at the Stillwater Mine in Montana, USA.

The findings of the RPM trials conducted seem to support the notion that running the TBM at a lower RPM gives a higher basic penetration in millimeter per cutterhead revolution, and that the rock breaking process is more efficient. The effect on the rock breaking process may be explained by how the loading rate between cutter and rock surface is influenced by the speed the cutterhead rotates with. Through analyzing shift logs from the TBM in areas of high rock fracturing it has also been found that lowering the RPM will give a higher basic penetration. In this case it is however not certain if this is due to how the rock break off the surface, or if it is caused by the fact that the penetration rate in areas of high rock fracturing is limited by the muck removal capacity of the TBM conveyor.

Through analysis of collected core sample data from probe drilling ahead of the TBM, it has been found that the rock mass fracturing has a strong correlation with the TBM penetration rate. It was also found that the rock mass fracturing highly influences the applicable thrust force of the TBM and thusly also has an indirect effect on the TBM performance. More work should be done at the Stillwater Mine regarding geological back mapping of the tunnel, in order to further assess the importance of the rock mass fracturing factor k_s.

A full laboratory testing of rock samples from the tunnel at the Stillwater Mine has been performed. Rock material in the form of both rock chips from the tunnel face and core samples from probe drilling have been tested. It was in the course of this testing observed that the Sievers' J test results are greatly different in rock chips compared with core samples. This is most likely caused by difference in mineralogy in the samples, and the fact that rock chips contain micro fractures from the rock breaking process. More work on assessing this difference should nonetheless be done.

Preface

This report is written as a part of my Master's Thesis in Construction Engineering at the Department of Civil and Transport Engineering at NTNU in the spring of 2014. The topic of this report is TBM tunnelling.

The interest for TBM came to me through the course TBA4150 Construction Engineering and from my six months as a research assistant at the Department of Civil and Transport Engineering. In this job I worked with among other things drillability testing of soils. A later job as student assistant in the Construction Engineering course helped to further spike the interest.

The overall objective of this thesis has been to document various conditions and parameters influencing TBM tunneling. In particular the influence of RPM on rock breaking and the effect of rock mass fracturing on TBM performance are investigated. This work is based on collecting and recording data from in a 10 week long field study at the Stillwater Mine in Montana USA, as well as performing laboratory research in Trondheim.

The thesis is part of an ongoing research at the Construction Engineering Department, and is done in cooperation with The Robbins Company.

Sassetta, June 24, 2014

Leon Nikolay Røren Eide

Acknowledgements

I would like to express my gratitude to the following who have helped me during the work of this Master's Thesis:

My main supervisor Professor Amund Bruland who has given me the opportunity to immerse myself in the field of TBM through excellent counseling when needed, and for helping me in obtaining the necessary funding for this thesis. Pål Drevland Jakobsen who as always has been an excellent support during this work. Yongbeom Seo for helping me in building the estimation models used. I would also like to offer a special thanks to Francisco Javier Macias Rico for being a great mentor during the last semester both in terms of excellent counseling when needed, and through his friendship which I have greatly appreciated.

The SINTEF laboratory for allowing me to perform the geological testing, which has been a great learning experience. A special thanks goes to Filip Dahl for always being available for questions.

Sindre Log of the Robbins Company for giving most useful feedback on my work with this report, and for helping me in facilitating the field stay at the Stillwater Mine.

The great people of the Stillwater Mine who gave me the opportunity to experience the true Montana. Thank you Curt Jacobs, Dwayne McKenny, Tom Cecil, Dylan Hertz and Bob Schuler for giving me a valuable experience and helping me in the process of bridging the gap between what I have learned at school and what real life at a construction site is like. The geology department at the mine represented by Mike Pasecznyk, Paul Holick and Kevin Butak also deserves a big thanks for all the good answers they have provided me both during the field stay and after the return to Norway, without which a great deal of this thesis could not have been completed. Also thank you Tim Cavanaugh for your company at the cabin.

And finally I would like to thank my dearest Anna, who supported me on the phone every day during the long field stay in winter-Montana.

Sammendrag

Når man skal vurdere bruken av TBM som et alternativ til konvensjonell boring og sprenging av tunneler er det viktig å utføre grundige og realistiske fremdriftsestimater. Feil i slike estimat vil kunne være fatale for bruken av TBM i hardt berg, ettersom et slikt prosjekt innehar høy geologisk risiko og i tillegg krever høye investeringer. Denne masteroppgaven har som hensikt å hente inn feltdata til bruk i arbeid med å oppdatere NTNUs estimeringsmodell. Spesielt effekten av RPM på brytningsforløpet i berget og fremdriften av en TBM, samt effekten oppsprekningsgraden i berget har blitt undersøkt. Masteroppgaven har også som hensikt å utføre borbarhetstester ved SINTEFs laboratorier i Trondheim for å finne indeksene DRI™ og CLI™ for geologisk materiale plukket i løpet av feltarbeidet. Datainnsamlingen er utført på en TBM brukt ved gruven Stillwater Mine i Montana, USA.

Funn gjort ved felt testing angående RPM virker til å støtte opp under hypotesen om at man ved å kjøre en TBM med lavere rotasjonshastighet oppnår en større basisinntrengning i millimeter per rotasjon av kutterhodet, og at brytningsforløpet av berget blir mer effektivt. Effekten som oppstår i brytningsforløpet kan være forårsaket av at overføringshastigheten av krefter mellom kutterne og berget forandrer seg med hastigheten kutterhodet roterer med. Gjennom å analysere borelogger fra TBMen i områder hvor berget er godt oppsprukket har det også blitt funnet at man ved å senke rotasjonshastigheten oppnår en høyere basisinntrengning. I dette tilfellet er det riktignok ikke sikkert om dette skyldes brytningsforløpet av berget, eller om det skyldes av at fremdriftsraten er begrenset av transportbåndets kapasitet til å fjerne brutt berg.

Gjennom å analysere innhentet kjerneprøvedata fra tunnelen har det blitt funnet at bergets oppsprekningsgrad har en sterk korrelasjon med fremdriftsraten til TBMen. Det ble også funnet at oppsprekningsgraden påvirket den anvendelige matekraften fra fremdriftssylinderne, noe som gir oppsprekningsgraden en indirekte effekt på ytelsen av maskinen. Mer arbeid bør bli utført ved gruven i Montana angående geologisk kartlegging av tunnellengden som har blitt drevet så langt, for å bedre kunne vurdere oppsprekningsgradens viktighet.

Laboratorietesting av materiale plukket fra tunnelen ble utført som planlagt. Dette materialet besto av både chips brutt ut på stuff og av kjerneprøver boret i forkant av tunnelen. Det ble i løpet av testingen observert at Sievers' J verdien for chips avviker i høy grad fra tilsvarende verdier fra kjerneprøver. Dette kommer mest sannsynlig av forskjeller i mineralogi, men også mikrosprekker fra chipsen ser ut til å påvirke resultatet. Mer arbeid bør utføres for å kartlegge om dette er en systematisk forskjell mellom chips og kjerneprøver.

Contents

1.   Introduction

The use of hard rock TBMs as an alternative to conventional Drill & Blast tunnelling is increasing worldwide, and now also in Norway. The first hard rock TBM in 20 year is currently being used for a hydroelectric project, and in the near future this kind of machinery will also be used for railroad tunnels in the two biggest cities of Norway. This increasing activity gives an increased need for knowledge regarding the technology. One needs to be able to make reliable predictions of performance and cost of a TBM in order to make sure it is a viable alternative for the big infrastructure projects.

1.1.   Background

The NTNU estimation model for hard rock tunnel boring has long been a good tool for obtaining the needed TBM tunnelling estimations. The model must however be kept updated as the years pass in order to stay relevant. In particular the effect of several machine parameters have to be reassessed as the TBMs used are getting bigger and more powerful. The understanding of how geological conditions such as fracturing effects TBM performance should also be elevated. The laboratory tests used for assessing drillability of rock and cutter life must also be understood as well as possible, as these are important input in the prediction models made at the NTNU.

1.2.   Purpose

The purpose of this Master's Thesis is to provide information and data to be used in the work of updating the NTNU model. In particular RPM and its effect on rock breaking and performance shall be investigated through field testing. Geological information with special respect to rock mass fracturing is also to be collected and presented. The purpose of this is to verify tunnelling performance against estimations and to increase knowledge about the tunnelling operations. The TBM investigated is a main beam open gripper TBM used to construct a ventilation and haulage level at the Stillwater Mine in Montana, USA.

The laboratory tests used to obtain input for the NTNU model are also to be evaluated through testing of geological samples collected at the Stillwater Mine.

1.3. Scope and Limitations

The scope of this work was to conduct a 10 week field study at the Stillwater Mine and collect as much data as possible from the TBM to bring home to the Department of Civil and Transport Engineering at NTNU for further research. Here it is processed and presented with respect to the parameters of interest. A comprehensive laboratory research of geological material collected is also performed.

As the amount of data available is quite high, the main work in this thesis is limited to investigate RPMs effect on basic penetration and the fracturing factors effect on net penetration. A simple and preliminary assessment of the rock fracturing factor through information given in core samples from the tunnel probe program is undertaken. General TBM performance is also presented and discussed.

1.4. Outline

The report is divided into eight chapters.

In chapter two a literature study investigating some of the most important mechanics and influences of the rock breaking process, and how they influence the efficiency of a TBM project is presented. This is important as the efficiency of a TBM highly influences the economy of such a project. The NTNU model is also briefly explained.

The third chapter will give an overview of the site at the Stillwater Mine where the field research of this master thesis has been conducted. Included in this chapter is also information regarding the TBM being used and the geology it is operating through.

The research methodology of the thesis is presented in chapter four. The methods of collection and processing of TBM performance data is presented, as well as the methods used in the field testing conducted. How geological information has been gathered and linked to the tunnel drive is also explained here, and all different laboratory test performed on the geological samples are presented and explained.

Chapter five presents the results of the processed TBM performance data, the field testing performed, the geological investigation of the tunnel and also the laboratory testing. These results are discussed in chapter six, trying to link findings to some of the theory presented in chapter two.

Conclusive remarks are given in chapter seven, while some thoughts about further work to be done after this thesis are presented in chapter eight.

2. Hard Rock TBM Tunnelling

This chapter will focus on some of the theoretical aspects of Hard Rock TBM Tunnelling. A brief explanation of how a TBM works is given, as well as some of the parameters that influence the performance of such a machine. In particular the rock breaking process has been investigated thoroughly in a literature review, as the understanding of this process is vital when performing a field study like the one in this thesis. The NTNU Model, on which the field testing of this thesis is based, is also presented.

2.1.   Tunnel Boring Machines

The description tunnel boring machine (TBM) refers according to Maidl et al. (2008) to a machine for driving tunnels in hard rock with a circular full-cut cutterhead, generally equipped with disc cutters. A TBM utilizes a rotating, crushing boring process to remove the rock from the surface of a tunnel drive. This is an alternative to using explosives when excavating a tunnel. To achieve this great force has to be applied to the head of the TBM, also called cutterhead, while it rotates. For each revolution the circular discs, or cutters, fitted on the cutterhead will penetrate further into the rock. These cutter rings are not powered, but roll in concentric circles against the rock face. A typical penetration value in hard rock conditions will be between 1 mm and 15 mm per revolution (Bruland, 1998d).

The definition of hard rock conditions is not well defined. Bruland (2000) presents some rough limits of the term hard rock, as used in the NTNU prediction model:

- The rock drillability expressed by the Drilling Rate Index DRI is in the range of approximately 20 to 80, roughly corresponding to a compressive strength σ_c in the range of approximately 350 MPa to 25 Mpa.
- The rock type has medium to low porosity, less than approximately 10 % (volumetric).
- The rock mass degree of fracturing expressed by the average spacing between weakness planes is larger than approximately 50 mm.
- The rock will break as chips (by brittle failure) between the disc cutters.
- The rock mass has a strength such that the excavated tunnel generally will need only light support in the form of rock bolts or shotcrete (except for weakness zones and other singular phenomena).

The mentioned Drilling Rate Index is explained in detailed in chapter 4.5.9 of this report.

2.1.1. Different Types of Hard Rock TBMs

There are several different kinds of TBMs which can be utilized when boring in hard rock conditions. The basic principle of how the rock is broken is the same for all of them, but they have different conditions in which they are most suited, especially when it comes to what kind of rock support is needed in the tunnel.

Gripper TBM

According to Maidl et al. (2008) the gripper TBM is the classical form of tunnel boring machines, and is often described as an open TBM. In rock conditions of medium to high stand-up time this kind of machine is most widely used as long as there are no strict regulations as to how much water may flow into the tunnel during boring. An example of a main beam gripper TBM can be seen in Figure 2.1.
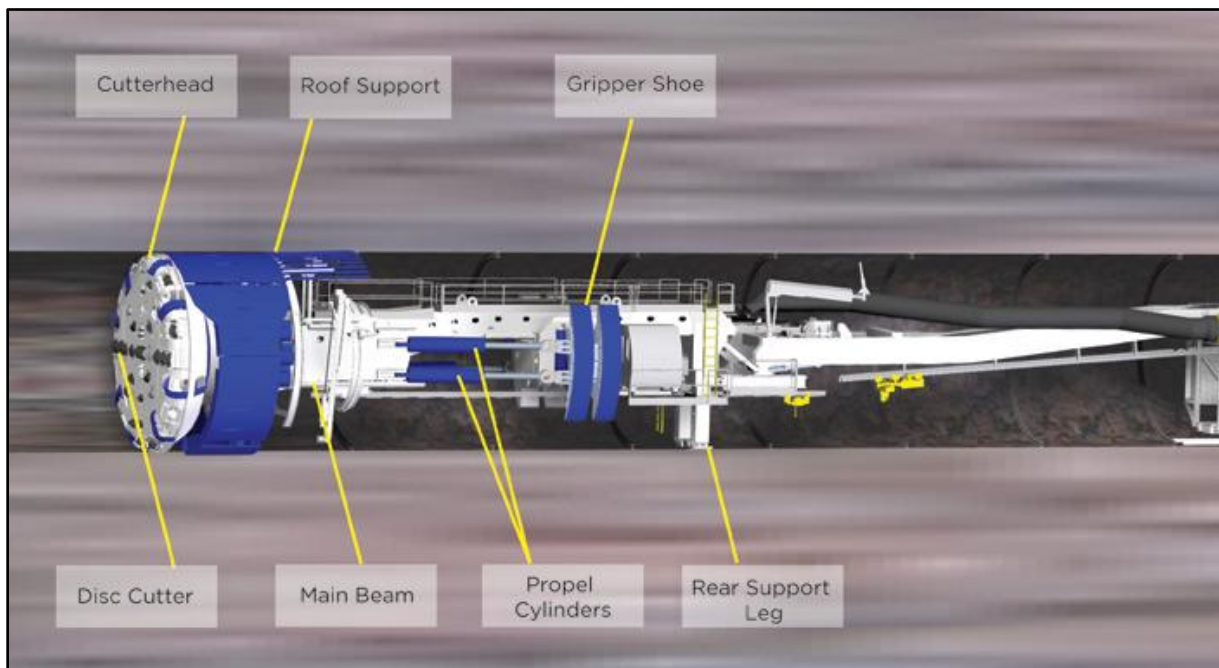

Figure 2.1: Example of a Main Beam Gripper TBM (The Robbins Company, n.d.)

An open gripper TBM utilizes the hydraulic gripper shoes to brace radially against the tunnel wall, and then applies pressure to the cutterhead through the hydraulic propel cylinders. After a full stroke of the propel cylinders is complete the TBM will rest on the rear support legs while the gripper shoes are retracted and regripped. The process then starts over again.

There are different kinds of open TBMs, some without any roof support and some with roof shields to protect the crew working behind the cutter head. The TBM may also be fitted with side steering shoes to steer the TBM during boring.

Single Shielded TBM

In rock conditions of low stand-up time a single shield TBM will be more suited. This TBM is equipped with a shield behind the cutterhead to protect the machine and the crew. The permanent rock support is installed under the protection of this shield in such a way that the rock surface never is exposed to the crew inside. Reinforced concrete segments are the most commonly used system today (Maidl et al., 2008). The thrust needed to break the rock is provided by jacks which push directly against the concreted elements installed. An example of a single shield TBM is shown in Figure 2.2.
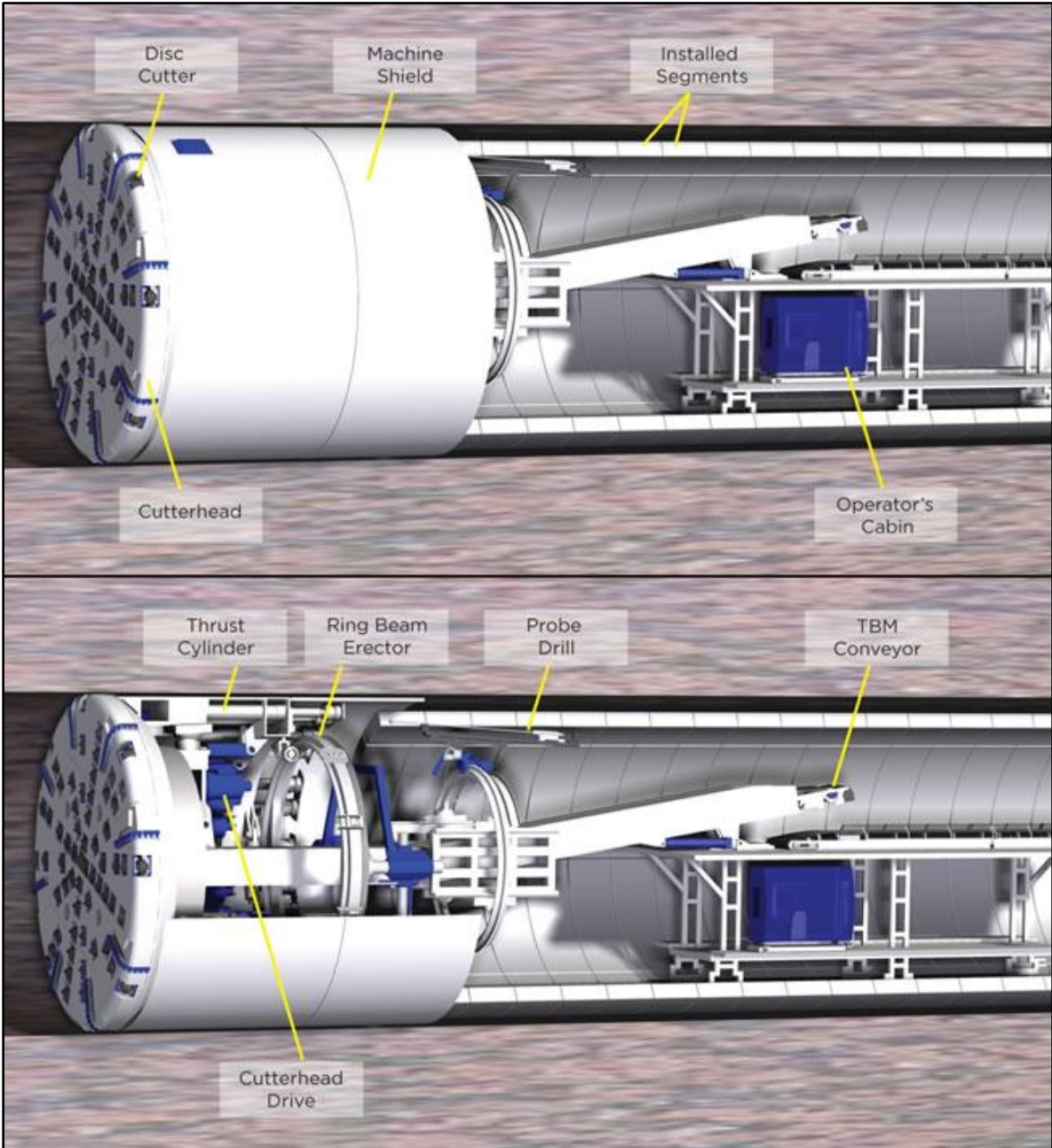

Figure 2.2: Example of a Single Shield TBM (The Robbins Company, n.d.)

Double Shielded TBM

Also known as a telescopic shield TBM, this machine type consists of two shields, a front shield and a gripper shield which are connected with telescopic jacks. In rock conditions that allow it, the machine will utilize gripper shoes and propel itself in the same way as a gripper TBM does. In this mode the concrete segments can be erected while the machine is boring. Should the rock conditions not allow gripping, the machine may be used in the same way as a single shielded TBM, where the necessary thrust is provided by jacks mounted at the installed concrete segments. As with a single shield TBM, the concrete elements may not be installed during boring in this mode. An example of a double shielded TBM is shown in Figure 2.3.
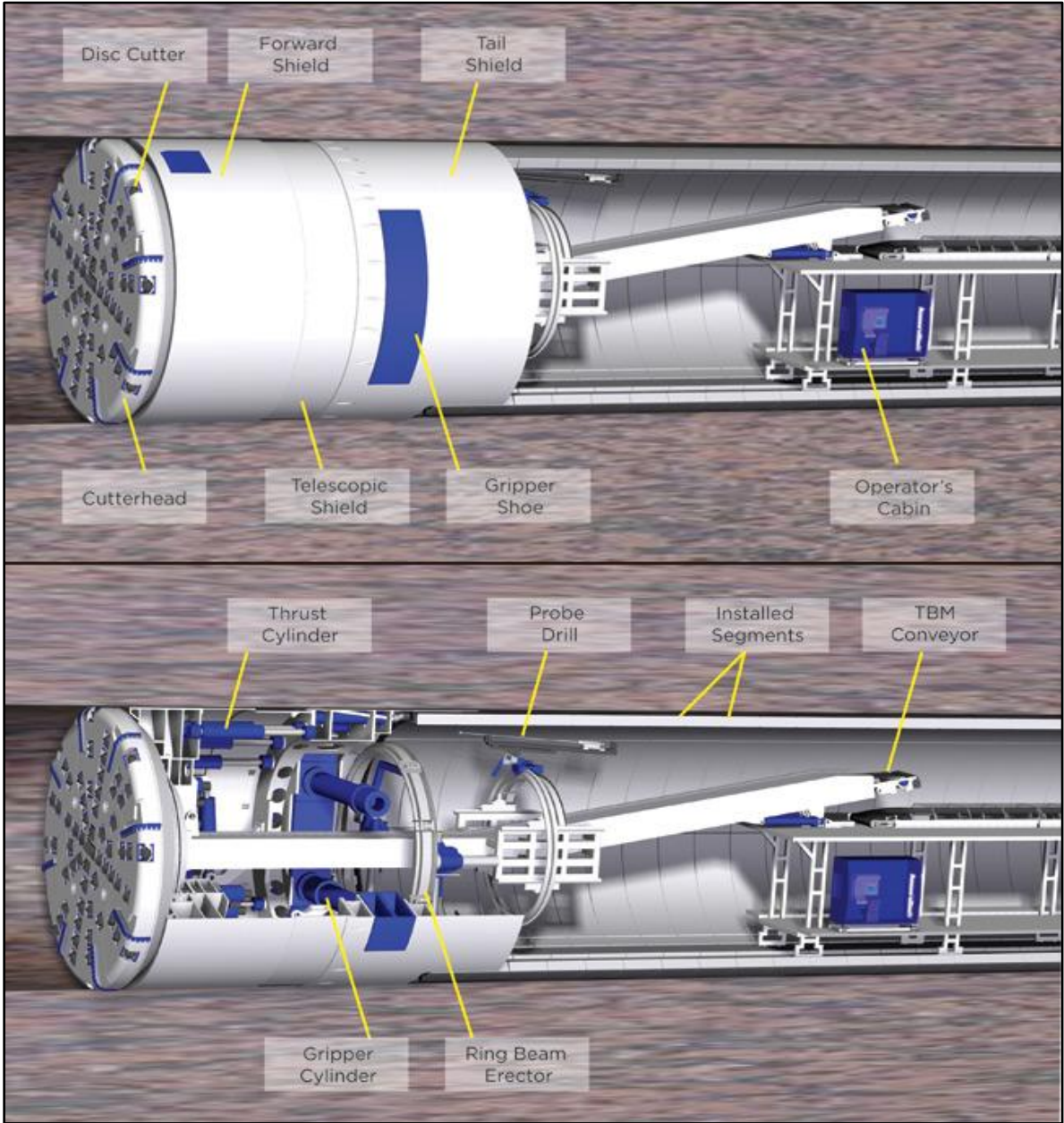

Figure 2.3: Example of a Double Shield TBM (The Robbins Company, n.d.)

2.1.2. TBM versus Conventional Drill and Blast Excavation

As presented by Maidl et al. (2008), the following lists can be shown as a summary of advantages and disadvantages of a TBM drive compared to a conventional drive using Drill and Blast technique:

<u>Advantages</u>

- Much higher advance rates possible.
- Exact excavation profile.
- Automated and continual work process.
- Low personnel expenditure.
- Better working conditions and safety.
- Mechanization and automation of the drive.

<u>Disadvantages</u>

- Better geological investigations and information are necessary than for drilling and blasting.
- High investment resulting in longer tunnel stretches being necessary.
- Longer lead time for design and building of the machine.
- Circular excavation profile.
- Limitations on curve radii and enlargements.
- Detailed planning required .
- Adaptation to varying rock types and high water inflow is only possible to a limited extent.
- Transport of the machine with trailers to tunnel portal.

In general it is possible to say that the flexibility of a TBM drive is less than that of a conventional drill and blast drive. However the technical, safety and economic advantages of using a TBM for a long tunnel could be substantial if the rock conditions are suitable. This is also in accordance with the findings of Macias and Bruland (2014). They also state that one should consider hybrid solutions of Drill & Blast and TBM whenever the circumstance allows it.

2.2.   The Rock Breaking Process in a TBM

By recording size and shape of rock chips one can assess how efficiently the boring process in a TBM drive has been. During the field work in this thesis rock chips have been collected and analyzed, and therefore processes behind the chipping are of great interest. The following sub-chapter will thusly focus on studying some of these processes and factors influencing them.

2.2.1. Chipping

During operations with a TBM the rock will break off from the surface wall in the form of chips. Most evidence shows that these chips are formed by the propagation of cracks that are induced by tensile fracturing of the rock (SME, 1992; Lindqvist and Rånman, 1980; Bruland, 1998d). This can be surprising, as the load applied by the cutter disc to the rock is one of compression. It is believed that the cutters generate tensile stresses in the rock by crushing a portion of the rock beneath the cutter tool and that this crushed material will dilate and induce tensile stresses that eventually leads to fractures developing in the surrounding rock.

Figure 2.4 shows the principle of chipping under a disc cutter as presented by Bruland (1998d). Notice how the planes of weakness in the rock will influence the process.
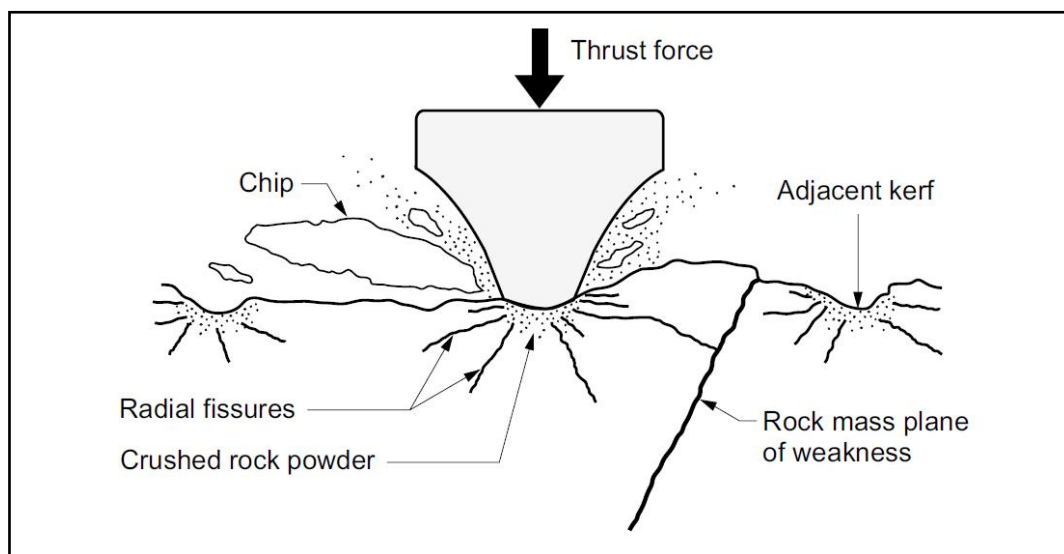
Figure 2.4: Example of rock breaking by a disc cutter (Bruland, 1998d)

The importance of the fracturing and weakness planes in the rock has been thoroughly investigated in the NTNU model, and the fact that they play an important role in the rock breaking process seems clear. The NTNU model will be further presented in chapter 2.3.

2.2.2. Indentation

Indention with mechanical tools is the most widely used technique for drilling holes ranging in diameter from less than 10 mm to several meters (SME, 1992). The indentation denotes the depth of which the cutter edge is pressed into the rock surface by cutterhead thrust. The indentation cannot be measured in situ by any practical method, but must be derived from analyses of chips and from laboratory tests (Bruland, 1998; Frenzel, 2010).

The principle of indentation is that the tool, in the case of TBM tunneling the disc cutters, is placed in contact with the rock. Then normal force is applied to the tool, so that stresses are built up underneath the area of contact. The rock directly beneath the contact point will crush, and cracks will then propagate from this area and to the surface, forming chips in the rock that break off. This is called surface chipping. It is widely believed that these cracks are formed by a tensile mode of failure, among others by Lindqvist et al. (1984), Bruland (1998d), SME (1992) and CSM (2008).

The process of fracturing rock from indention can be described using a *Flat Bottomed Punch* model, as can be seen in Figure 2.5 (SME, 1992).
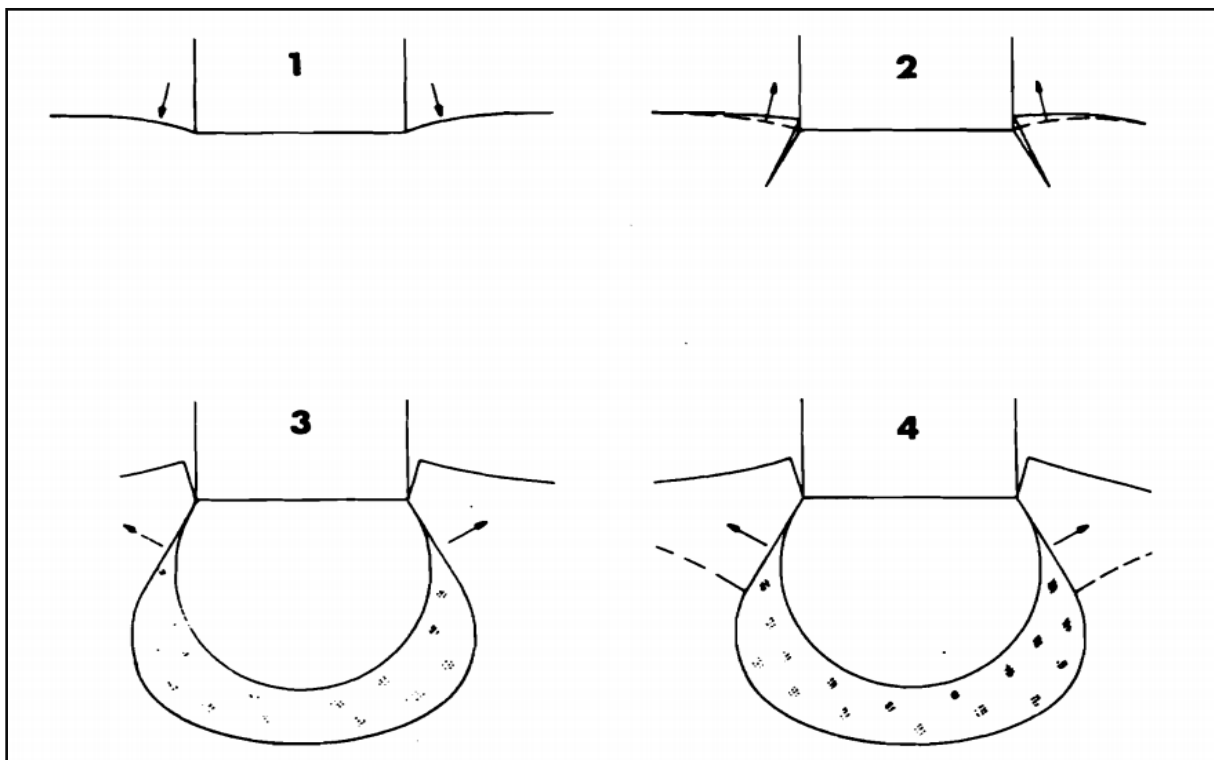

Figure 2.5: Illustration of the Failure Mechanism of Rock by a Flat-Bottomed Punch (SME, 1992)

According to this model, the rock surface will deform elastically as long as the stress from the flat-bottomed indenter, which is called a punch in this case, is low. Then as the stress increases, Hertzian cone cracks will be initiated in the rock from the corner of the tool. Further increase in the stress leads to crushing of the rock beneath the tool. Eventually, major fractures are initiated from the crushed rock zone and propagate to the surface to form chips. The next step in the process is the dilatation of the crushed material underneath the tool, which causes tensile stresses to be induced in the rock surrounding the crushed zone. The cracks that forms the chip will be initiated when this tensile stress exceeds the rocks tensile strength. In the last step of this model, chipping of larger fragments of rock occurs.

In a model presented by Lindqvist and Hai-Hui (1983), it can be observed that a zone will be formed in the rock material below the indenter where chips and fines are produced. This model is shown in Figure 2.6 and can be explained in six steps.

a – Crushed Zone Forms

b – Cone Crack Forms-
Chips Fly Out

c – Crushed Material
Redistributed

d – Second Crushing
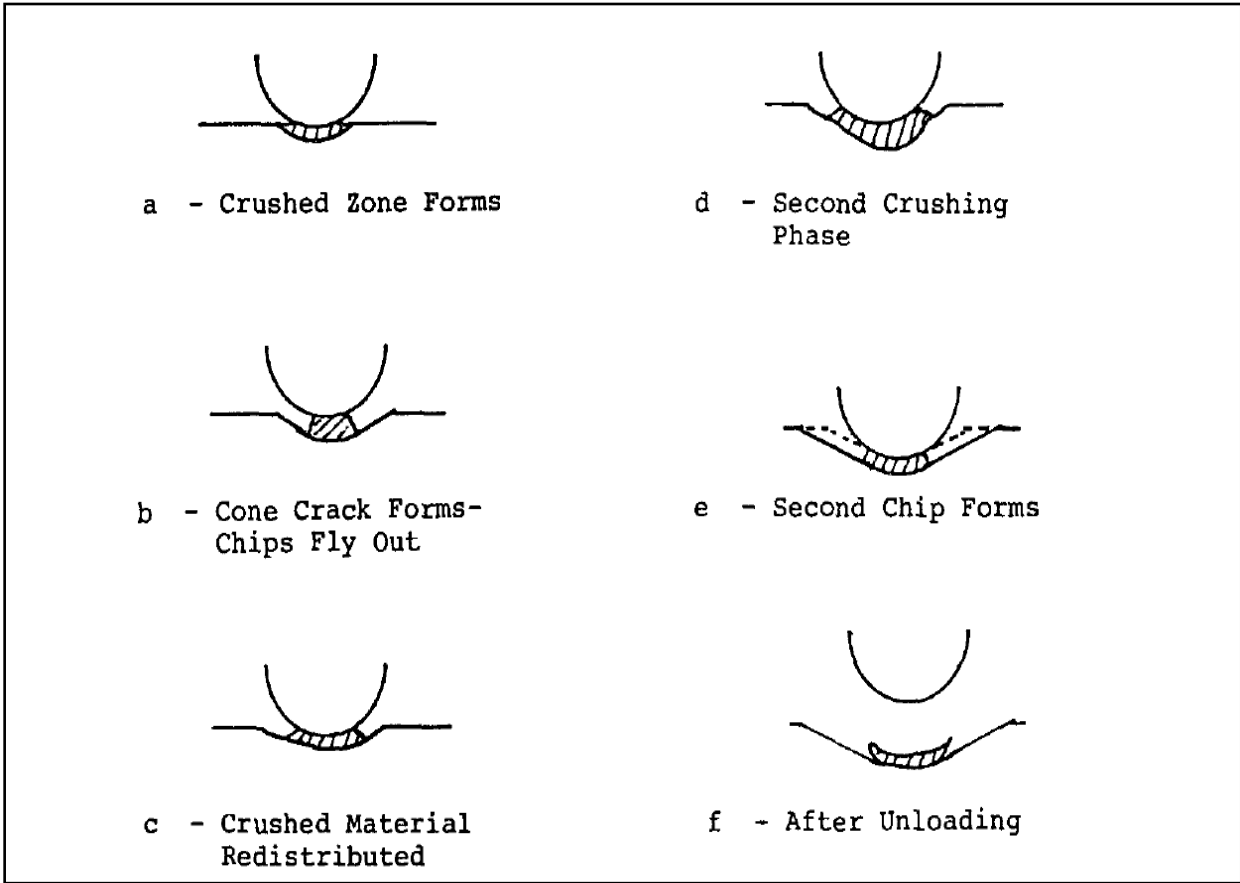Phase

e – Second Chip Forms

f – After Unloading

Figure 2.6: The sequence of events in hemispherical penetration in rock
(Lindqvist and Hai-Hui, 1983)

10

a) A zone of crushed rock is formed close to the contact point between the indenter and rock

b) Chips form and break out on the side of the contact zone due to radial fractures

c) The crushed fines are redistributed

d) A second crushing phase starts, where fines are also crushed again

e) Chips form a second time and breaks out

f) Unloading of the indenter

The model can be said to have similar mechanics as the process presented by Bruland (1998d). Bruland presents the same principles, but focusing on the rock breaking process for disc cutters used in TBMs. In this case the TBM will expose the tunnel face to several contact points, where chips will break out more efficiently due to the fact that chips will break out between adjacent kerfs and not from single points of contact. This is also the case of a model presented by CSM (2008), and an illustration of this can be seen in Figure 2.7.
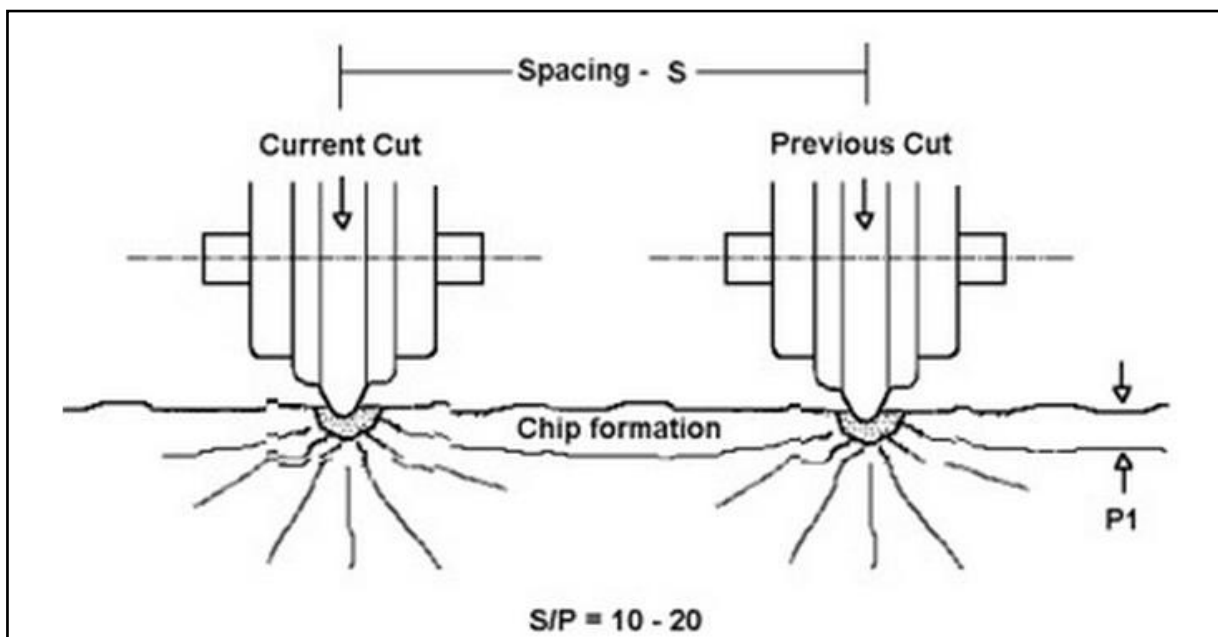

Figure 2.7: Illustration of how chips form between adjacent kerfs (CSM, 2008)

As seen in the models presented in Figure 2.4, Figure 2.6 and Figure 2.7 crushed material will be present beneath the indenter or cutter throughout the rock breaking process. It has been recognized that this crushed material is of importance. Models have been constructed by Gaye and Stephens (1981), as well as by Kutter and Saino (1982) and Saino (1985) which take into account how the crushed zone influences the breaking process between parallel kerfs made by

11

circular disc cutters. They argue that the required disc thrust force will increase due to the nature of the crushed zone. Lindqvist and Hai-Hui (1983) also argues that the crushed zone influences the penetration, and that the penetration will increase after removal of the crushed material in the zone, e.g. by flushing or other mechanical methods.

Understanding the indentation process is a key point in understanding the rock breaking process. This because the cutter edge indentation will determine the depth of crack formation into the rock face, and thereby how efficient the chipping will be (Bruland, 1998d). A more efficient chipping process will lead to a more efficient use of TBMs and thus make TBM an even more viable option for tunnelling compared to conventional Drill & Blast.

Figure 2.8 shows cross sections of chips taken during penetration tests of three cutter thrust levels. As the thrust increases the chips thickness also increases. An explanation of this change in size could be that the distribution between tensile and shear failure is different for the separate thrust levels, but in any case the tensile failure will be the dominating one.
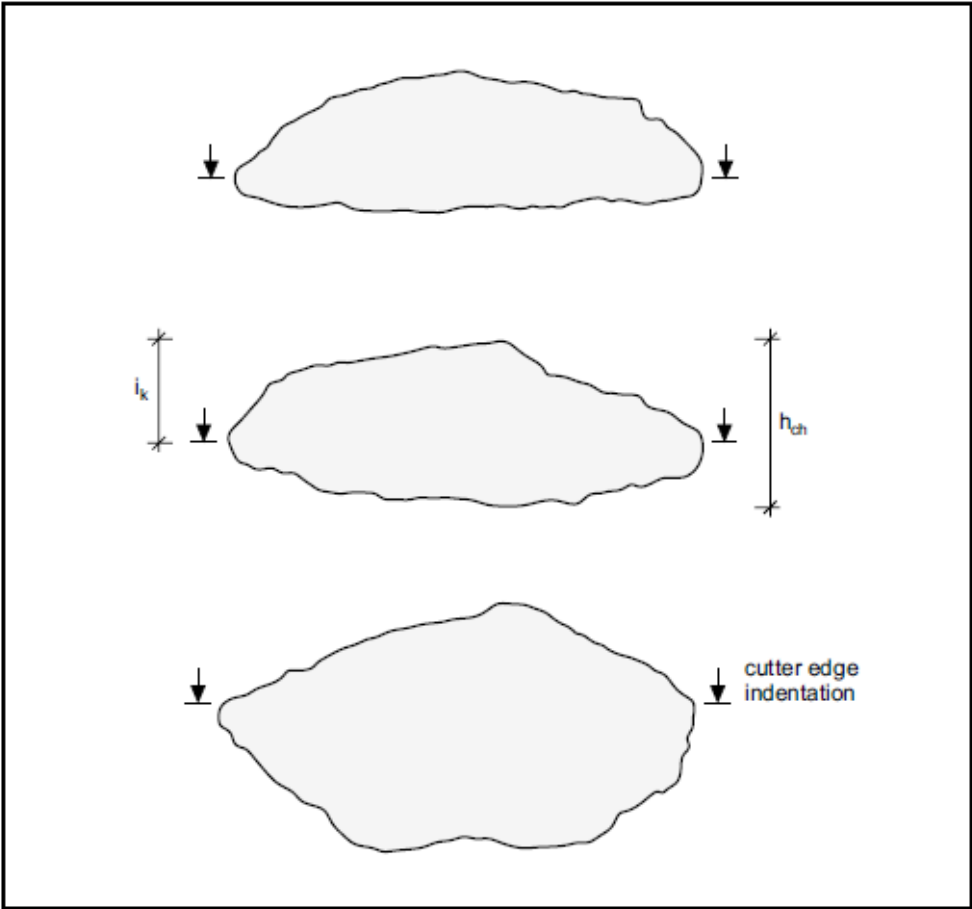

Figure 2.8: Rock chip shapes for different degrees of indentation (Bruland, 1998d)

2.2.3. Net Penetration

As opposed to indentation, which denotes the depth the cutter disc can penetrate into the rock, the penetration tells us how far the machine has advanced in one revolution. The difference between indentation and penetration can be seen in Figure 2.9.
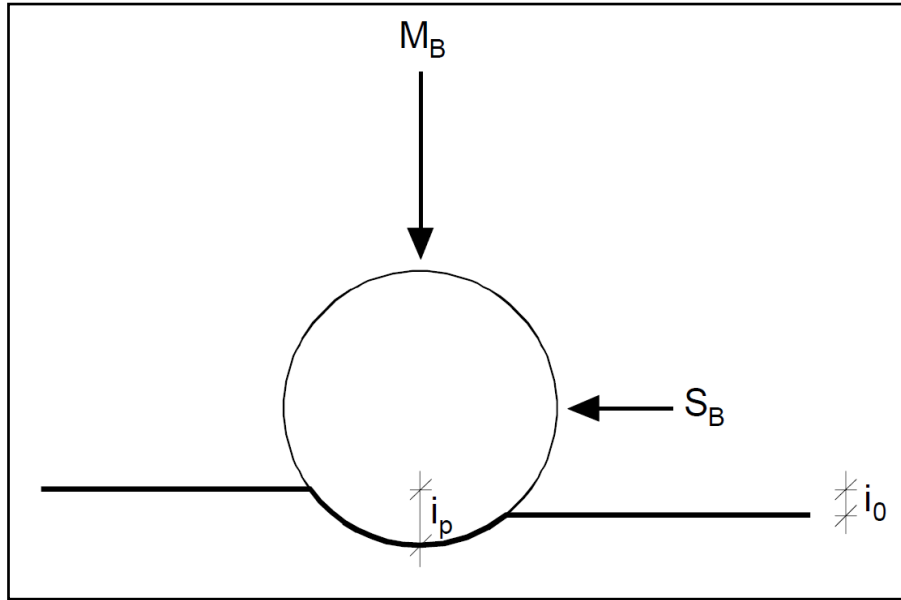

Figure 2.9: The penetration and indention of a disc cutter (Bruland, 1998d)

As seen in the figure, the penetration i_0 denotes the length the cutterhead advances after one revolution, while the indentation i_p shows the length the cutter disc is pressed into the rock. It is the penetration that is of interest when estimates for cost and time are made (Bruland, 1998d).

The basic penetration of the cutter in mm/rev is converted to net penetration I_0 given in m/h, based on the RPM being utilized, and can in systematically fractured rock mass without marked single joints be expressed in the following equation, as presented by Bruland (1998a):

$$I_o = i_o * RPM * \left(\frac{60}{1000}\right)$$

The inverse of the number of cutterhead revolutions required to achieve one total chipping of the face can be called the chipping frequency f_{ch}. The chipping frequency is also indicated by the thickness of the largest chips versus the penetration in mm/revolution (Bruland, 1998d).

Table 2.1, presented by Bruland (1998d) shows parameters influencing the penetration of a TBM. The influence should be understood as the influence on basic penetration when all other parameters are kept constant. Most of these parameters are explained in further detail in chapter 2.3.

Better Boreability	More Efficient TBM
- Increased degree of fracturing - Increased angle between the tunnel axis and the planes of weakness (when angle is 0° - 60°) - Increased rock drillability (reduced rock strength) - Reduced rock abrasivity	- Less cutter spacing (more cutters on the cutterhead - Less cutter diameter - Lower cutterhead *RPM* - Reduced cutter edge width - More stiff machine

Table 2.1: Factors influencing rock boreability and TBM efficiency (Bruland, 1998d)

2.3.   The NTNU Prediction Model

The NTNU tunnel boring model consists of four different parts, which are net penetration rate in mm/rev and m/h, cutter life in h/cutter, gross advance rate in h/km and finally excavation costs (Bruland, 2000). In the scope of this thesis the main interest is the penetration rate.

As can be seen in Table 2.2 the parameters influencing the net penetration calculated in the NTNU model can be divided into rock mass parameters and machine parameters.

Rock Mass Parameters	Machine Parameters
• Fracturing; frequency and orientation • Drilling Rate Index, DRI • Porosity	• Cutter thrust • Cutterhead rpm • Cutter spacing • Cutter size and shape • Installed cutterhead power

Table 2.2: Parameters influencing the net penetration rate of a TBM (Bruland, 1998a)

These parameters will be treated more in the following subchapters. Presently the NTNU prediction model is one of the most widely used prediction models for hard rock TBM tunnelling (Macias et al., 2014).

2.3.1. Rock Mass Parameters

Fracturing

According to Bruland (2000) the most important penetration rate parameter for tunnel boring is the rock mass fracturing. This can be understood by picturing that the rock mass has already been subject to part of the energy necessary to crush it through geological history, so that the specific energy needed from the boring process will be less. The shorter the distance between the fractures is, the greater they influence the penetration rate (Bruland, 1998a).

According to the NTNU model, this factor is of such importance that prediction models must have an input parameter describing the degree of fracturing. This is also supported by the penetration models of Büchi and Luleå (Bruland, 2000) as well as Gehring (1995). The rock mass fracturing factor used in the NTNU Model is explained in detail in chapter 2.3.3.

Rock Drillability

The DRI will be presented in detail chapter 4.5 of this report, but in short it is an index showing the drillability of the rock which shows a good correlation with field data regarding penetration rate from different TBM projects (Zare and Bruland, 2012).

Porosity

Bruland (1998d) also states that the porosity shows a clear influence on the penetration rate, but the exact size of the correction factor is uncertain. An explanation for the porosity's influence is that the pores in the rock mass act as crack initiators and amplifiers of crack propagation.

One could believe that this factor was accounted for in the DRI, but data shows that the effect of the porosity on the DRI is not large enough compared to the effect on penetration rate, when the porosity is less than 10-12 %. Thusly porosity has been included as a separate parameter in the NTNU model.

2.3.2. Machine Factors

Gross Average Cutter Thrust

Regarding the machine parameters presented in Table 2.2, the main parameter presented in the NTNU model is the cutter thrust represented by average cutter load. The reason for this is that with increasing cutter load the cutter edge will penetrate deeper into the rock. This will lead to that the indentation will increase, which in return leads to a more efficient rock breaking process. The energy transmitted from the cutterhead to the rock will be done so more efficiently when the indentation increases (Bruland, 2000).

The parameter used in the NTNU model for the cutter load is the gross average cutter thrust, which means that the total thrust of the cutterhead is divided by the number of cutters on the cutterhead. No corrections are made regarding drag or friction. This is chosen as the input parameter to get the most reliable and reproducible thrust measurements, without discussion about among other things the cutterhead support pressure and cutterhead friction. In Figure 2.10 the effect of the gross thrust per cutter disc on the basic penetration in mm/rev is shown.
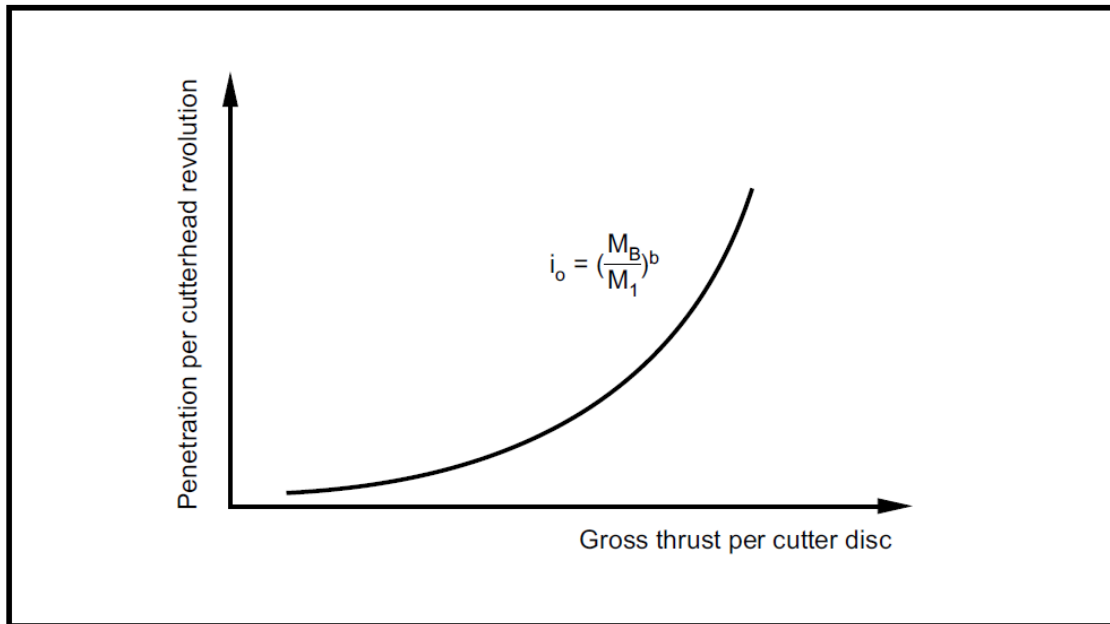
Figure 2.10: General progress of a penetration test curve (Bruland, 1998d)

As can be seen in the figure the basic features of the penetration curve are the following:

- M_b – Gross average thrust per cutter (kN/cutter)
- M_1 – Critical thrust to achieve a penetration of 1 mm/rev (kN/cutter)
- b – Penetration coefficient, which describes the effect of a change in the applied cutter thrust

To prevent the cutters from just rolling and wearing down against the rock surface, the penetration curve is normalized to a critical thrust M_1, which gives a penetration rate of 1 mm/rev. M_1 and b are found by performing a linear regression of the $\log_{10}$ values of the basic penetration in mm/rev and the thrust force applied.

According to the NTNU model the penetration rate increases rapidly with the cutter thrust. Also Gong et al. (2006) states that the penetration per cutterhead revolution increases in this manner with increasing thrust per cutter when it is higher than a critical value. They have analyzed muck sieves and found that with increasing thrust force, the muck size increases and the rock breaking process is more efficient. The chips they observe change shape from flat to elongated and flat as the thrust increases.

It has been argued by Bruland (1998a) that the material quality of the steel cutter ring is the limiting factor of the cutterhead thrust. This is also supported by the FAST-Tunn project (The Research Council of Norway, n.d.). Therefore one must consider the thrust capacity of the cutter rings along with the capacity of the cutter bearings and the main bearing when estimating the penetration rate.

The effect of increasing cutter thrust on the chip shapes can be seen in Figure 2.11, which shows how the shape of rock chips change with increasing thrust. This is of interest for the work in this thesis, as a part of the field work will be based on analysis of collected rock chips to assess the effect of variation in parameters such as RPM and thrust force.
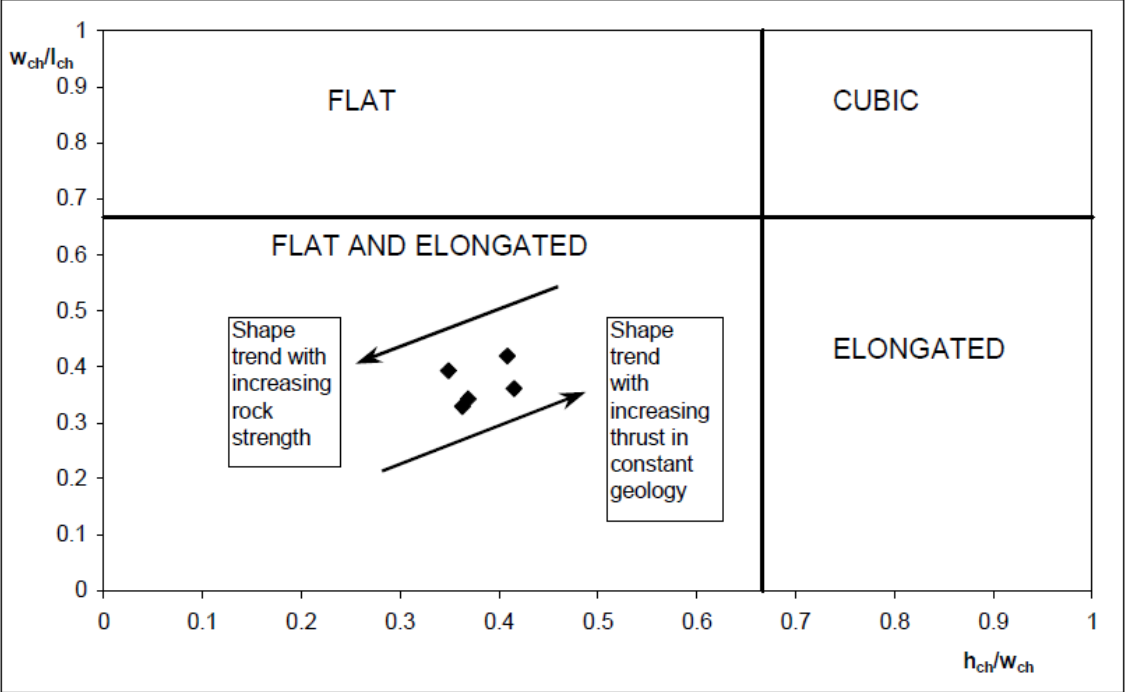

Figure 2.11: Change in rock chip shape with increasing thrust or increasing rock strength (Bruland, 1998d)

If the boring takes places in geology with marked single joints or heavy fractured rock, Bruland (1998a) states that it may be necessary to reduce the thrust to avoid high machine vibration, which will lead to poor working conditions on the TBM. The thrust should in this case also be reduced to prevent very high momentary cutter loads.

Bruland (1998d) also identifies some other limitations for thrust levels, and thusly penetration rates, in addition to vibration. These can be listed as follows:

- Cutters "butt with their hubs" due to very high indentation
- The muck removal capacity of the TBM is insufficient
- The cutterhead buckets are blocked in rocks with high hardness or in rock with high content of clay or other weak minerals

Average Cutter Spacing

Included in the NTNU model is the average spacing of cutters on the cutterhead. To find the average cutter spacing one simply has to divide the cutterhead radius by the number of cutters on the cutterhead. The cutter spacing must be adapted to the rock mass properties to achieve efficient chipping in a TBM drive, as the cutter spacing decides the distance the chip forming cracks have to propagate between the kerfs (Bruland, 2000).

Stempkowski (1996) identifies as well that the cutter spacing is of importance, as a reduction in cutter spacing reduces the necessary thrust to achieve the same penetration as if the spacing was bigger. He also states that the optimal spacing depends on the geology in question. Ewendt (1989) also presents how the thrust force varies with the cutter spacing, showing that increasing spacing demands a higher thrust force.

Cutter Size and Shape

Increased cutter diameter means that the thrust per contact point on the rock surface can be increased up to a limit where it is limited by the life of the cutter bearings, the ring steel quality and the ring fastening to the hub (Bruland, 1998d). Increased cutter diameter will also increase the size of contact point with the rock, and a higher total thrust from the TBM is demanded to set up the necessary rock stress to induce crack propagation.

As mentioned earlier, the quality of the steel cutter ring is believed to be a limiting factor for the cutterhead thrust. This means that the earlier trend to increase the cutter diameter has come to a halt until the problem of the steel quality has been solved. The size of the TBM itself is also a limiting factor for the cutter diameter, as the space available on the cutterhead determines the how big cutters can be fitted on it, and how complicated the loading system may be.

The shape of the cutters will also affect the boring performance, and the estimation model of Bruland (1998a) is based on Constant Cross Section cutter rings that are approximately 50 % worn. This shape of the cutters is especially important when considering cutter wear, but this will not be treated in detail in this report.

RPM

The RPM of the cutterhead is according to Bruland (2000) known to have substantial influence on the net penetration. It has been observed that cutterheads with substantially lower than designed RPM have a higher penetration per revolution, and the other way around for cutterheads with substantially higher than designed RPM. This is also observed by Macias et al. (2014a). One possible explanation for this is that the loading rate of forces from the cutterhead to the rock face will affect the deformation and strength properties of the rock.

The RPM of a TBM is inverse proportional to the cutterhead diameter (Bruland, 1998a; Stempkowski, 1996). This takes into account that the rolling velocity of the peripheral cutter has to be limited. The cutterhead RPM is at the present not a parameter in the NTNU prediction model, but Bruland states that as a part of future development of the mode a correction factor for the cutterhead RPM must be added. Research on this field is currently also being conducted by The Robbins Company (Log, 2013).

Installed Power and Torque

In cases with high net penetration or fractured rock it is of importance that the installed cutterhead power is high enough to utilize the estimated thrust (Bruland, 1998a). Should the installed power be too low to rotate the cutterhead at a given penetration, the torque will be limited. In this case the thrust will have to be reduced enough to reduce the required torque.

The importance of the torque and torque limit is also recognized by Schneider et al. (2012), who show how the penetration model of Gehring (1995) correlates in a significantly better way with actual effective penetration values when a factor for among other things limited torque is included.

The required torque of the TBM drive is dependent on among other things the cutterhead diameter, the number of cutters on the cutterhead and the gross average cutter thrust.

Utilization

The utilization of the machine is the net boring time in percentage of the total tunneling time. Total tunneling time includes the following activities:

- Boring
- Regripping
- Cutter change and inspection
- Repair and service of the TBM and Backup
- Miscellaneous

2.3.3. The Rock Mass Fracturing Factor - k_s

When talking about rock boreability, one could define this as the resistance, ease or difficulty that a TBM can penetrate in a rock mass (Macias et al. 2014). The rock boreability is composed of the intact rock properties which in the NTNU model is described mainly by the Drilling Rate Index, and by the rock mass parameters, in particular the rock mass fracturing.

According to the NTNU model, there are two aspects of the rock mass fracturing that must be taken into account. Firstly there is the degree of fracturing, which means the fracture type and spacing between them. Secondly one should also consider the angle between the tunnel axis and the plane of weakness.

These two parameters have been combined into one rock mass fracturing factor, also called k_s. This factor is the most important parameter in the NTNU Model for calculating penetration rate, where a higher value for the k_s means better rock mass boreability. Table 2.3 shows fracture classes with the spacing between the planes of weakness. This table from Macias et al. (2014) is a modified version of the classification presented in Bruland (1998b).

Fracture Class (Joints / Fissures)	Average Spacing between the Planes of Weakness a_f (cm)	Range Class (cm)
O	∞	$240 - \infty$
O +	190	$160 - 240$
O - I	140	$110 - 160$
I -	90	$60 - 110$
I	40	$37.5 - 60$
I +	35	$32.5 - 37.5$
I-II	30	$27.5 - 32.5$
II -	25	$22.5 - 27.5$
II	20	$17.5 - 22.5$
II - III	15	$12.5 - 17.5$
III	10	$8.75 - 12.5$
III - IV	7.5	$6.25 - 8.75$
IV	5	$4 - 6.25$

Table 2.3: Fracture classes with average spacing between the planes of weakness
(Macias et al. 2014)

The orientation of the weakness planes is found by the following equation (Bruland, 1998a):

$$\alpha = \arcsin(\sin \alpha_f * \sin(\alpha_t - \alpha_s))$$

Where α_s is the strike angle, α_f the dip angle and α_t the tunnel direction. When the fracture class and the average angle between the planes of weakness and the tunnel axis is found, the k_s value is calculated from the graph shown in Figure 2.12 given by Bruland (1998c).
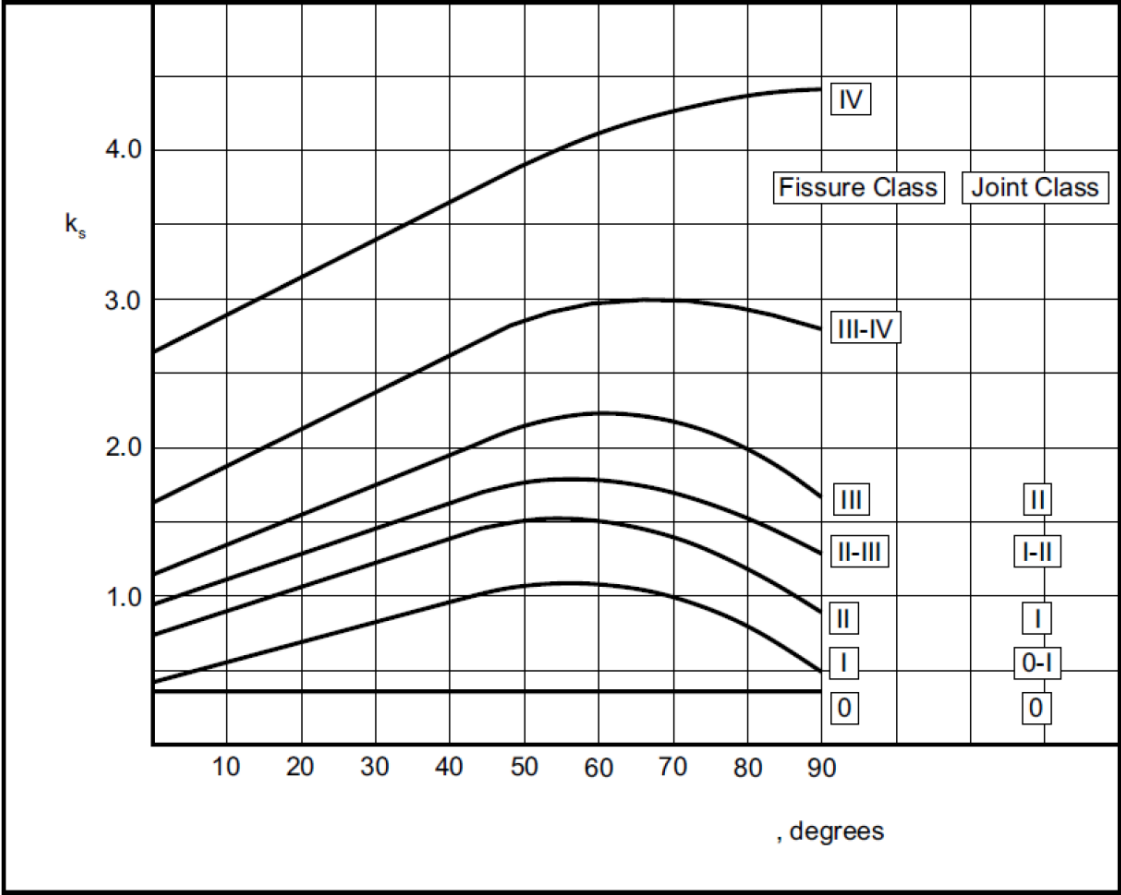

Figure 2.12: Graph used to calculate the Rock Mass Fracturing Factor ks (Bruland, 1998c)

One can see from this graph that the optimum angle is around 60 degrees, except for in the highest fracture class St 4 where an angle of 90 degrees gives the maximum fracturing factor.

After calculating the k_s for all sections in a given tunnel interval, the average k_s value is found by the following equation (Macias et al., 2014):

$$k_{s-avg} = \frac{\sum_{i=1}^{n} l_i}{\sum_{i=1}^{n} \frac{l_i}{k_{s-i}}}$$

Where l_i is the tunnel length of fracturing class *i* of the section and k_{s-i} is the k_s factor of fracturing class *i* of the section.

When more than one set of weakness planes exists, the total fracturing factor can be calculated by the following equation (Bruland, 1998a):

$$k_{s-avg} = \sum_{i=1}^{n} k_{si} - (n-1) * 0.36$$

Where k_{si} is the fracturing factor for set of weakness number *i* and *n* is the number of fracturing sets.

By studying the actual performance of a TBM and the rock mass fracturing in the tunnel by geological back mapping, it has been found that the k_s as expected has a high influences on the penetration rate of the TBM (Macias et al., 2014). It is also found in this case that the k_s value has an influence on the applicable cutter thrust, as a lower thrust level was observed when the rock mass fracturing increased. This is believed to be an operational decision to avoid cutter and machine damages.

3.   The Stillwater Mine

This chapter will give a brief presentation of the site visited for the field study of the thesis. This includes a description of the Blitz Project at the Stillwater Mining Company, as well as the TBM used and the geology it is operating through.

3.1.   General

The Stillwater Mine is one out of two mines that the Stillwater Mining Company operates along the eastern portion of the J-M Reef in south-central Montana, USA (Stillwater Mining Company, n.d.). The reef is the world's richest known deposit of platinum group metals. The platinum group metals consist primarily of palladium, platinum, but there is also a small amount of rhodium to be found. The Stillwater Mining Company is the largest primary producer of platinum group metals in North America (Luxner, 2014).

3.2.   The Blitz Project

East of the existing Stillwater Mine, still along the J-M Reef, the Stillwater Mining Company also controls an area called the Blitz Area. The development of this area is referred to as the Blitz Project, and was started in 2010 (Luxner, 2014). The goal of this project is to provide additional ore reserves, and will possibly increase the total production of the Stillwater Mine. The company estimates that the full Blitz development will take about six year to complete. An overview of the project compared to the existing mine is shown in Figure 3.1.
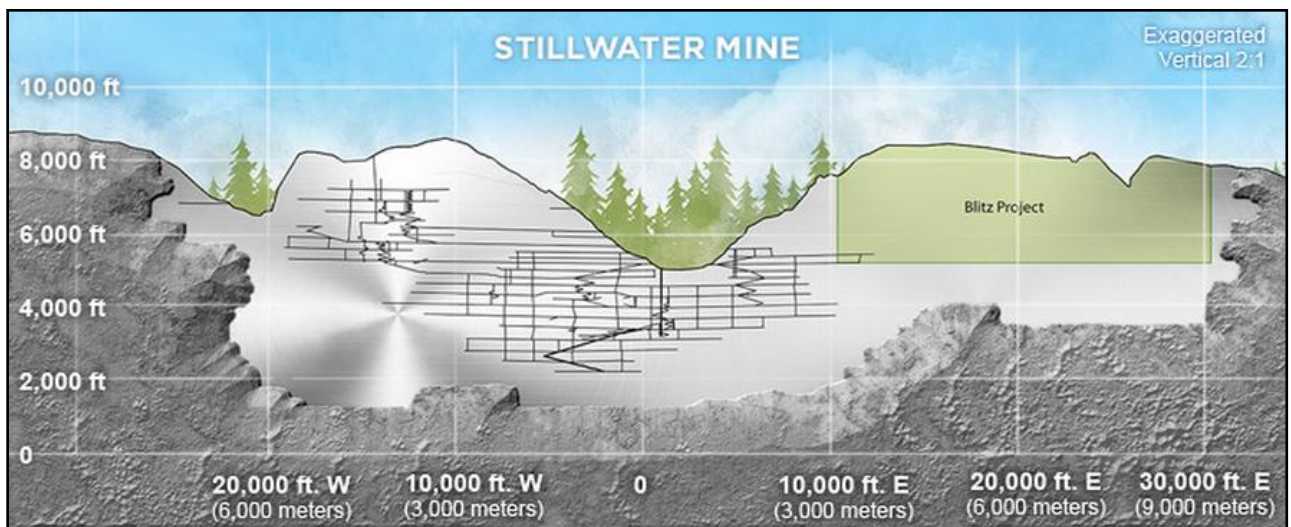

Figure 3.1: Details of The Stillwater Mine (Stillwater Mining Company, n.d.)

25

One of the main goals of the Blitz project is to advance a 6, 975 meter ventilation and haulage level. This level is being driven by the use of a TBM. The bored drive will also be used for ore body investigation.

3.3. The TBM

The manufacturer of the TBM is The Robbins Company, who has extensive experience in building TBMs. Especially their pioneer work within the hard rock TBMs and cutters is well known. They have produced over 200 open gripper machines (The Robbins Company, 2011).

The machine being utilized in the Blitz Project is a 5.5 meter diameter remanufactured open gripper type hard rock TBM. This gives a face area of approximately 24 m^2. Originally the machine was supposed to be fitted with two diamond drills. One to be used to probe in front of the TBM, and one to probe for ore body. Due to insufficient space the diamond drills were not installed on the machine, but are rather brought in and set in the "pit" below the bridge during probe stops. The probe drilling program for investigation is done approximately every 150 meters (Luxner, 2014). The TBM used in the Blitz project is shown in Figure 3.2.
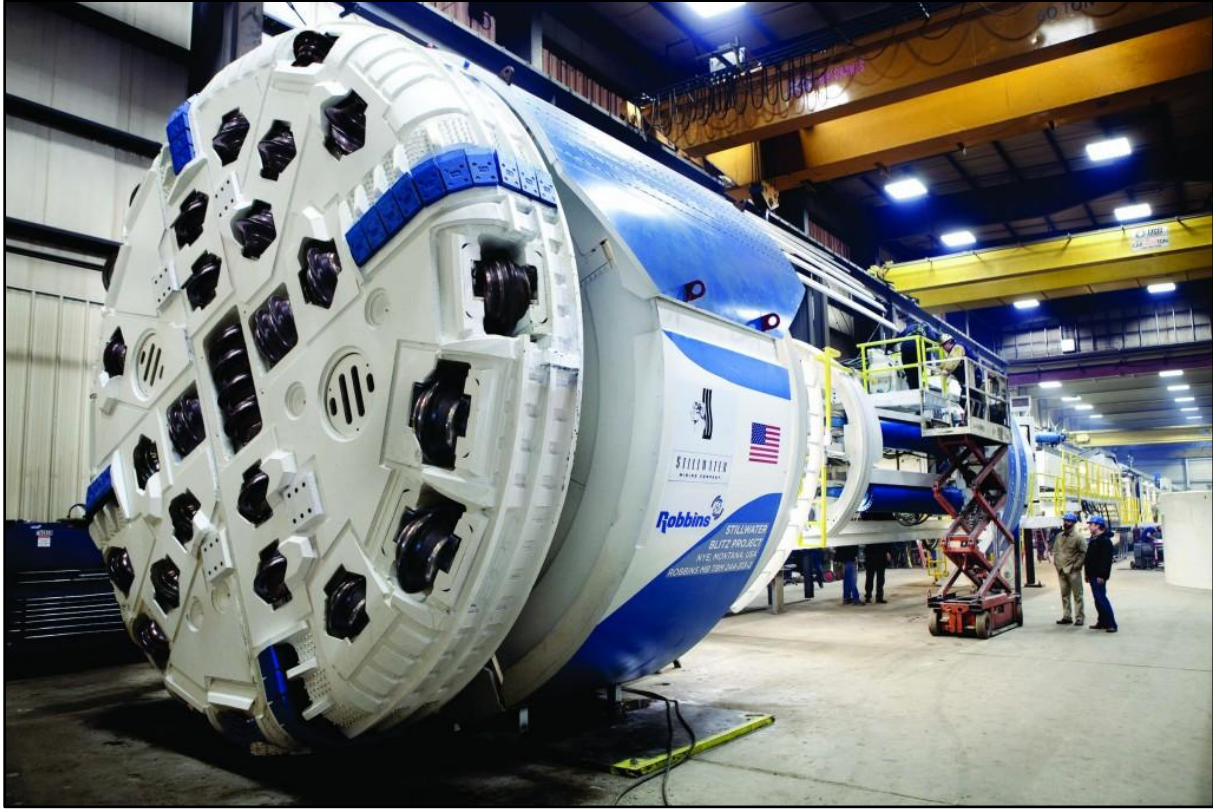

Figure 3.2: The TBM used in the Blitz Project (The Robbins Company, 2011)

The ground support the machine offers consists mainly of roof bolts, wire mesh slats and possible ring beams. Shotcrete or cable bolts are also be utilized when necessary. The main bolting pattern in the TBM is 0.9 x 0.9 meters of 1.5 meter Split Sets, and 1.8 x 1.8 meters of 2.4 meter Dywidags. A picture showing the tunnel profile with installed rock support can be seen in Figure 3.3. In addition to these measures the roof shield is modified to incorporate Robbins own "McNally" slat type support system, which focuses on containing fractured rock for better safety for the personnel working on the TBM (The Robbins Company, 2011). The area behind the TBM cutterhead can be seen in Figure 3.4.

A summary of some of the most important machine specifications is given in Table 3.1.The cutters of the TBM are back loading. The volume per stroke is approximately 73.5 m^3.

Machine diameter	5.5 meters
Cutters	483 mm (19 inches)
Number of disc cutters	33
Recommended individual cutter load	311 kN
Recommended operating cutterhead thrust	10 885 kN
Cutterhead power	6 x 330 kW = 1 980 kW
Cutterhead speed	Up to 10 RPM
Cutterhead torque	1 900 kNm at 10 RPM
Thrust cylinder stroke length	1.83 m
TBM weight	Approximately 360 tons

Table 3.1: TBM specifications (The Robbins Company, 2011)

3.4.   Geology

In general when using TBM one should strive to know as much as possible about the geology the machine will operate through. This is because TBMs are in general sensitive to unforeseen changes in the geology, as the machines are custom designed to handle specific geological conditions.

The Beartooth Montains, in which the Stillwater Complex is situated, contains some of the oldest rocks occurring on the North American continent (Stillwater Mining Company, 2011). The Stillwater Complex is an igneous saucer-shaped layered intrusion, which contains the PGM rich J-M Reef that is being mined.

The TBM part of the Blitz Project will be driven within layers of norite and gabbro-norite. The targeted rock types for the drive are plagioclase rich rocks, meaning more than 60 %. Layers of melano units can also be encountered at times. These melano units consist of more than 50 % dark minerals such as olivine, bronzite and augite.

The compressive strength of the rocks in the area range from the weakest olivine rocks at approximately 7 MPa to the hardest plagioclase rocks at about 140 MPa (Stillwater Mining Company, 2011). The norites encountered are typically between 70 and 85 MPa.

Several large transverse cross faults are expected to occur during the project (Luxner, 2014). These are often highly faulted with small angular block size. The faults will usually contain a core of clay rich fault gouge, at times as wide as 15 meters. The ground around the faults is also anticipated to be highly fractured. It is expected that gripping to push the machine through these clay rich zones will be a challenge, as the strength of the clay is no more than approximately 3.5 MPa.

The rock of the Stillwater Mine is an igneous rock with poor porosity (Stillwater Mining Company, 2011). Water will probably be found in open fractures associated with the faults, and it is anticipated that water bearing formations will be encountered, which will need to be grouted off before allowing the TBM to continue.

In summary the Stillwater Mining Company has a good understanding of the geology encountered during the Blitz project. However the probe drilling program is vital in order to add more detailed information about the conditions ahead of the TBM in the areas beyond exiting mine infrastructure.

Figure 3.3: Tunnel profile with installed rock support

Figure 3.4: Area behind the TBM cutterhead

4.   Research Methodology

The research methodology of the thesis is presented in this chapter. The selection of methods is based on similar research in the field of TBM tunnelling, and in particular the doctoral thesis of Professor Amund Bruland at the NTNU has been used as a guideline to perform the necessary work. The work can be divided into recording of TBM data, processing and calculation of this data, performing field testing and finally laboratory testing at the SINTEF Engineering Geology Laboratory in Trondheim. Additionally a small literature study of the rock breaking process has been performed.

4.1.   Literature Study

The theory behind this report, including TBM tunnelling and laboratory research, is investigated through a literature search and review of the topics in question. The topics of the rock breaking process and the different laboratory tests is based on the author's preliminary study of TBM tunnelling which was written during the fall of 2013. More work has however been put into also these chapters to update and specify the topics for the work of this thesis.

4.2.   Collecting and Processing TBM Performance Data

The collection of TBM performance data is based mainly on shift logs written by the TBM operator at the end of each shift, as there is no computer logger on the TBM in question. These shift logs have been digitalized into an Excel spreadsheet, which can be found as a digital appendix to this thesis.

Each shift log contains information regarding the following:

- Time and date of boring operations
- Machine hours at the start and end of each shift
- Averaged TBM data for selected strokes during a shift
    - Amperage [A]
    - Propel Pressure [psi]
    - Gripper Pressure [psi]
    - RPM of the cutterhead
- Distance bored each stroke
- Amount of rock support installed

As there was no systematically registered chainage at the start of each shift, the author has calculated cumulative values for chainage based on the distance bored in each shift. In some periods the shift logs have been noted by the crew without including the machine hours of the TBM. To obtain a value to be used in calculations, the machine hours was in these cases estimated based on meters bored and average boring time for the area where the machine hour values are missing. When controlling these calculated values with the next known value the maximum deviation is approximately 15 %.

Based on the input given in each shift log the following is calculated and used as parameters to assess the TBM performance:

- Boring time in machine hours
- Meters per shift
- Average amperage per shift
- Average torque per shift
- Gross average cutter thrust in kN/cutter
- Penetration rate in m/h
- Basic penetration in mm/cutterhead revolution
- Utilization of the machine in percentage boring time

To average torque is calculated based on the following equation given by Bruland (1998c):

$$T_B = \frac{U_B \cdot I_B \cdot \sqrt{3} \cdot (\cos\phi \cdot \eta) \cdot 60 \cdot n_m}{2 \cdot \pi \cdot 1000 \cdot RPM} \qquad \text{(kNm)}$$

U_B = applied operating voltage of the cutterhead drive motors (V)
I_B = applied amperage (A)
$\cos\phi\cdot\eta$ = efficiency of the motors at the given amperage, see Section 3.3
    (if unknown, $\cos\phi\cdot\eta = 0.8$ is a good approximation)
n_m = number of motors on the cutterhead
RPM = cutterhead revolutions (rev/min)

Figure 4.1: Equation to calculate torque (Bruland, 1998c)

The value of 0.8 is chosen for the efficiency of the motors. Applied operating voltage of the drive motors is 660 volts and the number of motors in the cutterhead is six.

Each shift at the Blitz Project at the Stillwater Mine has a duration of 11.5 hours. However, as this is not a conventional tunnelling project but a tunnel constructed at a mine, it was decided to calculate the utilization based on an available time in the tunnel each day of 10 hours. This gives a more correct picture of the utilization of the machine, as the crew spends time each morning conducting a safety meeting and traveling to the site of the TBM. This means less available excavation time compared to a civil tunnelling project where shifts change in the tunnel to give more time to excavate.

All averaged values are calculated as weighted averages with respect to the time used, in accordance with Bruland (1998c).

4.3.   Field Testing

One of the quantitative research methods for this thesis has been to conduct field testing at the TBM in the Blitz Project. The main focus of the field testing in this case has been to document the effect the RPM has on TBM performance and the rock breaking process. Some few net penetration tests has also been performed in order to assess the effect of thrust force as well. To give additional value to the tests performed, geological sampling in the form of rock chip collection has been done. All testing has been done following the procedures presented by Bruland (1998c). This kind of testing is simple to perform and can give valuable information as to how the TBM performs.

4.3.1. Net Penetration Test

The principle behind this test is to keep all other parameters in the TBM as fixed as possible while varying the thrust force. Typically one would want to measure five different levels in thrust, for example 70 - 80 - 90 - 100 - 110 % of what is considered to be normal thrust used in the TBM. Each level would normally be run for at least 3 minutes each while registering the following information from the TBM for each level:

- Cutterhead penetration
- Average cutterhead thrust
- Average amps and torque
- Penetration, thrust and torque of the previous and following strokes
- Register other relevant info like vibration levels and where in the stroke the test was performed

If possible one should manually check the penetration of the TBM by measuring on one of the thrust cylinders. In addition to registering this data, rock chips that have been broken off during each thrust level should be sampled. Usually 20-30 rock chips are picked, and then the 15-20 biggest of these are kept for analysis. When performing a net penetration test, one wants the TBM to operate in as similar geology as possible throughout the entire test.

In the field testing performed at the Blitz Project the amount of rock chips picked was for practical reasons limited to picking the 10-15 biggest rock chips. The reason for this was that due to safety regulations the rock chips could not be picked from the conveyor, but had to be picked off the muck cars on the train after each test level had been performed. Each thrust level was therefore performed within one single stroke each, as the same person had to gather TBM data and sample the rock chips. Usually this test should be performed by at least two individuals in addition to the TBM operator.

The TBM data collected is after testing processed and analyzed to assess if the TBM performance is in accordance with the theory presented in chapter 2.3 of this report.

4.3.2. RPM Trials

The principle of the RPM trials performed in the work of this thesis is very much similar to the net penetration tests. The difference is that within each level of thrust, the RPM is varied. This means that the thrust is varied as described for the net penetration test, but within each increment of thrust the RPM is also be varied to be for example 70 - 80 - 90 - 100 -110 % of what is considered normal RPM used in the TBM. An ideal RPM trial would therefore consist of 25 levels of testing, five different RPM levels within five different thrust levels.

The rock chip sampling during the RPM trials is performed in exactly the same way as presented for the net penetration test, where a complete sample is picked for each level of RPM tested. Some of the geological material sampled during the RPM trials was sent to the SINTEF Engineering Geology Laboratory in Trondheim to be tested for amongst other things drillability. This gives further information in order to understand what influences the TBM performance, and also the rock breaking process.

4.4. Geological Investigation

As a part of this kind of research, it is always of high value to compare the performance data of the TBM with geological back mapping (Bruland, 1998c). Due to safety regulations at the Stillwater Mine, a geological back mapping could unfortunately not be performed. Instead the geological information available from the probe drilling done in front of the TBM has been used to assess the geological conditions along the tunnel. Information about these core samples and how they are collected is presented in this part of the report, along with the treatment and calculations performed in order to assess the geological conditions.

4.4.1. Core Logging at the Stillwater Mine

As it is important for a mine like the Stillwater Mine to stay informed about the whereabouts of the ore body they are mining, they have an extensive core drilling program in place. This same program is also utilized when probe drilling in front of the TBM at the Blitz Project, except without looking for ore body minerals in the core samples. Each core drillings is logged, and information about the following is noted (Stillwater Mining Company, 2010):

- Date(s) of drilling
- Location of probe drilling in the form of a northing, an easting and an elevation relative to the mine grid used at the Stillwater Mine.
- A unique hole number selected sequentially as drill proposals are designed.
- The orientation of the drilling based on the mine grid
- Inclination of the drilling measured in degrees
- Core size
- Depth of drilling in feet

Based on the performed diamond drilling, the following geological and geotechnical information is logged, usually for each 3 meter of core:

Lithologies

The rock lithology is logged to the nearest 0.1 foot of core based on the mineralogical content. In the rock of the J-M Reef at the Stillwater Mine one will typically only see four different cumulate minerals; plagioclase, bronzite, augite and olivine. The typical rock type of the TBM drive is norite.

Angle between core and structures

The angle between the core sample and the most prominent structures of fracturing are noted when possible.

Recovery of core [%]

The length of the core between blocks divided by the interval length drilled.

Rock Quality Index (RQD) [%]

The length of core between blocks that exceeds 4 inches (10.16 cm) in length without a fault/fracture break divided by the interval length drilled. Fractures associated with "discing" are considered a fracture for RQD purposes.

Fracture count

The number of original open fractures (Healed fractures or breaks made by the drillers putting the core into the box does not count). Fractures associated with "discing" are considered a fracture. For a 3 meter (10 feet) sample the maximum fracture count noted is 50.

Joint sets (Jn)

The number of clearly identifiable joint sets are noted with the following classification:

- 0.5 - Massive (no fractures or faults)
- 2.0 - One set
- 3.0 - One set + Random
- 4.0 - Two sets
- 6.0 - Two sets + Random
- 9.0 - Three sets
- 12.0 - Three sets + Random
- 15.0 - Four sets + Random
- 20.0 - Crushed

For example when there is one dominant joint set with multiple fractures, and a single fracture from another set that would be classified as 3.0.

Joint roughness (Jr)

The most unfavorable joint set is classified by the following notation:

- 4.0 - Massive, no fractures
- 3.0 - Rough and wavy
- 2.0 - Smooth and wavy
- 1.5 - Rough and planar
- 1.0 - Smooth and planar, or filled
- 0.5 - Slickensided and planar

Joint alteration (Ja)

The joint alteration is classified by the following notation:

- 0.75 - Healed
- 1.0 - Stained (Surface can be scratched with a knife)
- 1.5 - Very slightly altered
- 2.0 - Slightly altered (Surface can be scratched with a fingernail, feel slippery)
- 3.0 - Coated
- 4.0 - Clay coated (Surface can be dented with a fingernail, feel slippery)
- 5.0 - Thick clay coated
- 6.0 - Stiff clay <5mm
- 7.0 - Soft clay <5mm
- 10.0 - Stiff clay >10mm
- 12.0 - Swelling clay >5mm
- 15.0 - Clay >5mm
- 18.0 - Soft clay >5mm
- 20.0 - Swelling clay >5mm

Fill

Fracture fill is broken down into three categories. If there is alteration just on the surface it should be included in the "no fill" category.

- 0 - No fill
- 1 - Serpentine, Chlorite and Talc
- 2 - Clay
- 3 - Carbonate and zeolite

Point Load Index (PLI)

A piece of core that best represent the interval is chosen to perform a point load test.

An example of parts of a core sample used for logging by the Stillwater Mining Company is shown in Figure 4.2, and an example of a diamond drill log used in the drilling of such a core is given in Appendix B.

Figure 4.2: Example of core sample taken at the Blitz Project

The usual procedure for logging is to log the presented geological and geotechnical information in intervals of 3 meters (10 feet), which is approximately the same amount as is shown in the example picture. Sampling intervals of less than 3 meters can also be utilized.

4.4.2. Correlation of Core Sampling Information to Tunnel Chainage

Based upon previous mining in the same area, the TBM was allowed to bore 372 meters before the probe drilling program was started (Luxner, 2014). The first probe stop was started the 27.03.2013. By the end of the field stay at the Blitz Project, the TBM had advanced a total of 1828 meters and had performed eight probe stops.

The geotechnical data from all of these eight probe stops as well as associated diamond drill logs was received by email the 07.04.2014 from the geology department at the Stillwater Mine. Geotechnical data was gathered in an Excel spreadsheet, which was further treated to compile necessary information to assess the geological conditions in the tunnel.

The entire Excel spreadsheet used in the work of assessing geological properties is given as an digital appendix to this thesis.

The first point of treatment of the core data was to correlate the information to a tunnel chainage. The cores are drilled in front of the tunnel at an angle of approximately 5 degrees relative to the tunnel axis, so that the information from the core is not directly representative to the geological conditions met in the tunnel drive. A simplified version of how the core drilling is situated related to both the tunnel axis and fracturing structures is shown in Figure 4.3. From which side of the tunnel the core drilling is performed varies from probe stop to probe stop.
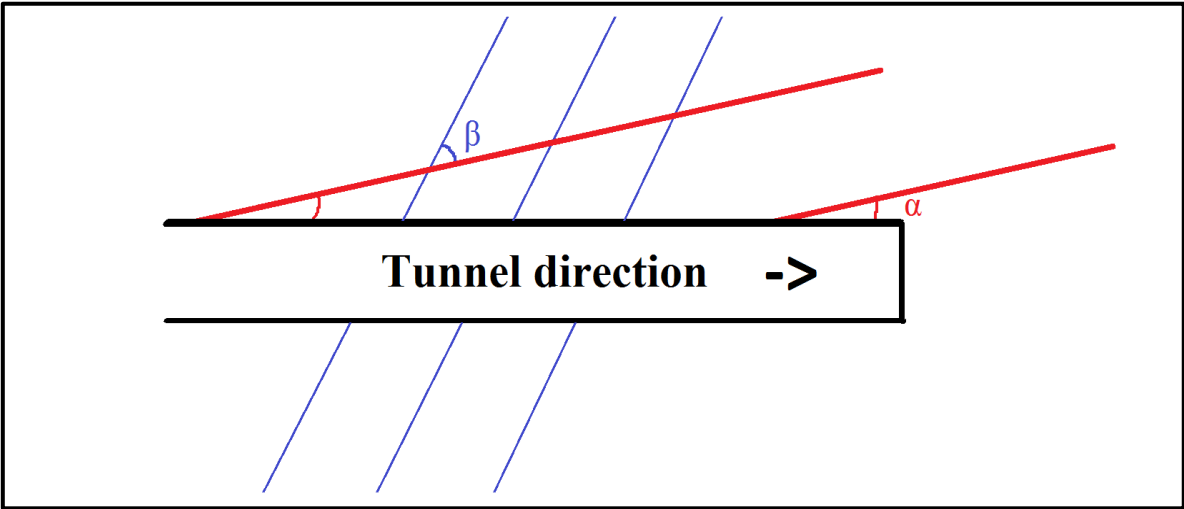
Figure 4.3: Simplified drawing of core samples in red and fracture structures in blue relative to the tunnel drive seen from above. The angle between the tunnel and core sample is exaggerated.

Assuming that the geological and geotechnical properties of the rock mass will follow the structures that the tunnel drives through, it is possible to correlate the properties of a certain point in the core sample to a point in the tunnel by using the law of Sines, as all the angles needed are given. The angle α is stated to be approximately 5 degrees for the straight ahead probes like these according to the geology department of the Stillwater Mine. The angle β between the core samples and the fracturing structure is given for various intervals in the diamond drill logs from each probe stop. This method of correlation will naturally be an approximation. When the angels are as shown in Figure 4.3 there will be an error caused by the fact that the properties of a length of core will represent a shorter length of tunnel chainage, and the opposite when the angle β is greater than a certain value. For the practical use in the model established in this thesis, this error is neglected.

An overview of the probe stops with drill hole numbers as given by the mining company as well as approximated tunnel chainage represented by each probe is shown in Table 4.1.

Probe stop	Diamond drill hole no.	Tunnel chainage represented [m]
1	36409	372 - 594
2	36894	594 - 818
3	37013	818 - 1025
4	37293	1025 - 1198
5	37412	1198 - 1344
6	37487	1344 - 1471
7	37591	1471 - 1695
8	37682	1695 - 1828

Table 4.1: Overview over probe stops used for the geological assessment

As can be seen in the table the different cores represent various lengths of tunnel, while normal geological investigation usually divides the tunnel into intervals of equal length, for example 20 meters. All of the cores had some amount of overlap with the following core sample. It was therefore decided to only include information from a core until the point where the next core started. This because the margin of error in the correlation between core sample and tunnel chainage will increase with the length of the core sample since the distance to the tunnel always increases. It would have been a possibility to compare the overlapping values of two core samples to see how well the approximation fits, but this was however not done.

4.4.3. Treatment of Compiled Geotechnical Data

The goal of treating the geotechnical data from the core samples was to get information of the geological conditions of the tunnel drive, which could then be used to assess the performance data calculated from the TBM through the collected shift logs. The main parameter that was assessed in this case was the Rock Mass Fracturing Factor (k_s), as described in chapter 2.3.3 of this report.

The calculation of the k_s was done with the help of two PhDs at the Department of Civil and Transport Engineering, namely Francisco Javier Macias and Yongbeom Seo. Based on work they had previously conducted at a TBM tunnel at the Faroe Islands, the k_s of the core samples was calculated in the same manner. The following preconditions and assumptions apply for the calculation performed.

Fracture sets

As a simplification only one fracture set was consequently used it the calculations. This was done due to the lack of more geological information from the core samples. In reality there were often more than one fracture set present, but no information regarding these additional sets makes it hard to estimate values for strike and dip.

Strike and dip of the fracture set

The strike of the fracture set was calculated based on the core orientation and the angle between the core and the fracture set. The dip of the sets was set to 70 degrees for the entire tunnel, based on consultation with geologists at the Stillwater Mine. This is highly simplified, but as the dip is not noted systematically during core sampling the geologist could only generalize based on the lithological structures in the geological area of the tunnel.

Average spacing between fractures

The average spacing between fractures was calculated as follows (Bruland, 1998b):

$$Average\ spacing = \frac{l_c * sin\ \beta}{n_f}$$

l_c = length of core section (m)

β = angle between core and fracture

n_f = number of fractures in the given core section

Fracture classes

Based on the calculated average spacing between fractures, each core interval was classified as shown in Table 4.2, which is a modified version of Table 2.3 shown in chapter 2.3.3 of this report. The classes was chosen in order to fit the graph used to calculate k_s, which was shown in Figure 2.12. In this calculations it was assumed that all fractures are fissures (St).

Fracture Class	Spacing Range (cm)
St 0	>180
St 1	30 - 180
St 2	17.5 - 30
St 2-3	12.5 - 17.5
St 3	8.75 - 12.5
St 3-4	6.25 - 8.75
St 4	0 - 6.25

Table 4.2: Fracture classes used in the calculation

Orientation of joints and calculation of k$_s$

The orientation of joints was calculated based on the tunnel orientation and the strike and dip of the fracture set in accordance with Bruland (1998d) and the equation given in chapter 2.3.3:

$$\alpha = \arcsin(\sin \alpha_f * \sin(\alpha_t - \alpha_s))$$

Where α_s is the strike angle, α_f the dip angle and α_t the tunnel direction. The tunnel direction was found from tunnel maps provided by the mining company. An example of such a map is given in Appendix C.

The k$_s$-value for each core interval was calculated based on the fracture class and the orientation of the fracture sets using Figure 2.12 shown in chapter 2.3.3 of this report. The formulas used in the Excel spreadsheet to perform the calculation for fracture class was borrowed from the work done by previously mentioned PhDs Javier Macias Rico and Yongbeom Seo. The k$_s$ was then averaged over each of the eight core samples using the equation presented earlier in this report:

$$k_{s-avg} = \frac{\sum_{i=1}^{n} l_i}{\sum_{i=1}^{n} \frac{l_i}{k_{s-i}}}$$

Where l_i is the tunnel length of fracturing class i of the section and k_{s-i} is the k$_s$ factor of fracturing class i of the section.

4.4.4. Correlation of Geological Data to TBM Performance

In order to correlate the calculated k$_s$-values to the TBM performance data gathered, it was decided to section performance data into tunnel lengths matching the eight probe stops. This means that the lengths compared vary from section to section, while a normal procedure like this would divide into intervals of 50 or even 20 meters in order to compare performance data with geological information.

Based on the tunnel intervals from the probe stops, data from the TBM performance was averaged into one value representative for the section. This averaging was as previously mentioned in the report done with respect to time used.

4.5.   Laboratory Testing

As a big part of the work in this thesis a comprehensive laboratory testing has been performed by the author of this thesis. This was done at the SINTEF Engineering Geology Laboratory in Trondheim, Norway. The different tests performed are presented in this part of the report.

4.5.1. Brittleness Value (S_{20})

The Brittleness Value test is used to determine rock brittleness. The test utilized by NTNU/SINTEF has been used its current version since the end of the 1950s to determine rock drillability (Dahl et al. 2011). The principle of the test is shown below in Figure 4.4, and a picture of the apparatus used is shown in Figure 4.5.
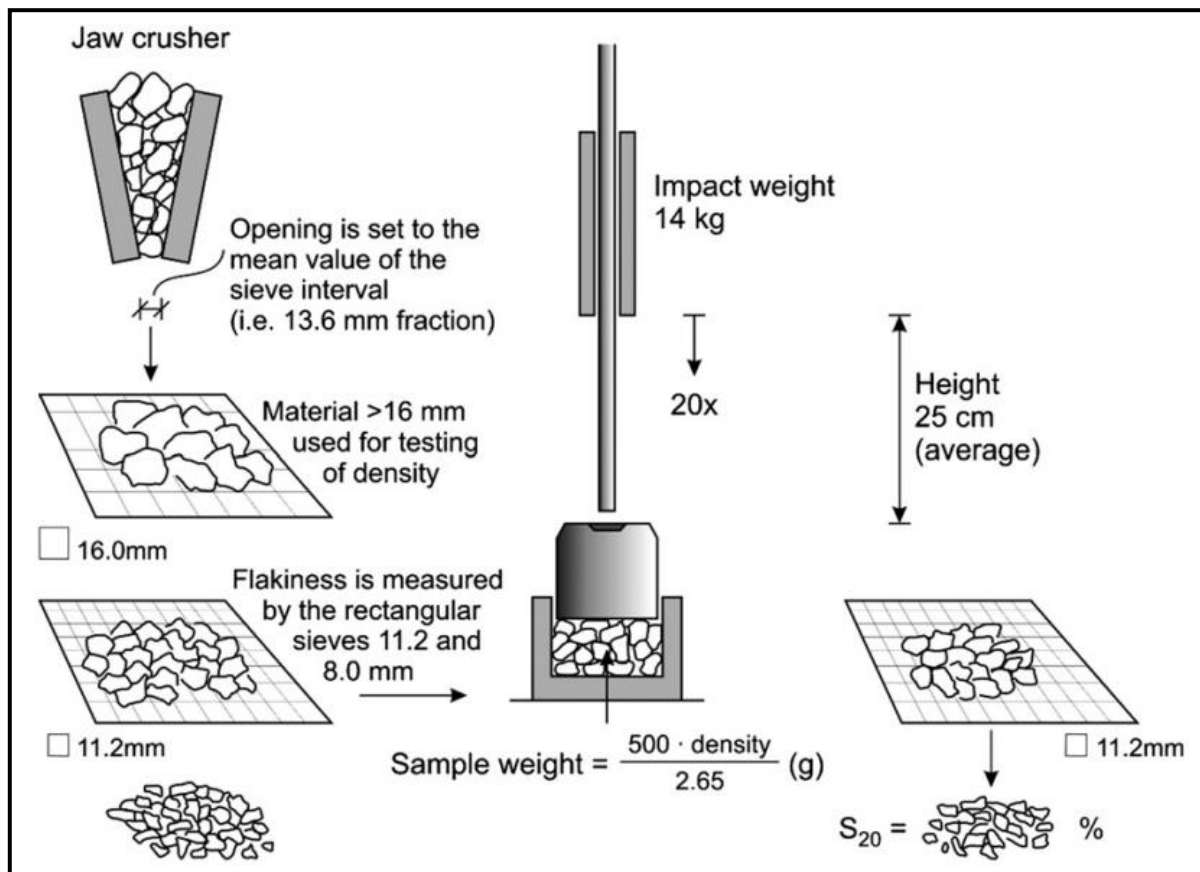
Figure 4.4: Outline of the brittleness value test (Dahl et al. 2011)

Figure 4.5: Picture of the brittleness test apparatus

The test measures the rocks ability to be crushed by repeated impacts from the impact weight, as can be seen in Figure 4.4. The rock sample is pre-sieved, and then undergoes 20 impacts in the apparatus. The targeted value of the test, the S_{20}, is defined as the percentage of the crushed material that passes through a 11.2 mm sieve after the impacts. Thus a high S_{20}-value implies that the rock has a high ability to be crushed and is therefore more brittle.

The test is normally performed on three extractions from one representative and homogenized sample of crushed and pre-sieved rock material, and the final S_{20}-value is the mean value of these three tests. To classify the brittleness test results, Table 4.3 is used (Dahl et al., 2011).

Category – brittleness	S_{20}-value (%)	Cumulative percentage (%)
Extremely high	$\geqslant 66.0$	95–100
Very high	60.0–65.9	85–95
High	51.0–59.9	65–85
Medium	41.0–50.9	35–65
Low	35.0–40.9	15–35
Very low	29.1–34.9	5–15
Extremely low	$\leqslant 29.0$	0–5

Table 4.3: Classification of the brittleness test results (Dahl et al., 2011)

According to Dahl et al. (2011) the S_{20}-value is influenced by factors like mineralogical composition, grain size, grain binding and to a great extent by the degree of weathering/alteration, micro fracturing and foliation.

4.5.2. Sievers' J-Value (SJ)

The Sievers' J-miniature drill test was developed in the 1950s, and gives a measurement of the rock surface hardness, or resistance to indentation (Dahl et al. 2011). In this test, a rock sample is drilled with an 8.5 mm miniature drill bit for 200 revolutions, as can be seen in Figure 4.6.
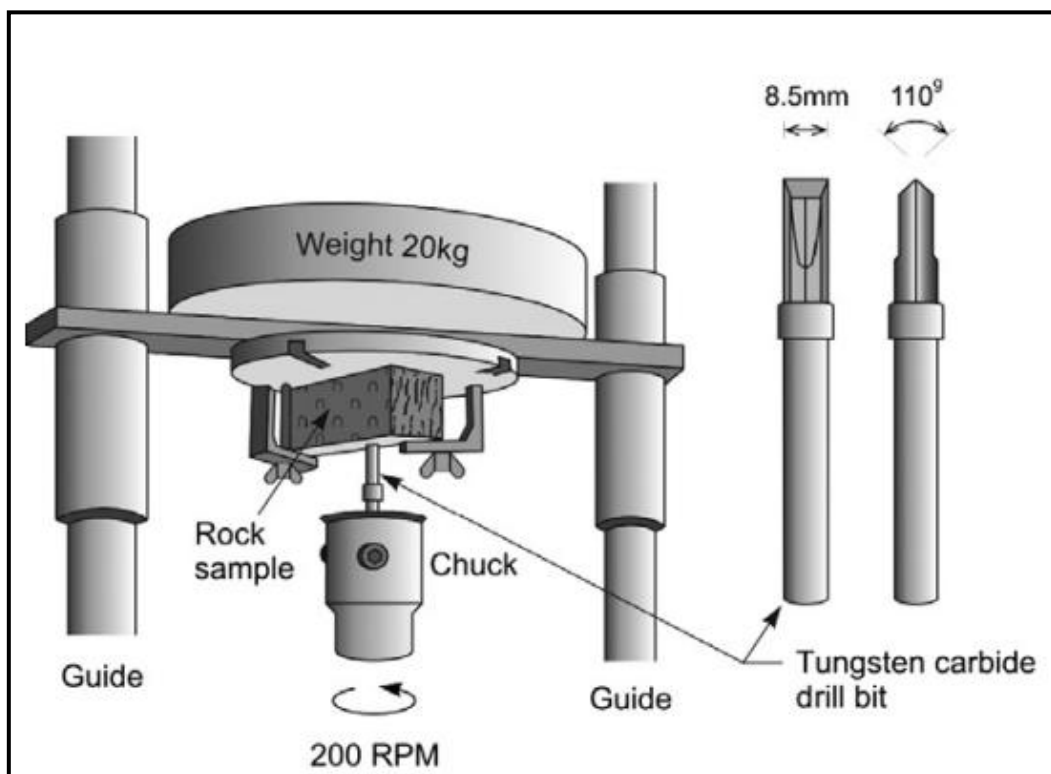
Figure 4.6: Outline of the Sievers' J-value miniature drill test (Dahl et al. 2011)

45

The SJ-value is then defined as the mean value of drillhole depths after this procedure for 4-8 drillings, given in 1/10 mm. The amount of drillings depends on the variations in the samples texture. If the values should vary by too much, more than 8 drillings may be necessary to achieve a representative mean value. The classification of the test results is shown in Table 4.4 as presented by Dahl et al. (2011).

Category – surface hardness	SJ value (mm/10)	Cumulative percentage (%)
Extremely high	$\leqslant 2.0$	0–5
Very high	2.1–3.9	5–15
High	4.0–6.9	15–35
Medium	7.0–18.9	35–65
Low	19.0–55.9	65–85
Very low	56.0–85.9	85–95
Extremely low	$\geqslant 86.0$	95–100

Table 4.4: Classification of the Sievers' J test results (Dahl et al., 2011)

According to Bruland (1998e) the pre-cut surface of the rock sample must be parallel or perpendicular to the foliation of the rock. The SJ value used in the Drilling Rate Index is the one found when measuring parallel to the foliation. Additionally if the SJ-value found drilling perpendicular to the foliation differs from the value found drilling parallel to the foliation, the Drilling Rate Index will likely vary with drilling direction with respect to the foliation.

The SJ-value is also influenced by the same factors as the S_{20}-values. However, the mineralogical composition shows a higher influence in the case of the SJ-value. A picture of the test apparatus is shown in Figure 4.7.

Figure 4.7: Picture of the Sievers' J test apparatus

4.5.3. Siever's J Interception Point (SJIP)

Based on the drillings performed in the SJ test one can analyze the penetration depth and speed during this testing. According to Dahl et al. (2007) one can generally divide the drilling into two separate parts, one "effective drilling" part and one "worn out drill bit" part.

The interception point of the tangent lines of these two separate parts is called the Sievers' J Interception Point, or SJIP. It has been shown that the value of this interception point can be used to obtain a direct cutter life estimate. The test expresses the "effective lifetime" of the sharpened edge on the drill bit, and the results have been found to correlate with other cutter life estimation tests, such as the Cutter Life Index and the Cerchar Index (Dahl et al., 2007).

The main advantages of the SJIP test are that it is based on a scaled drilling test and that it can be performed on a small but representative rock sample. The main rock properties that influence the results of this test are such as mineralogy, texture, grain shape, grain binding and grain size. In order to classify the test results in respect to cutter life, the following preliminary classification for SJIP "Steepest" given by Dahl et al. (2007) is used:

Category test values	Cumulative percentage	SJIP "Start"	SJIP "Steepest"
Extremely low	0–5	<2.0	<2.2
Very low	5–15	2.1–2.6	2.3–2.7
Low	15–35	2.7–3.8	2.8–3.6
Medium	35–65	3.9–10.2	3.7–8.1
High	65–85	10.3–18.5	8.2–14.3
Very high	85–95	18.6–27.0	14.4–20.6
Extremely high	95–100	>27.0	>20.6

Figure 4.8: Preliminary classification of SJIP values (Dahl et al., 2007)

4.5.4. Abrasion Value Cutter Steel (AVS)

The Abrasion Value Cutter Steel test gives a measure of the rock abrasion or ability to induce wear on a test piece of steel taken from a TBM cutter ring. This test is based on a test called Abrasion Value test (AV), which was developed in the early 1960s. This test measures the abrasion on a test piece made of tungsten carbide instead of cutter steel (Dahl et al. 2011).

The principle of the AVS test is shown in Figure 4.9. Note that the figure also shows the principle for the Soil Abrasion Test (SAT), which is the same procedure but measures the ability to induce wear from soil material instead of rock. A picture of the test apparatus is shown in Figure 4.10, while Figure 4.11 shows a test being performed.
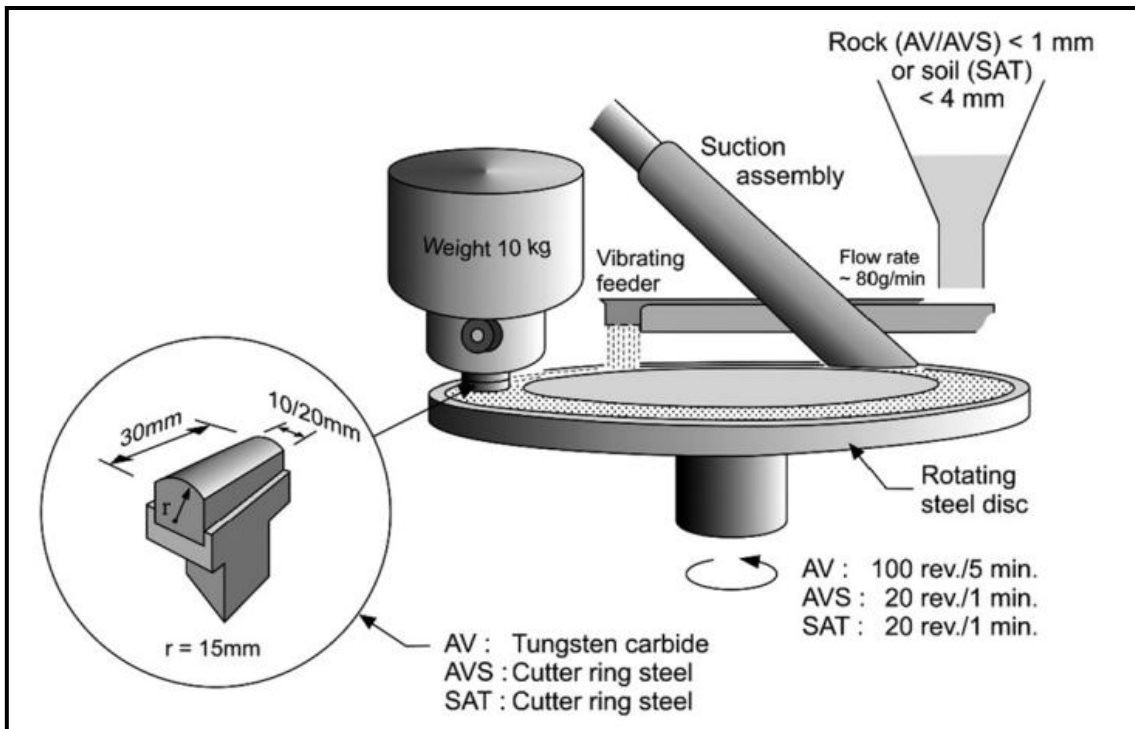
Figure 4.9: Outline of the Abrasion Value Cutter Steel test (Dahl et al. 2011)

Figure 4.10: Picture of the AVS test apparatus

Figure 4.11: AVS test being performed

The abrasion powder used in the AVS test in normally prepared by use of test material from the extractions used to find the S_{20}-value of the same material. The material will therefore be regarded as representative and homogenized sample material. The AVS-value is defined as the mean value of weight loss of the steel test piece in milligrams after one minute of testing for 2-4 test pieces. The variation between these 2-4 test pieces should not exceed 5 milligrams of weight loss if the test is performed correctly.

The classification of the test results is given in Table 4.5 (Dahl et al., 2011). For the AVS-value, Dahl et al. (2011) states that the mineralogical composition, grain shape, grain size and grain binding are the factors that influence the result the most.

Category – abrasion on cutter steel	AVS (mg)	Cumulative percentage (%)
Extremely high	$\geqslant 44.0$	95–100
Very high	36.0–44.0	85–95
High	26.0–35.9	65–85
Medium	13.0–25.9	35–65
Low	4.0–12.9	15–35
Very low	1.1–3.9	5–15
Extremely low	$\leqslant 1.0$	0–5

Table 4.5: Classification of the AVS test results (Dahl et al., 2011)

4.5.5. Sieve Curve

The sieve curve of TBM muck can give an indication of the efficiency of the rock breaking process. A muck sieve with higher percentage of large chips and rock fragments will indicate a more efficient rock breaking process.

Finding the sieve curves of the muck material is done according to the procedure described by Bruland (1998c). In this procedure, the sieves used are square and the recommended sizes of the sieve are 64, 45, 32, 16, 8, 4, 2, and 1 mm.

These sizes are only recommended to study the rock breaking and boring process, as standard sieve test will utilize smaller fractions down to 0.063 mm or less. In the work of this thesis the largest sieve of 64 mm is not utilized due to lack of equipment.

In this procedure a manual verification of the size of each chip is needed, as flat and elongated chips may not pass through the sieves because of their shape. These chips are therefore fitted through the sieve manually, as shown in Figure 4.12.
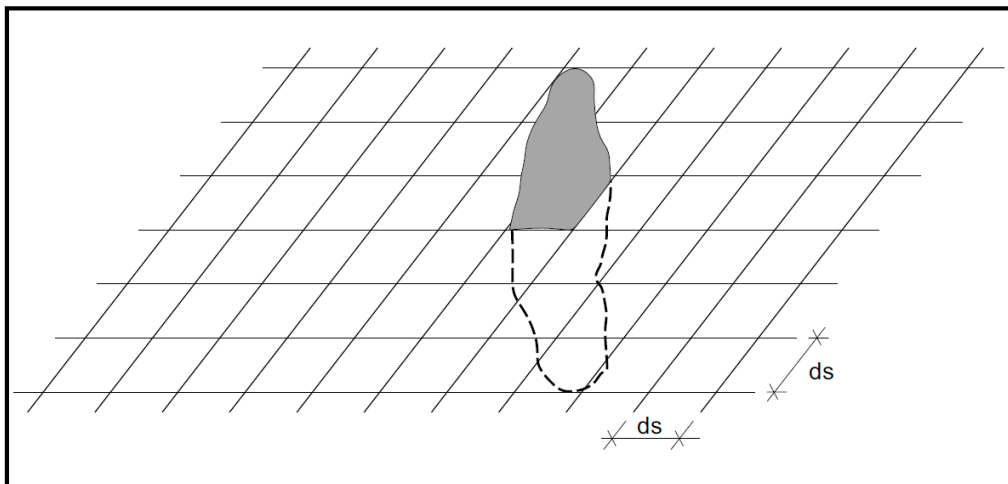
Figure 4.12: Manual sieving of TBM chips (Bruland, 1998c)

4.5.6. Cerchar Abrasivity Index (CAI)

The CAI is an index used for estimation of the cutter life and was first introduced by the Centre d'Etudes et Recherches des Charbonnages de France in 1971. This test may be performed on chips from the TBM boring process (Bruland, 1998b).

The test used for this index is a scratch test which utilizes a steel pin against the rock surface (Rostami et al., 2005). It is easy to perform and the rock sample needed is small. The CAI is mainly determined by the mineralogical composition of the rock (Suana and Peters, 1981).

To classify the test results the SINTEF Engineering Geology Laboratory uses Table 4.6, which is from the *ASTM Standard Test Method for Laboratory Determination of Abrasiveness of Rock Using the Cerchar Method* (Dahl, 2014). The performed tests utilize pins with Rockwell Hardness of 43, and the classification for HRC = 40 is used in this case. A picture of the test apparatus used is shown in Figure 4.13.

Category	CAI (HRC = 55)	CAI (HRC = 40)
Very low abrasiveness	0.30 - 0.50	0.32 - 0.66
Low abrasiveness	0.50 - 1.00	0.66 - 1.51
Medium abrasiveness	1.00 - 2.00	1.51 - 3.22
High abrasiveness	2.00 - 4.00	3.22 - 6.62
Extreme abrasiveness	4.00 - 6.00	6.62 - 10.03
Quartzitic	6.00 - 7.00	N/A

Table 4.6: Classification of Cerchar Abrasivity Index According to ASTM (Dahl, 2014)

Figure 4.13: Test Apparatus used for the Cerchar Abrasivity Index Testing

4.5.7. X-ray diffraction (XRD)

To determine the mineralogy of the rock samples used in the laboratory research, a X-ray diffraction (XRD) is performed at the SINTEF Engineering Geology lab in Trondheim. For this test a small rock sample is sufficient (Bruland, 1998c). The material needed is 40 grams, and is crushed down to fractions smaller than 20 micrometers.

4.5.8. Vickers Hardness Number Rock (VHNR)

After measuring the mineral content of the rock sample, one can combine the Vickers Hardness Number (VHN) of each mineral to one hardness number for the rock (VHNR) (Bruland, 1998e).

The Vickers Hardness Number Rock can be a measure for the abrasiveness of the rock, and is also a parameter in the NTNU model for estimating cutter life.

4.5.9. The Drillability Indices

Three of the tests explained above, the S_{20}, SJ and AVS, all give information about rock properties that are input for calculating the indices DRI and CLI. These indices are indirect measures for the drillability of rocks (Bruland, 1998e).

These indices have been developed at NTNU/SINTEF and combine various rock properties, as opposed to e.g. the UCS or CAI, which only represent one specific rock property (Dahl et al. 2011). DRI and CLI are registered trademarks of SINTEF and NTNU (Dahl et al. 2010).

Drilling Rate Index (DRI™)

Based on the values for S_{20} and SJ, the Drilling Rate Index may be calculated. According to Bruland (1998e) the DRI may be described as the Brittleness Value (S_{20}) corrected for the rocks surface hardness. A higher DRI indicates better drillability.

To find the value of the DRI, one should utilize the diagram showed in Figure 4.14. Note that if a rock material has a SJ-value of 10, the DRI equals the S_{20}-value.
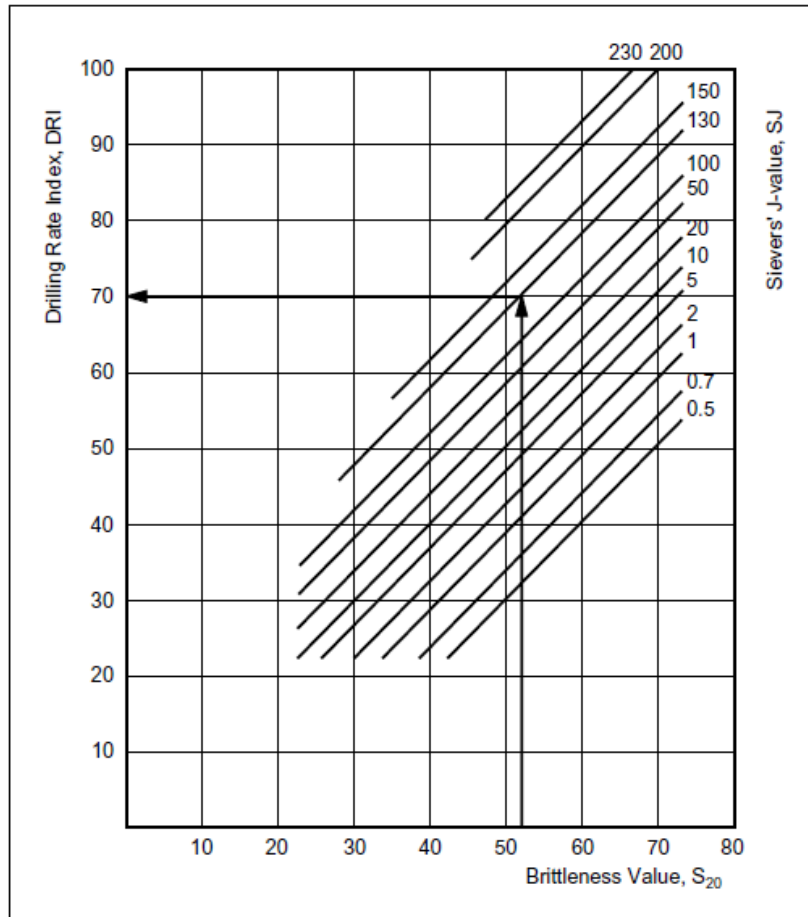
Figure 4.14: Diagram for used to find the DRI of a rock sample (Bruland, 1998e)

The Drilling Rate Index is used in the NTNU advance rate model (Bruland, 1998a). DRI has been found to be the most important rock drillability parameter used in the NTNU model, both for TBM and for conventional drill and blast tunneling (Zare and Bruland, 2012).

Cutter Life Index (CLI™)

Based on the values for SJ and AVS, one can calculate the CLI with the following equation (Bruland, 1998e):

$$CLI = 13.84 \times (\frac{SJ}{AVS})^{0.3847}$$

The calculated CLI expresses life in boring hours for cutter disc steel used in a TBM. The basis of the CLI is normalized field data for actual cutter life vs. tested rock parameters.

Table 4.7 shows a classification of the indices DRI and CLI, as suggested by Bruland (1998e). The table has been modified to exclude the Bit Wear Index (BWI), which has not been treated in this thesis.

Category	DRI	CLI
Extremely low	- 25	< 5
Very low	26 - 32	5.0 – 5.9
Low	**33 - 42**	**6.0 – 7.9**
Medium	**43 - 57**	**8.0 – 14.9**
High	**58 - 69**	**15.0 - 34**
Very high	70 - 82	35 - 74
Extremely high	82 -	≥ 75

Table 4.7: Recommended category intervals for the DRI and CLI (Bruland, 1998e)

4.5.10. Uniaxial Compressive Strength (UCS)

The uniaxial compressive strength of rock is widely used as a parameter in designing surface and underground structures (Bruland, 1998c; Kahraman, 2001). The procedure for measuring this rock strength has been standardized by both the American Society for Testing and Materials (ASTM) and the International Society for Rock Mechanics (ISRM). The test performed at the SINTEF Engineering Geology lab follow the ISRM standard (Dahl, 2013).

According to Dahl (2013) the material required to perform the UCS test is a block of the rock material in question of at least 200x200x300 mm in dimension to be able to obtain the 32 mm cores that will be used in the test.

4.5.11. Point Load Index (I_{s50})

As the collection of material needed for the UCS testing is time consuming and expensive, an alternative is to perform a test of the Point Load Index. This is an indirect test to predict the UCS and shear strength of rock, and can easily be used in field (Bruland, 1998c). The test was first standardized in 1972 by the ISMR. A more recent method can be found in ISMR (1985) which is followed in this thesis.

It has been found that the Point Load Index has a strong linear correlation with the compressive strength of several rock types (Kaharman, 2001).

The conversion factor between I_{s50} and the UCS value is chosen in accordance with the procedures at the SINTEF Engineering Geology Lab shown in Table 4.8 (Dahl, 2014).

Compressive Strength σ_c [MPa]	Point Load Index I_{s50} [MPa]	Factor k_{50}
25 – 50	1.8 – 3.5	14
50 – 100	3.5 – 6	16
100 – 200	6 – 10	20
> 200	> 10	25

Table 4.8: Conversion factor between Point Load Index and Compressive Strength (Dahl, 2014)

The test may be performed on both chips and core samples. In case of testing on pieces or lumps that are not circular, it will according to Brook (1985) be necessary to calculate an equivalent core diameter to be used in calculation of the Point Load Index. The principle of this is shown in Figure 4.15.
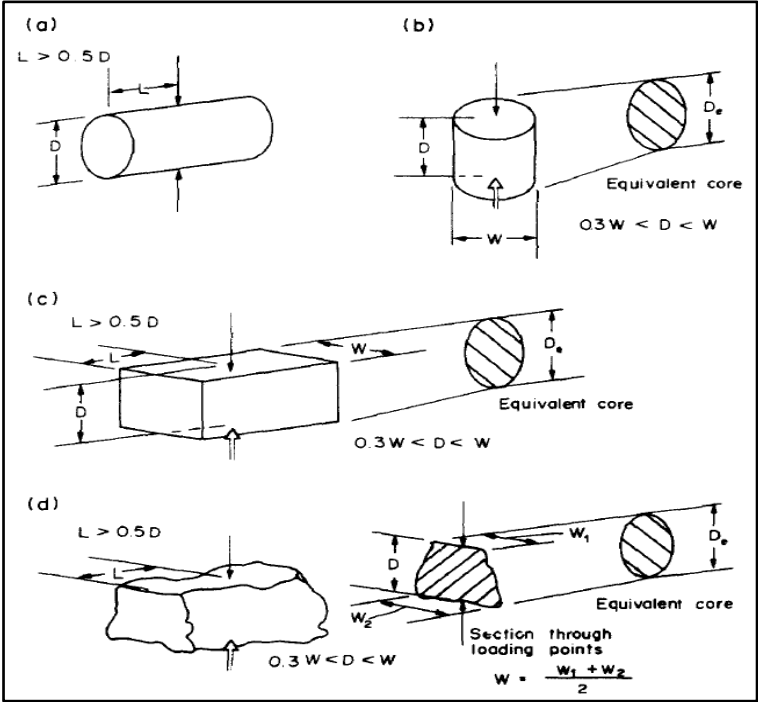
Figure 4.15: Types of specimens for Point Load Testing (Brook, 1985)

After testing is complete the samples may be classified based on the following classification from Bieniawski (1975) shown in Table 4.9.

Classification	Point Load Strength
Very low strength	< 1 MPa
Low strength	1 – 2 MPa
Medium strength	2 – 4 MPa
High strength	4 – 8 MPa
Very high strength	> 8 MPa

Table 4.9: Classification of Point Load Strength (Bieniawski, 1975)

4.6.   Communication

As a final method used in the work of the thesis to collect and treat data is various forms of communication. This includes personal conversations with key personnel at the Blitz Project, at the laboratory where the testing is performed and also the supervisors of this thesis. Correspondence via email is also utilized to communicate with the mentioned people.

The personal conversations with experienced crew of the TBM can be of high value in order to assess both the validity and the reliability of the empirical data collected during the different tests performed and through the shift logs.

In order to best understand the laboratory test results, an interview with Filip Dahl, the laboratory manager at the SINTEF Geological Engineering Laboratory is also performed (Dahl, 2014).

5.   Results

This chapter presents the data gathered during the field work at the Stillwater Mine and results of the related processing and calculations. The results of the laboratory testing are also presented. The duration of the field study was nine weeks in the time period between January 20th and March 21st of 2014, and the laboratory testing was performed in the time period between 23.04.2014 and 12.05.2014. Most test in the laboratory were performed by the author under supervision of SINTEF personnel.

5.1.   TBM Performance Data

The results in this subchapter are calculated from hand written shift logs from the TBM which have been digitalized in an Excel Spreadsheet. Based on information given by Luxner (2014), the shift logs starting from the 01.01.2014 has been used in these calculations, as this was the first month where the TBM was fully operational after assembly.

5.1.1. Monthly Advance Rate

The monthly advance rate of the TBM since it was fully assembled is shown in Figure 5.1. At the end of the field stay the TBM had an cumulative average of 137 meters per month.
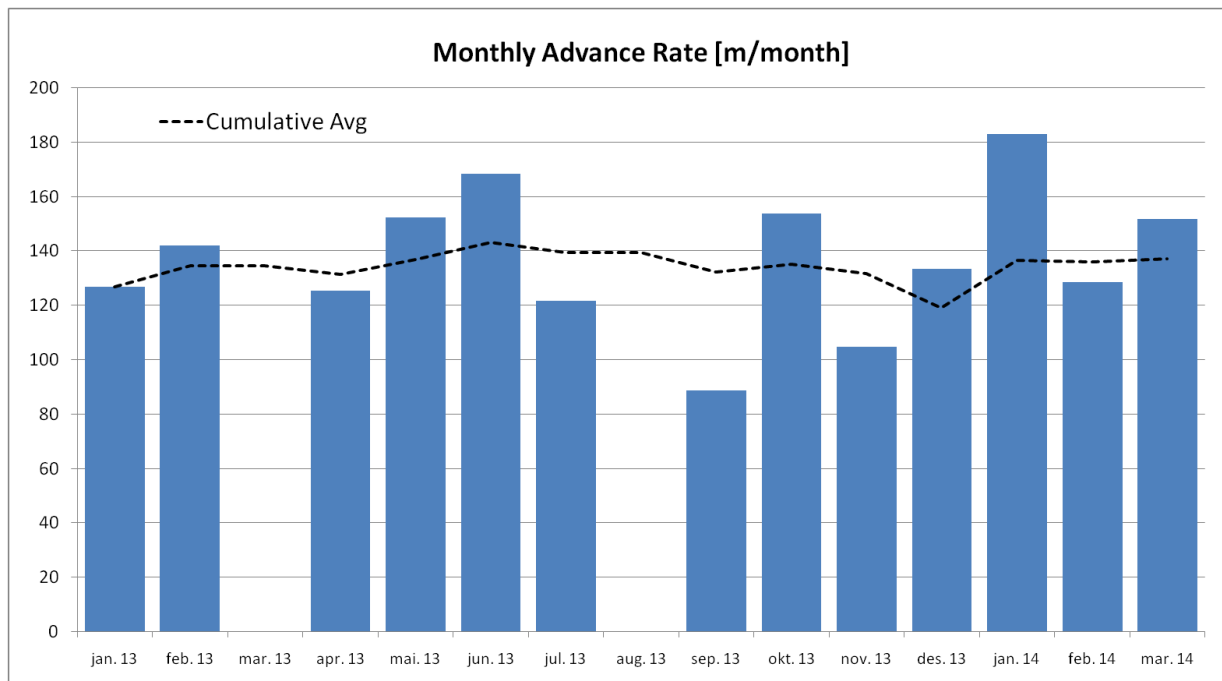
Figure 5.1: Monthly advance rate of the TBM

The monthly advance rates of the TBM are not very high, but this is also a tunnel being driven at a mine, which means it cannot be directly compared with similar civil construction projects. This tunnel is driven with one shift only, working Monday through Thursday at 11.5 hours per shift, from which approximately 10 hours is available excavation time. This gives an excavation time of 40 hours per week. This is also the reason why the advance rate is presented per month instead of per week as is more common, since the weekly advance rate would have been highly influenced by downtime in the TBM. The best month produced 183 meters, and the best day in the observed months was 20.12 meters.

5.1.2. Penetration Rate

The average monthly penetration rate in meters per machine hour of boring is presented in Figure 5.2. The cumulative average by the end of the data collection period was 4.8 meters per hour of boring time.
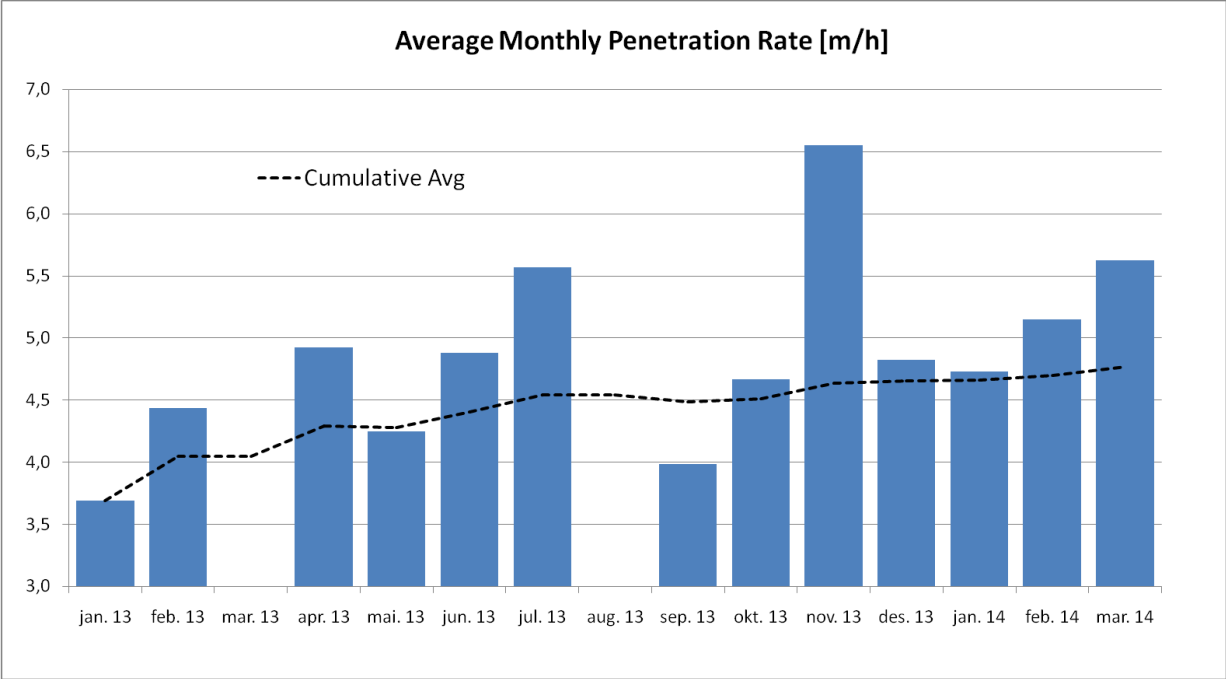
Figure 5.2: Average monthly penetration rate for the TBM

The cumulative average penetration rate is increasing for the first months of boring. This is to be expected, and probably follows the learning curve of the TBM crew. As time progresses the crew gets experienced and the cumulative average flattens out. At this time the geological conditions are probably the factor that influences the penetration rate the most. The highest average penetration rate for a month is found to be 6.6 meters per hour, which is quite high.

The month of November 2013 is observed to have the highest penetration rate, which is most likely due to favorably geological conditions with a high degree of fracturing. This is also most likely the case in the months of July 2013 and March of 2014. This will be further discussed in the results of the geological investigation performed which is presented in chapter 5.3 of this report.

5.1.3. Utilization

The average monthly utilization of the machine in percent boring time is shown in Figure 5.3. As described previously in the report, this utilization is based on an available excavation time of 10 hours per shift for the crew.
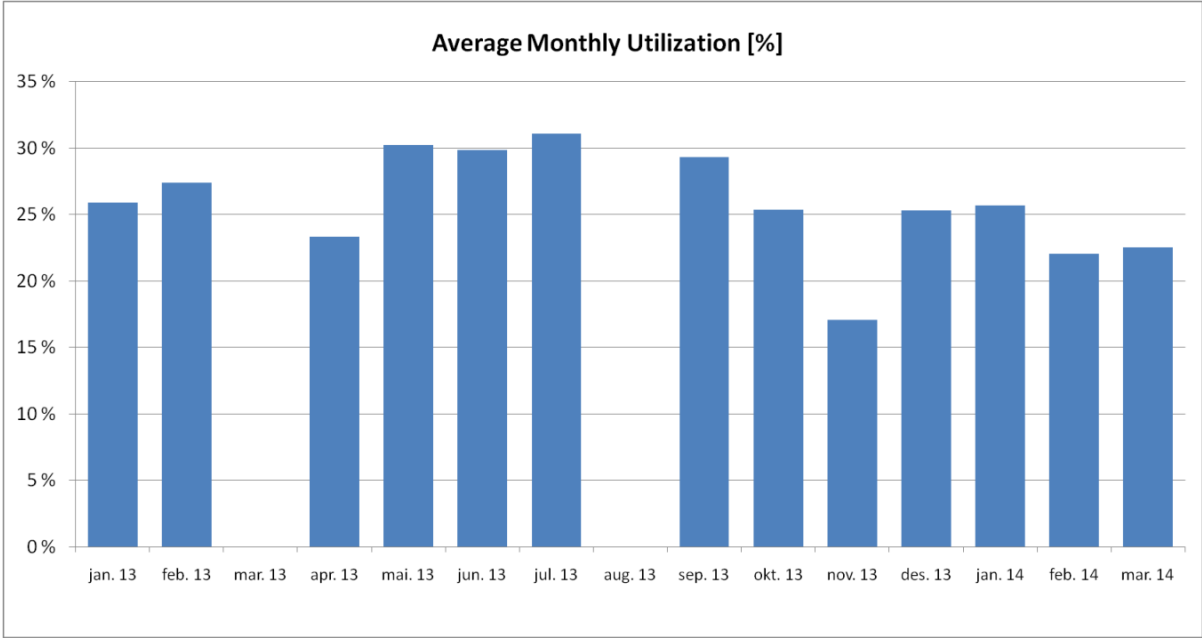
Figure 5.3: Average monthly utilization for the TBM

The best month of the period observed had an utilization of 31 %, and the worst month 17 %. The total average utilization of the machine is over all the months calculated to 26 %. This is not a very high value, but one must consider that this is not a civil tunneling project where time and utilization is the main focus. The utilization could be dependent on geological factors, as when penetration rate is high and more strokes are made during a day more time is also used for waiting on the train to return to the TBM for further excavation to start or waiting for rock support to be installed. This can be seen especially in the month of November, which has the lowest utilization but also the highest average penetration rate.

5.1.4. Gross Average Thrust per Cutter

In Figure 5.4 the gross average cutter for each month is shown. The highest averaged value is 327 kN/cutter and the lowest is 213 kN/cutter. One can observe the same trend for this graph as was seen in Figure 5.3 for the utilization of the machine. This could be explained by the same argument, that the machine utilization is dependent on the penetration rate, and the penetration rate is expected to be highly influenced by the gross cutter thrust.
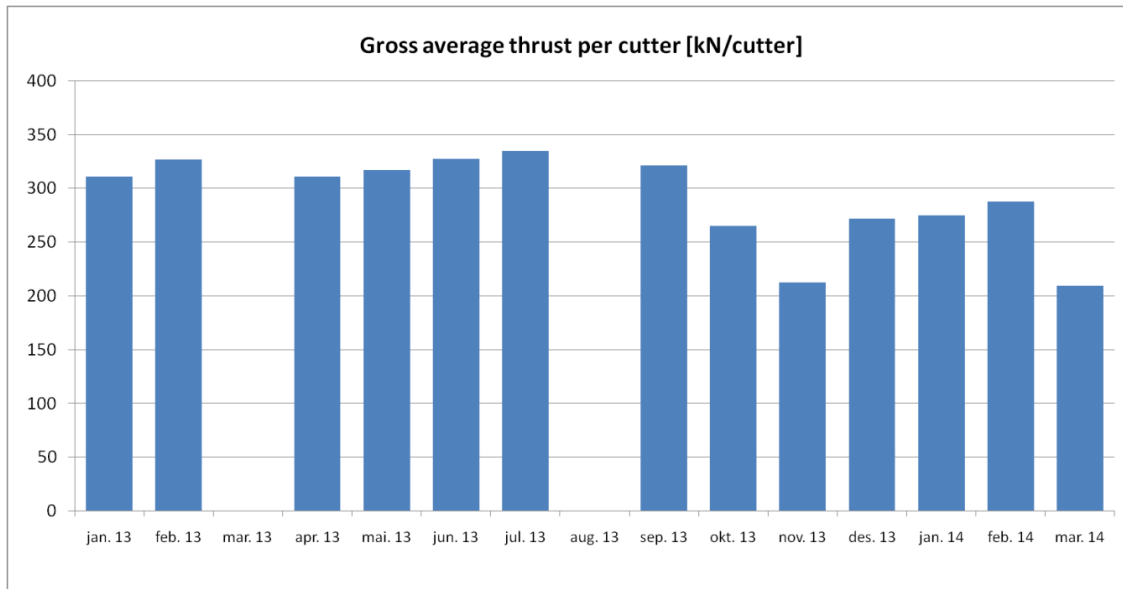
Figure 5.4: Gross average thrust per cutter

The highest observed cutter thrust in the period was 349 kN/cutter. As is the procedure in the NTNU model, no correction has been made for drag or friction in the TBM. However, the cutter thrust values would have been lower if adjusted for the weight of the backup system that is towed during boring. Considering this and the fact that losses from drag and friction usually makes up approximately 10 % or less of the gross thrust, the value of the gross cutter thrust would have been within the recommended maximum loads for the cutters.

It can be observed that there is not a as good correlation between gross cutter thrust and penetration rate (m/h) as would be expected. This can be caused by several factors, but probably mostly by the following: The values of propel pressure that is noted by the TBM operator is not an correct average over the full shift, but more a value that best represent the time when the operator decided to note it down. The penetration rate is highly dependent on the rock mass fracturing, as high fracturing gives a high penetration according to the NTNU model. When the fracturing is very high, it could be difficult to apply more than a certain amount of thrust without causing damage to the machine and the cutters.

62

5.1.5. Average Amps and Torque

The recorded average amps for each month is shown in Figure 5.5. The highest value in this chart is 281 A while the lowest is 186 A. The highest value of amperage that was noted by the TBM operator during the months in this period was 318 A.
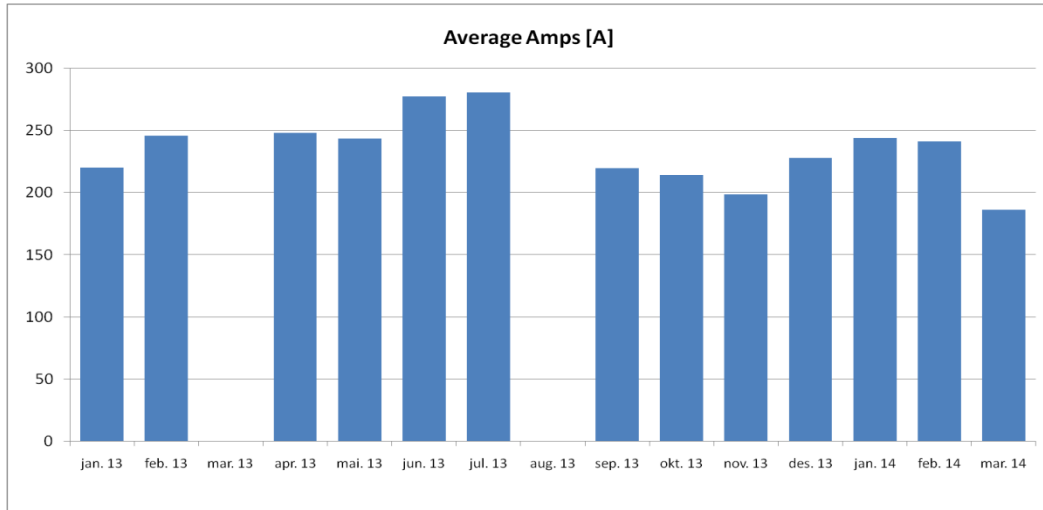

Figure 5.5: Average amps for the TBM

Based on the average amps shown above, the average torque per months was also calculated based on the procedure given in chapter 4.2 of this report. The results of this are shown in Figure 5.6. The highest value in this chart is 1822 kNm and the lowest 1537 kNm. The highest value of torque observed in the period calculated from amps was 2405 kNm.
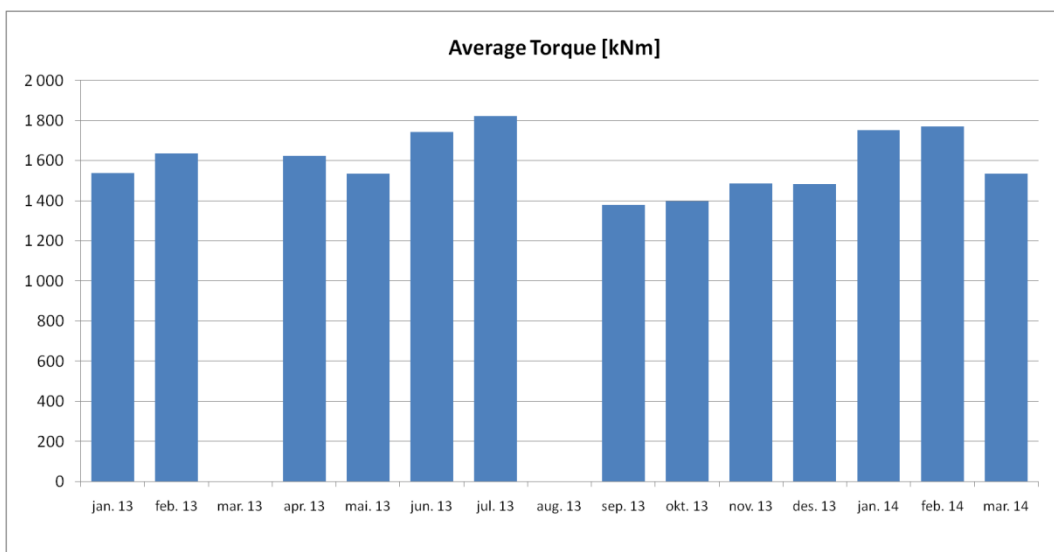
Figure 5.6: Average torque for the TBM

5.1.6. RPM versus Basic Penetration Rate

As parts of the field testing that was performed at the Blitz Project was about assessing the RPMs influence on basic penetration rate (mm/rev), it is also of interest to look at data from the daily shift logs from the TBM regarding RPM and basic net penetration achieved.

In Figure 5.7 the collected data from the shift logs with respect to basic penetration rate and RPM is shown. Each data point represents the averaged value from each shift noted. One can easily see that the most utilized RPM on the TBM has been 10.
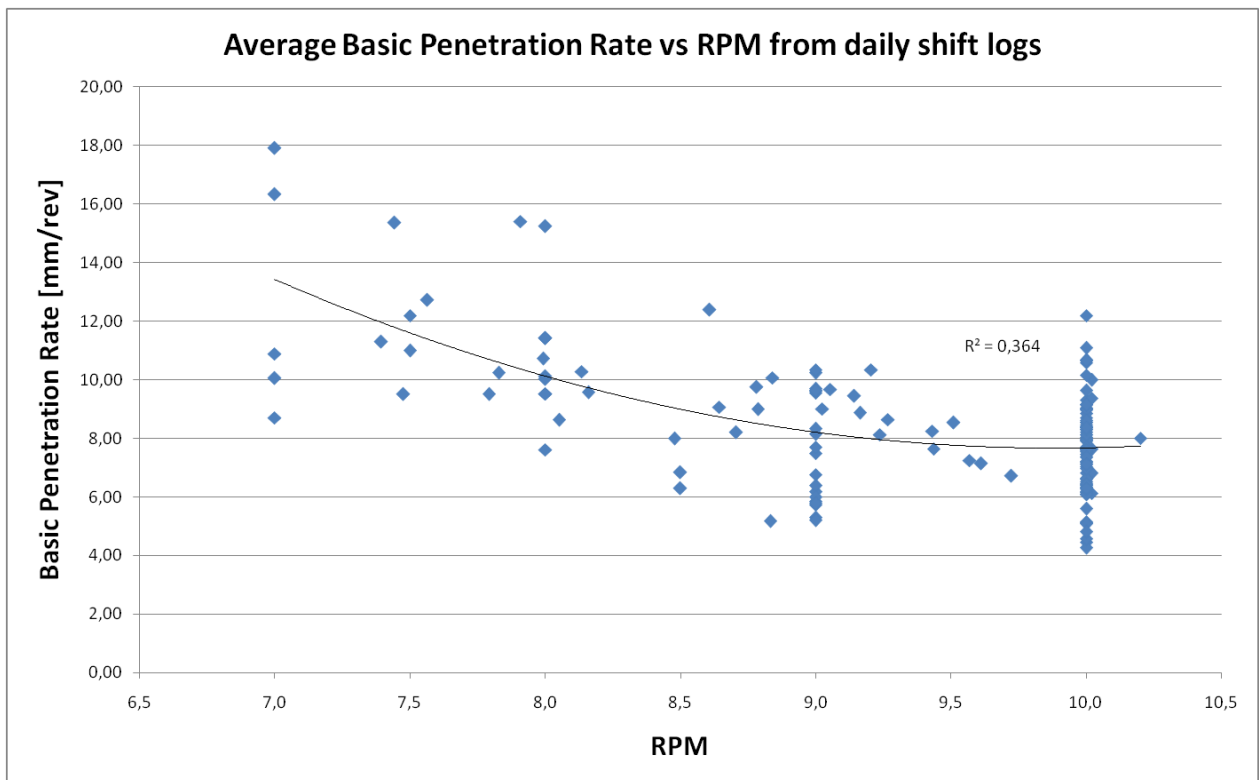
Figure 5.7: Basic penetration rate versus RPM from daily shift logs

From the figure it is possible to observe a trend for the data, namely that lower RPM gives a higher penetration per cutterhead revolution. The reason for this could be how the rock breaks when RPM is lowered. But perhaps more important is the fact that when the TBMs advance is limited by for example the muck removal capacity of the TBM conveyor or that the rock mass fracturing is so high that advance must be slowed down to not damage the machine or cutters, it matters less which RPM is utilized. If the advance rate is limited by something unrelated to RPM a lower RPM will naturally give a higher penetration per revolution in any case.

5.2.   Field Testing

In this part of the report the results from the field testing done at the Blitz Project is presented. This includes results from penetration tests and RPM trials with geological sampling, as well as some RPM trials done without geological sampling. The main goal of this field testing was to assess the influence of RPM on the basic penetration rate of the TBM given in millimeters per cutterhead revolution. The Excel spreadsheets used to treat the test data are given as digital appendices to this thesis.

5.2.1. Penetration Tests

In the beginning of the field work a couple of penetration tests were performed according to the procedure presented in Bruland (1998c). This was done to verify that the rock breaking process in the TBM was as expected before starting the RPM trials.

The TBM studied in this field work had no automatic computer logger. This means that data for thrust force, penetration rate, amps and torque had to be manually logged. Because a sensor in the TBM conveyor was broke, the operator had to focus on watching the belt to prevent an overload and thereby clogging up the cutter head, and could therefore not be used as help in performing the penetration tests. All data logging and chip sampling was therefore performed solely by the author of this report. This is less than ideal according to the procedures presented by Bruland.

As chips had to be collected in the back of the TBM from the muck carts, the amount of chips collected in both the penetration tests and the RPM trials was for practical reasons reduced from 20-25 to 10-15 per test. This also made it difficult to perform more than one increment in thrust force per stroke length. This means that each level of cutter thrust force in the penetration tests and each level of RPM in the RPM trails are done within separate strokes of 1,8 meters. The tests was been tried executed in the middle of each stroke. Each test was performed with a duration of 5 minutes. Before starting the testing, the machine's penetration rate according to the onboard computer was controlled on one of the thrust cylinders, and was found to be accurate.

All data and calculations behind the results of the penetration tests and the RPM trials are given as a digital appendices to this thesis.

Penetration Test 1

This penetration test was performed the 04.02.2013 and 06.02.2013. The normalized penetration curve can be seen in Figure 5.8. Information regarding chip sizes and shape can be seen in Figure 5.9-Figure 5.12 and a picture of the rock chips gathered can be seen in Figure 5.13. Note that the presented charts in this report have the Norwegian notation for decimals, where "," is used instead of ".".
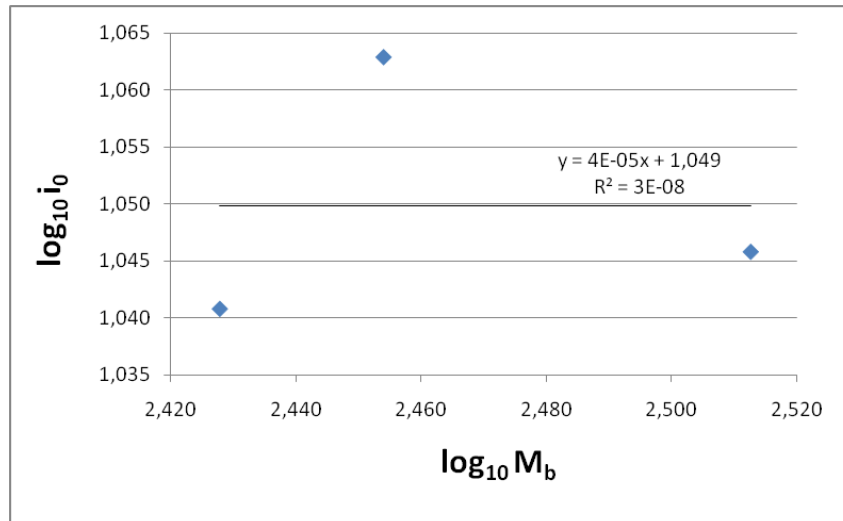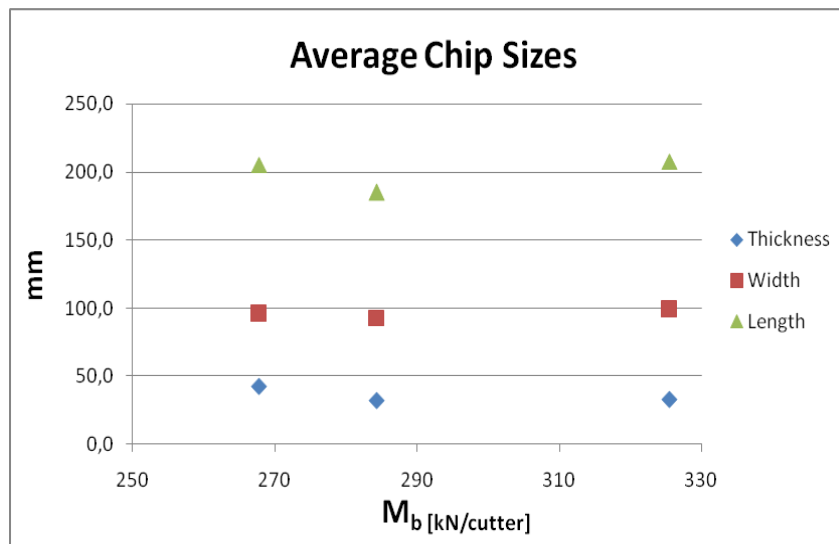

Figure 5.8: Logarithmic values for i_o and M_b for penetration test 1

Figure 5.9: Average chip sizes for penetration test 1
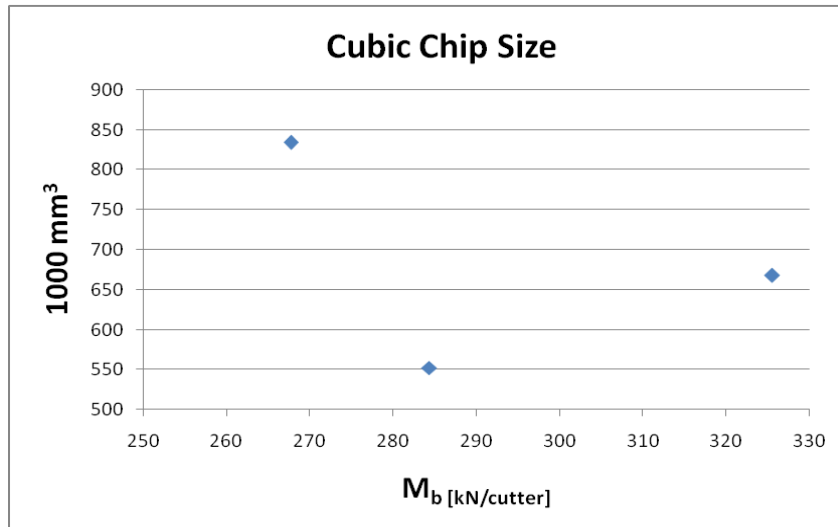
Figure 5.10: Cubic chip sizes for penetration test 1
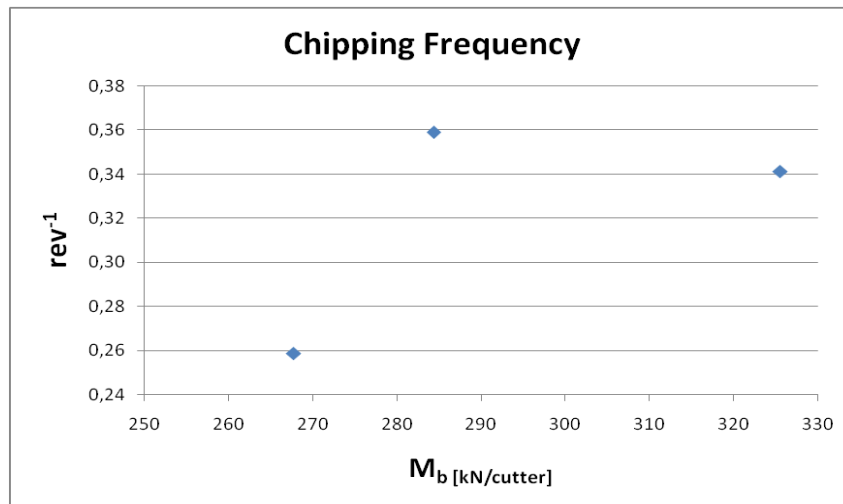
Figure 5.11: Chipping frequency for penetration test 1
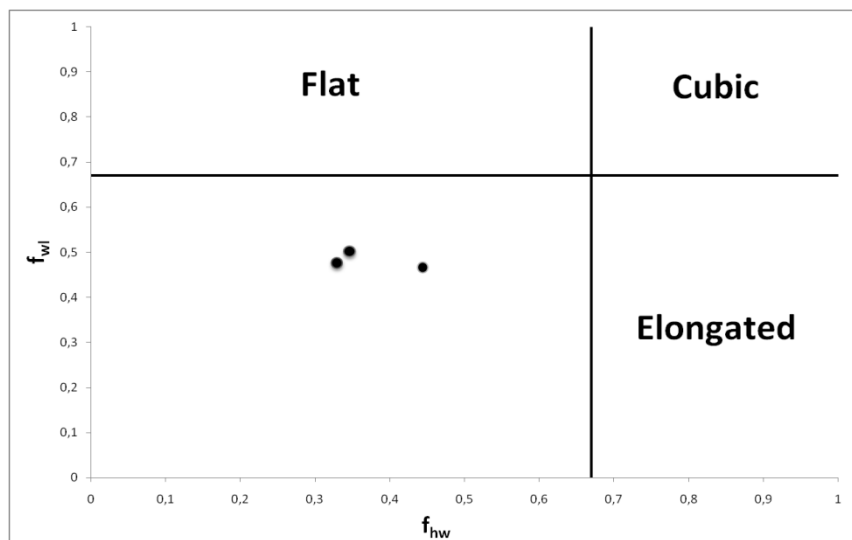
Figure 5.12: Chip shapes of the average chip sizes of penetration test 1

67

Figure 5.13: Rock chips picked during penetration test 1. Thrust levels from top row to bottom: 3100 PSI (325 kN/c), 2550 PSI (268 kN/c), 2700 PSI (284 kN/c). The mean thickness of the bottom row was 32.2 millimeters.

The penetration curve is not as expected according to Bruland (1998c). This can be explained by the fact that during the second level of thrust, the machine encountered a highly fractured and blocky geological section. In the final thrust level the rock mass got less fractured again. However the final stroke was stopped after the test was completed, as the rock mass encountered in the second thrust level had to be extensively bolted before further progress.

As can be seen in Figure 5.13 not all of the chips picked has the expected chip shape. As this was the first test of the field study, rock chip sampling was not performed very well. Rock samples were picked regardless of shape and size, and some of the samples are probably not from face cutters, but also from the gauge cutters and center cutters. Considering the nature of this first test, it is hard to say much about how chipping efficiency was when assessing the chip sizes and shapes. The average standard deviation for the chip sizes was 19 % for the length, 18 % for the width and 28 % for the thickness.

Penetration Test 2

The second penetration test was performed on the 11.02.2013. The normalized penetration curve can be seen in Figure 5.14. Information regarding chip sizes and shapes can be seen in the Figure 5.15-Figure 5.18 and picture of the chips gathered is shown in Figure 5.19.
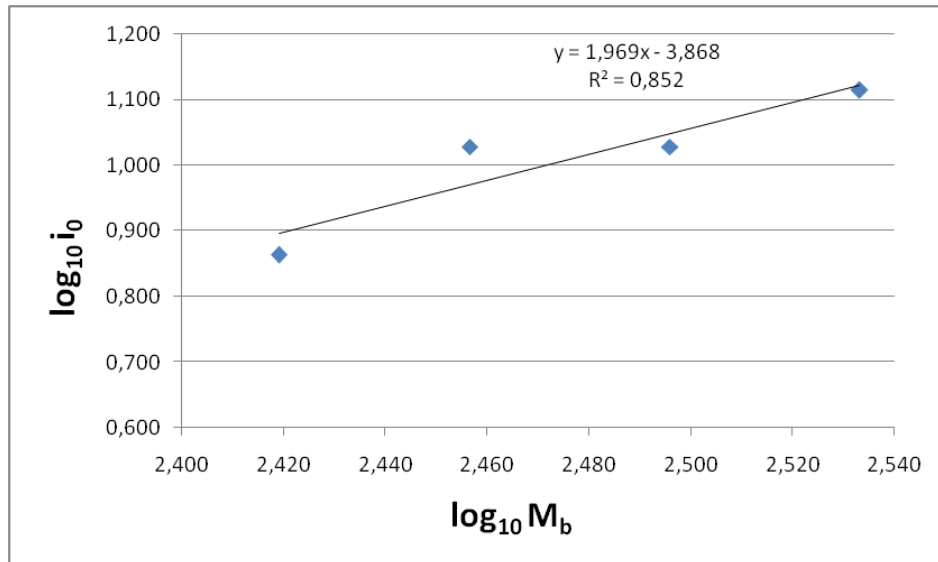

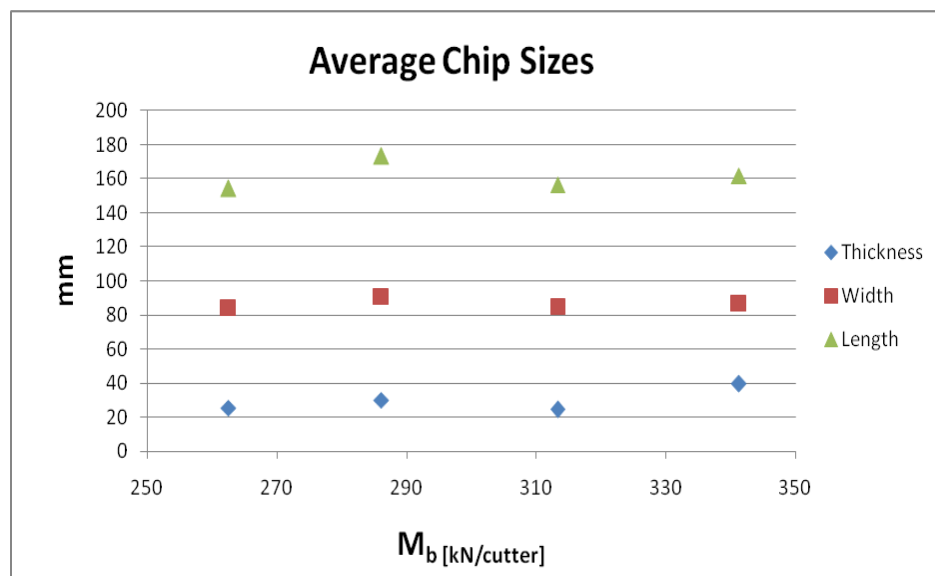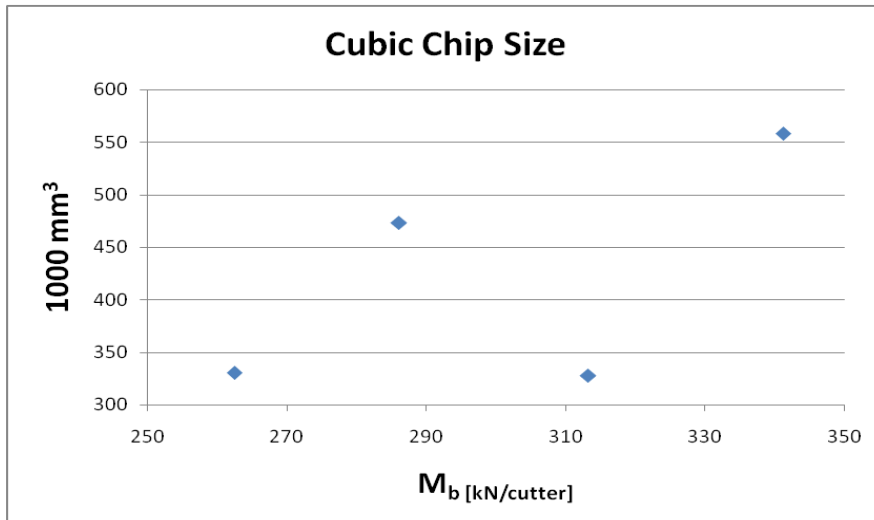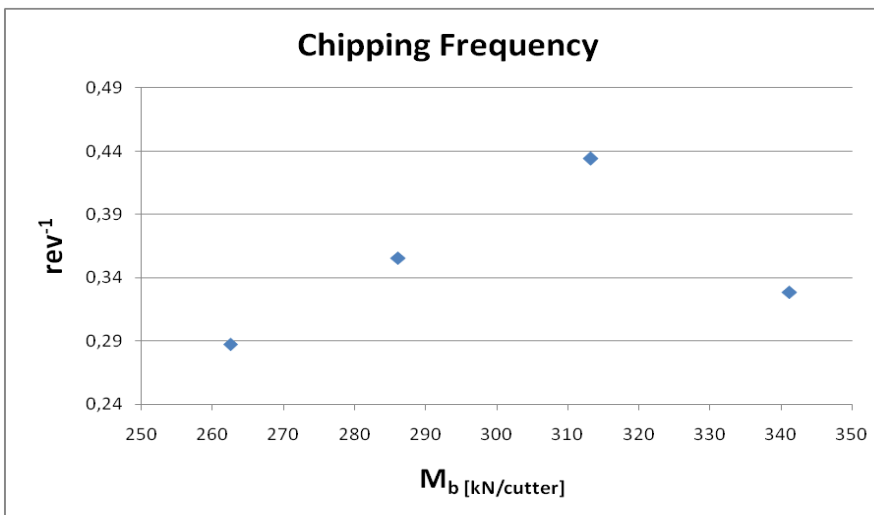Figure 5.14: Logarithmic values for i_o and M_b for penetration test 2

Figure 5.15: Average chip sizes for penetration test 2

Figure 5.16: Cubic chip sizes for penetration test 2

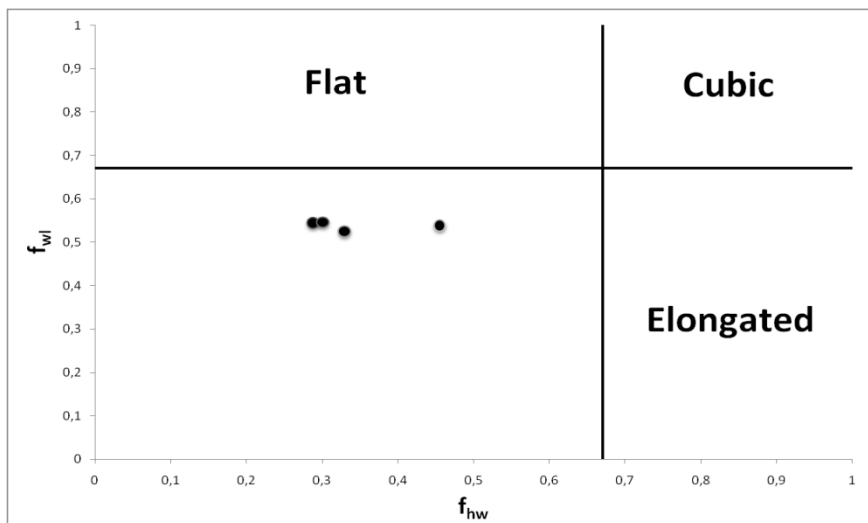Figure 5.17: Chipping frequency for penetration test 2

Figure 5.18: Chip shapes of the average chip sizes of penetration test 2

Figure 5.19: Rock chips picked during penetration test 2. Thrust level from top row to bottom: 3000 PSI (313 kN/C), 2750 PSI (286 kN/c), 2500 PSI (263 kN/c), 3250 PSI (341 kN/c). The mean thickness of the bottom row was 39.6 millimeters.

The rock mass stayed fairly consistent during this test, and no unforeseen stops occurred in the time period of the four strokes in which testing took place. The strokes before and after the test were also observed, and the same conditions prevailed also for these.

This penetration test is more in accordance with Bruland (1998), where a linear relationship between the logarithmic values of basic penetration and the cutter load is expected. This shows that the basic penetration will increase exponentially with increasing cutter load.

When considering the penetration curve presented in Figure 2.10 in chapter 2.3 of this report, the logarithmic values of the basic penetration and the cutter thrust from this test gives us the following information based on the calculations presented by Bruland (1998c):

- Critical thrust to achieve a penetration of 1 mm/rev (M_1) = 92.14 kN/cutter
- Penetration coefficient (b) = 1.97

The rock chip sampling gives no definite answer to how the chipping efficiency was during this test, except for that the thickness of the chips seems to increase with increasing thrust force, which is expected. There was some uncertainties regarding the chip sampling that led to the fact that chips also from gauge cutters and center cutters was included. This was corrected in the sampling of the following RPM trials. The mean standard deviation for the chip sizes was 13 % for the length, 17 % for the width and 25 % for the thickness.

5.2.2. RPM Trials

After completing the two penetration tests, the focus was shifted to performing the planned RPM trials. The RPM levels 7, 8, 9 and 10 were chosen, as these were values already utilized by the operator of the TBM.

At first the RPM trails was executed as planned, which means that rock chips were sampled during each level of the tests. After a couple of tests the geological conditions changed rapidly and prevented the completion of the planned thrust levels. Only tests for 90, 100 and 110 % of the normal thrust level were conducted with geological sampling. For the 100 % level only two different RPM was tested and for the 90 % level only one RPM was tested, before the geological conditions got so unstable that further testing was made impossible.

After almost a month stop in the RPM testing it was decided to perform additional tests, but this time without geological sampling. This was due to limited time at the site. Because of highly fractured rock mass in this area the TBM could only be operated at a maximum of 1700 PSI, which is 55 % of normal thrust. This was to avoid the cutter head from clogging up due to insufficient removal capacity of the TBM conveyor. The result of the RPM trials both with and without geological mapping are presented in the following part of the report.

Tests with Geological Sampling

3300 PSI - 345 kN/cutter
This test was performed on the 12.02.2014, and represents the RPM trial at 110 % of normal thrust for the TBM. The geological conditions were consistent over the five strokes in which this test was conducted. The strokes before and after the test were also observed, and showed the same results regarding penetration rate.

The penetration rate of this test is showed in Figure 5.20, and the basic penetration in mm/rev is shown in Figure 5.21. Information regarding the chip sizes and form can be seen in Figure 5.22-Figure 5.25 and a picture of the chips gathered is shown in Figure 5.26.
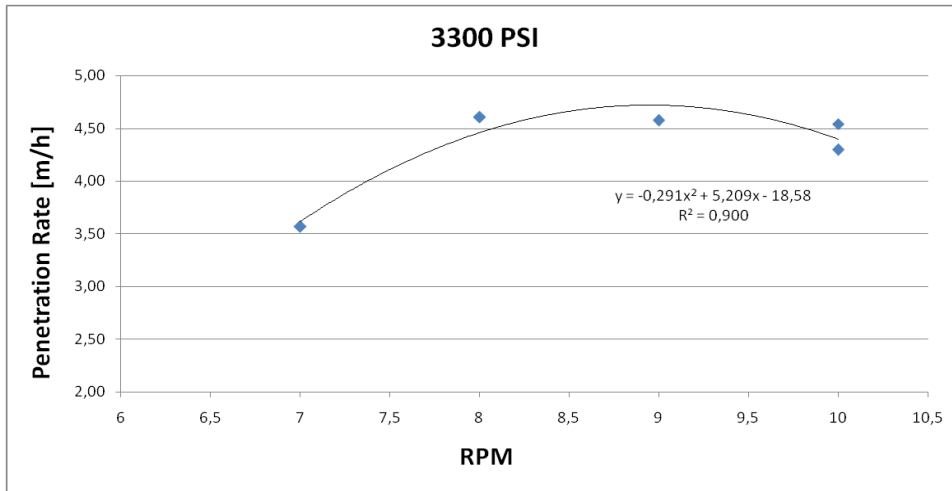
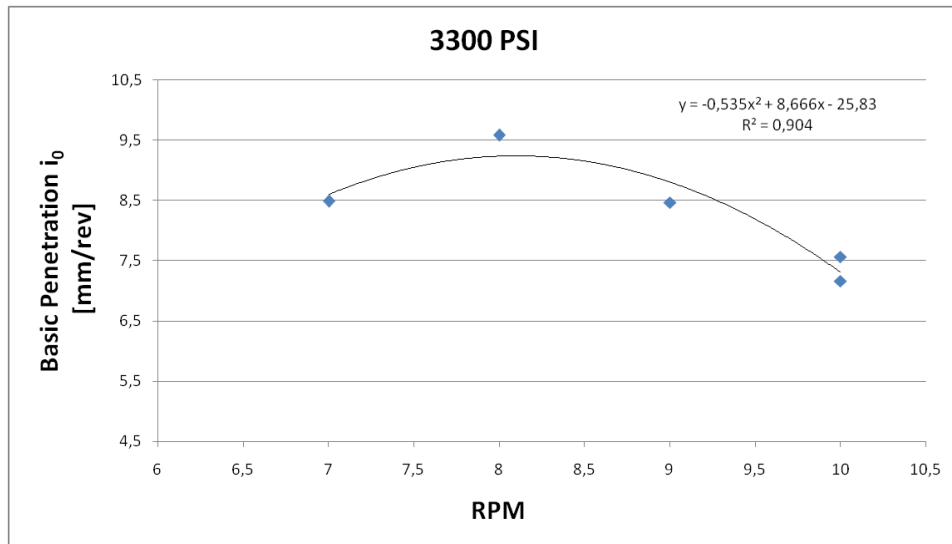Figure 5.20: Penetration rate for RPM trial - 3300 PSI

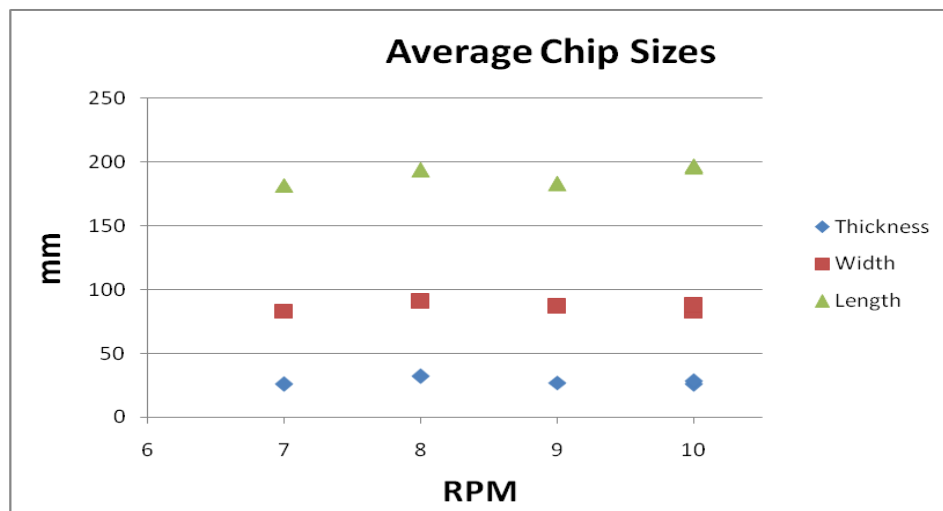Figure 5.21: Basic penetration in mm/rev for RPM trial - 3300 PSI

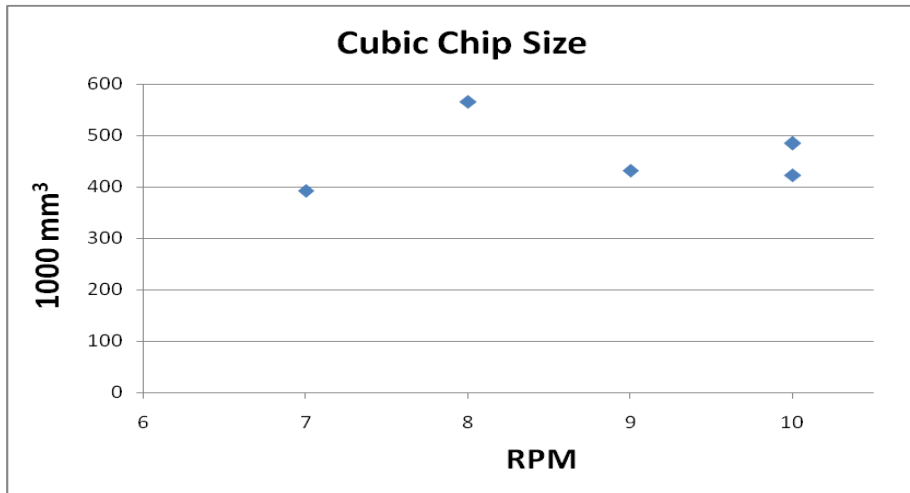Figure 5.22: Average chip sizes for RPM trial - 3300 PSI

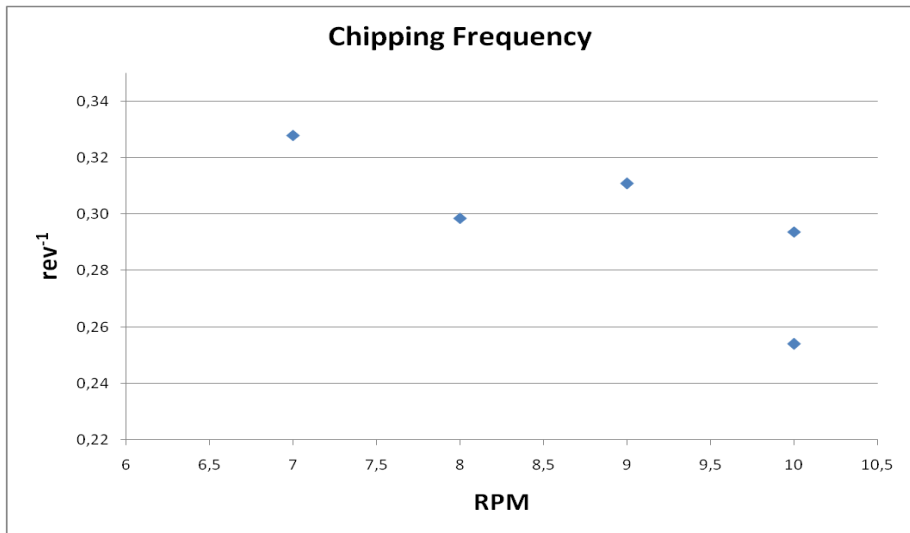Figure 5.23: Cubic chips sizes for RPM trial - 3300 PSI

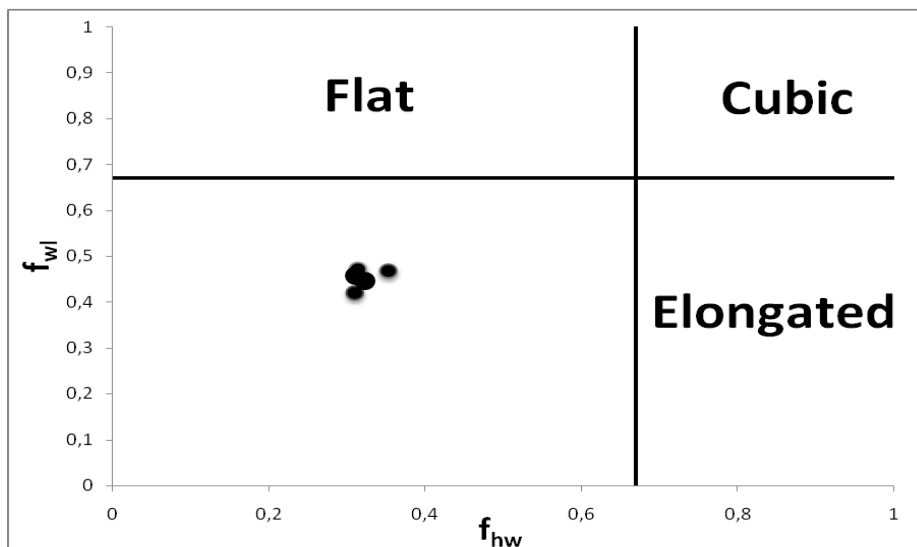Figure 5.24: Chipping frequency for RPM trial - 3300 PSI

Figure 5.25: Chip shapes of the average chip sizes for RPM trial - 3300 PSI

74

Figure 5.26: Rock chips picked during RPM trial - 3300 PSI. RPM levels from top row to bottom: 10, 9, 8, 7, 10. The mean thickness of the bottom row was 28.2 millimeters.

As can be seen in the presented graphs, the penetration rate is increasing with increasing RPM up to a certain point before it flats out, while the basic penetration is increasing with decreasing RPM down to a certain point before it drops again. The cause of this could be a more beneficial loading rate between the cutter and the rock surface at a lower RPM.

Based on the collected data of chips sizes and shapes it is possible to see that the rock breaking can be said to have been most efficient for the RPM level 8. In this case both thickness and width of the rock chips are the largest, which also gives this RPM level the largest cubic size of chips. Also this could be caused by that at this RPM the most beneficial loading rate between the cutters and the rock occurs. The trend of the chipping frequency also shows that the rock breaking is more efficient for the lower RPMs, as the frequency goes up with decreasing RPM.

The rock chip sampling was satisfactory at this test as a better understanding of which chips to pick from the muck cart was achieved. The mean standard deviation for the rock chip sizes was 10 % for the length, 11 % for the width and 24 % for the thickness.

3000 PSI - 315 kN/cutter

This test was conducted on the 17.02.2014, and represent the RPM trial at 100 % of what is considered normal thrust force for the TBM. Because of rapidly changing geological conditions the testing was stopped after only two levels of RPM.

The penetration rate of this test is shown in Figure 5.27 and the basic penetration in mm/rev is shown in Figure 5.28. Information regarding the chip sizes and form can be seen in the Figure 5.29-Figure 5.32 and picture of the chips gathered is given in Figure 5.33.
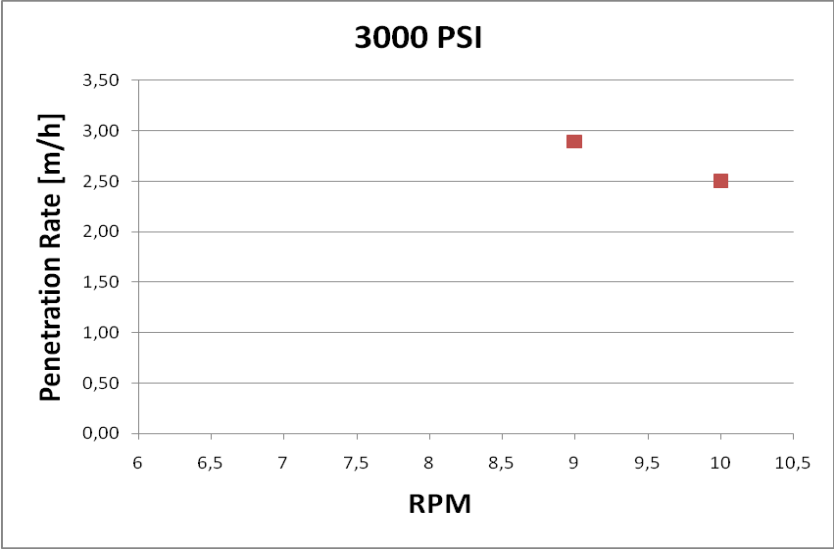

Figure 5.27: Penetration rate for RPM trial - 3000 PSI

Figure 5.28: Basic penetration in mm/rev for RPM trial - 3000 PSI
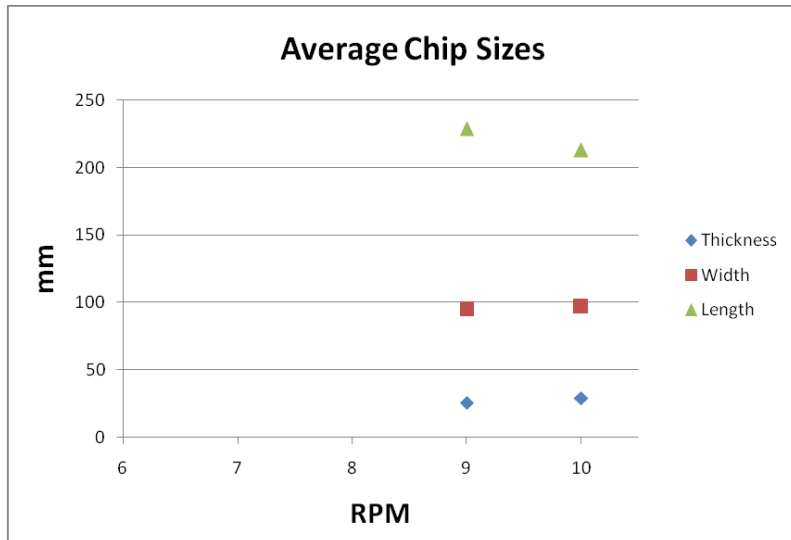
Figure 5.29: Average chip sizes for RPM trial - 3000 PSI
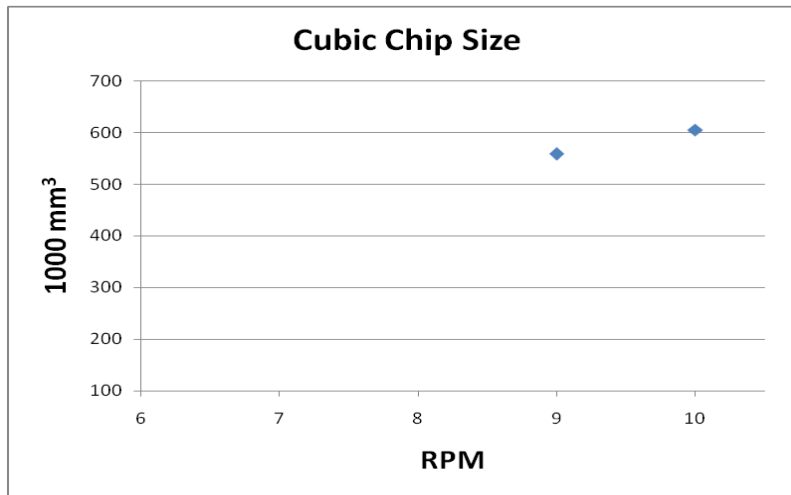
Figure 5.30: Cubic chips sizes for RPM trial - 3000 PSI
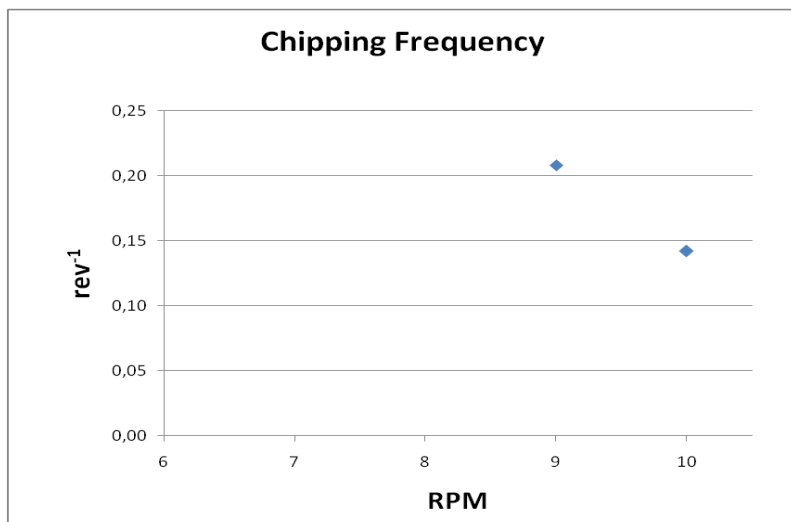
Figure 5.31: Chipping frequency for RPM trial - 3000 PSI
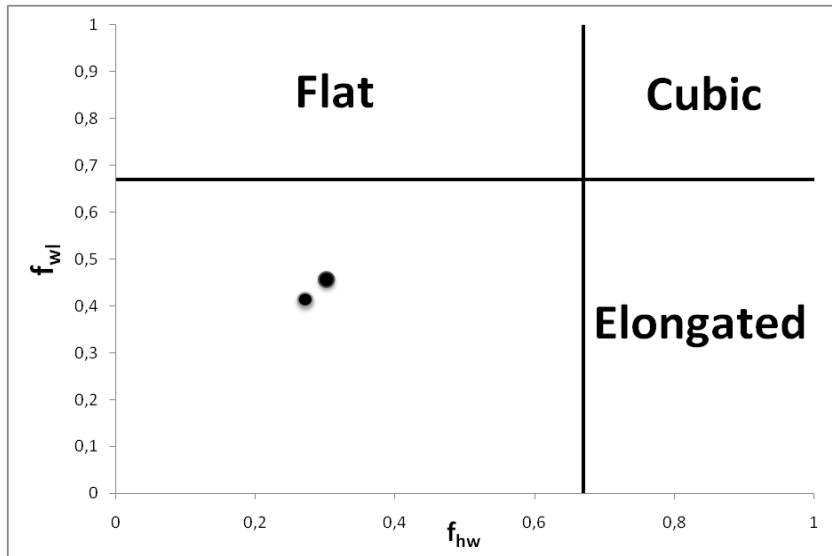
Figure 5.32: Chip shapes of the average chip sizes for RPM trial - 3000 PSI

Figure 5.33: Rock chips picked during RPM trial - 3000 PSI. RPM levels from top row to bottom: 10, 9. The mean thickness of the bottom row was 25.8 millimeters.

As can be seen in the graphs, the penetration rate of this test is lower than that of the test with 3300 PSI propel pressure. This is to be expected as lower thrust level should give a lower penetration rate. However the rock mass also got less fractured, which resulted in the penetration rate dropping roughly 20-25 %. This was shown by comparing the penetration rates at 100 % of normal thrust for the two RPM tests.

For this test the penetration rate decreases with increasing RPM, as does the basic penetration in mm/rev. The fact that only two points of data were collected for this test makes it difficult to say something certain about this.

The chip samples show the opposite trend in this test compared to the previous RPM trial, as the chip sizes and therefore the cubic chip size increases with increasing RPM. Only the values for length are higher for 9 RPM compared with 10 RPM. The chipping frequency however shows a more efficient chipping for 9 RPM than for 10. The mean standard deviation for the chip sizes was 12 % for the length, 15 % for the width and 20 % for the thickness.

2700 PSI - 285 kN/cutter

This test was conducted the 19.02.2014 and represents the RPM trail at 90 % of normal thrust force for the TBM. Due to the geological conditions this test was cut short after only one RPM level, as the TBM operator had great problems stabilizing the thrust force.

One data point is far from enough in order to analyze the effect of lowering the thrust force. Nevertheless the results of the one RPM level is presented in order to compare it to the previously presented RPM trials at 3300 and 3000 PSI. The penetration rate of the test in m/h is shown in Figure 5.34 while the basic penetration in mm/rev can be seen in Figure 5.35. Information regarding the rock chips picked during the test can be found in the Figure 5.36-Figure 5.39 and a picture of the rock chips picked during the test is shown in Figure 5.40.

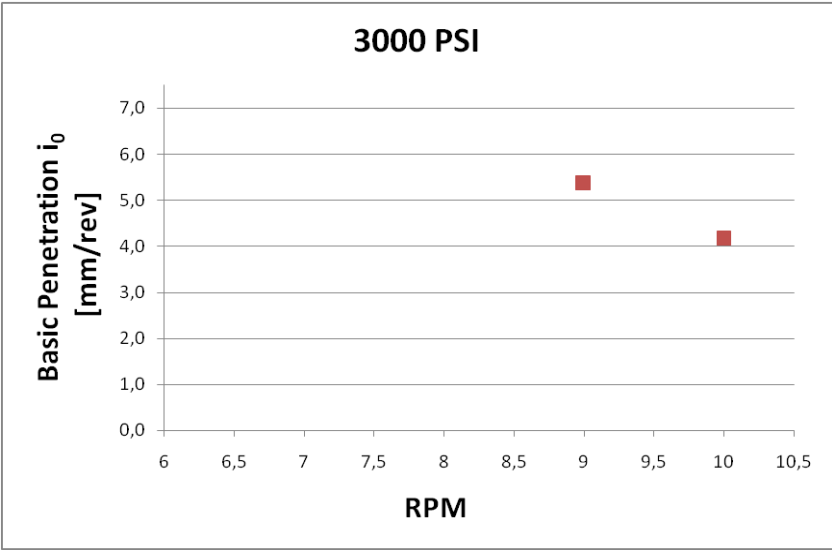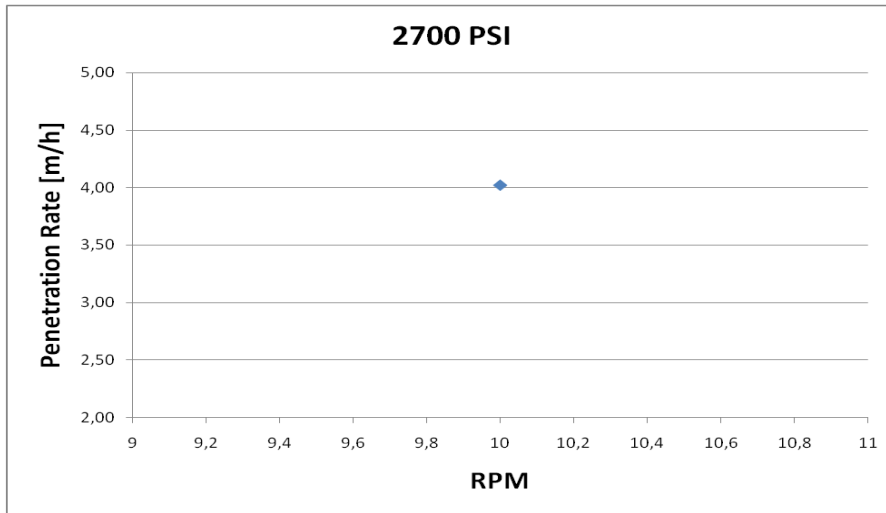Figure 5.34: Penetration rate for RPM trial - 2700 PSI
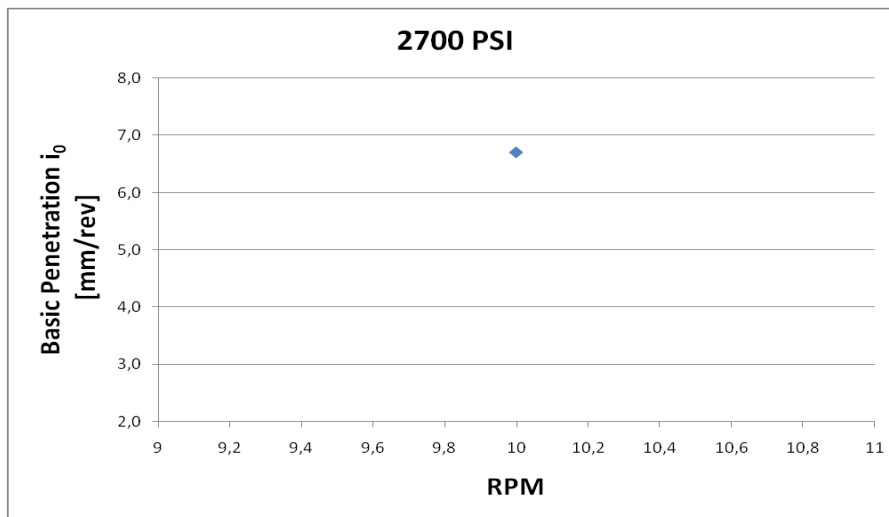
Figure 5.35: Basic penetration in mm/rev for RPM trial - 2700 PSI
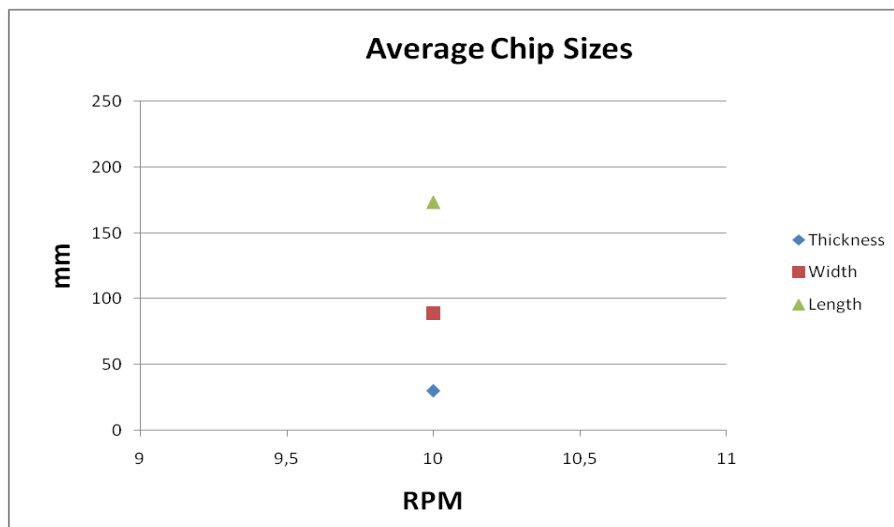
Figure 5.36: Average chip sizes for RPM trial - 2700 PSI
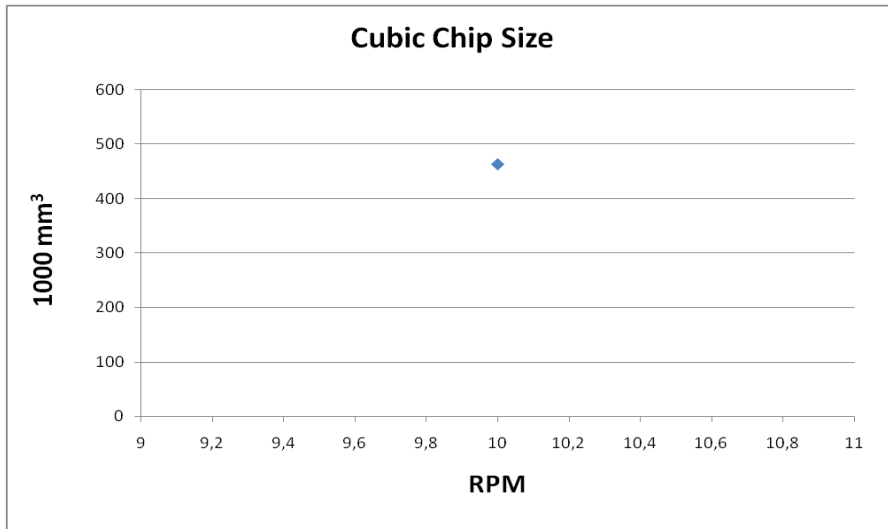
Figure 5.37: Cubic chips sizes for RPM trial - 2700 PSI
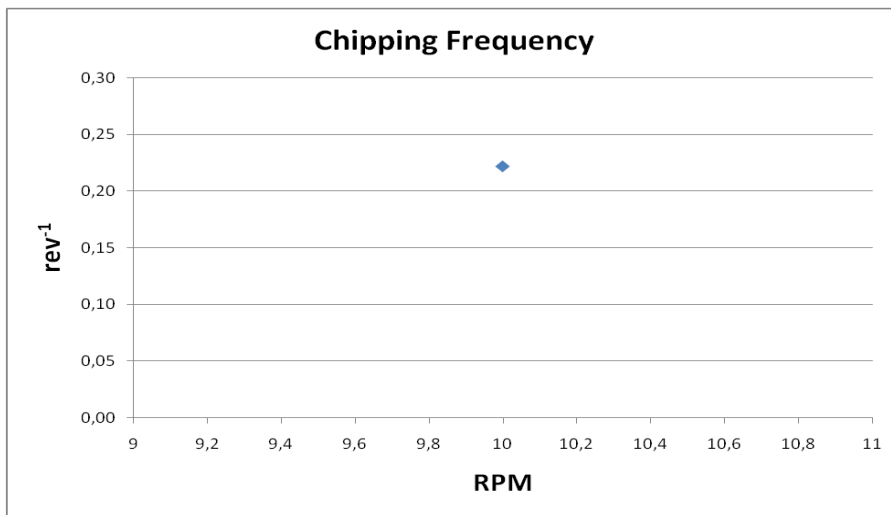
Figure 5.38: Chipping frequency for RPM trial - 2700 PSI
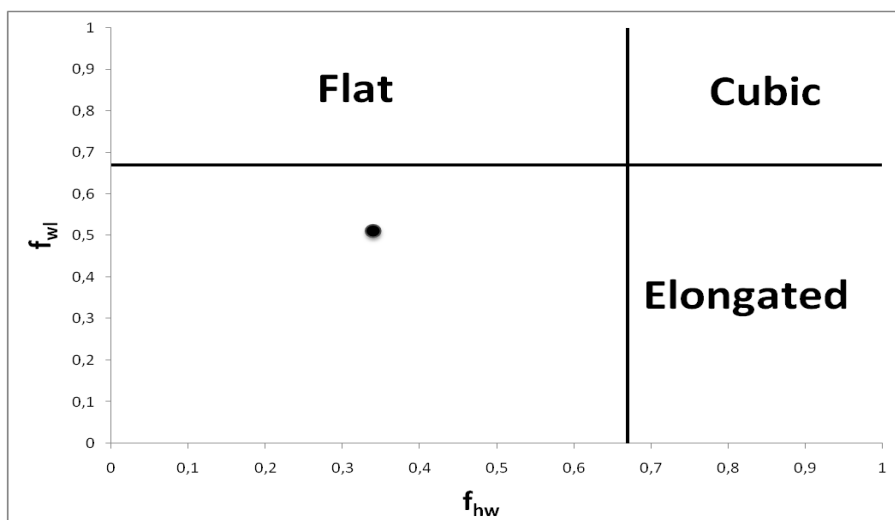
Figure 5.39: Chip shapes of the average chip sizes for RPM trial - 2700 PSI

81

Figure 5.40: Rock chips picked during RPM trial - 2700 PSI. RPM level 10. The mean thickness of the chips was 30.2 millimeters.

Both the penetration rate in m/h and the basic penetration in mm/rev is for this thrust level higher than expected, when comparing to the thrust levels of 3300 and 3000 PSI. The reason for this is most likely the fact that the rock became highly fractured, which was also the reason for stopping the testing after only one level of RPM.

Regarding the rock chips one can see that the average chip sizes and cubic chip size are somewhat lower than what is the case for the same RPM at higher thrust levels. This is to be expected, as the rock breaking efficiency should go down with less thrust. The mean standard deviation for the chip sizes was 12 % for the length, 5 % for the width and 19 % for the thickness.

Tests without Geological Sampling

1700 PSI - 180 kN/cutter

These two tests were conducted on the 17.03.2014. The geological conditions during the tests was fairly consistent, but the second test was cut short after only two levels RPM due to overloading of the TBM conveyor. From observation of the transport conveyor it was clear that the rock was heavily fractured, as chips of any notable size were absent.

Graphs showing the penetration rate and the basic penetration for the tests can be seen in Figure 5.41 and Figure 5.42.
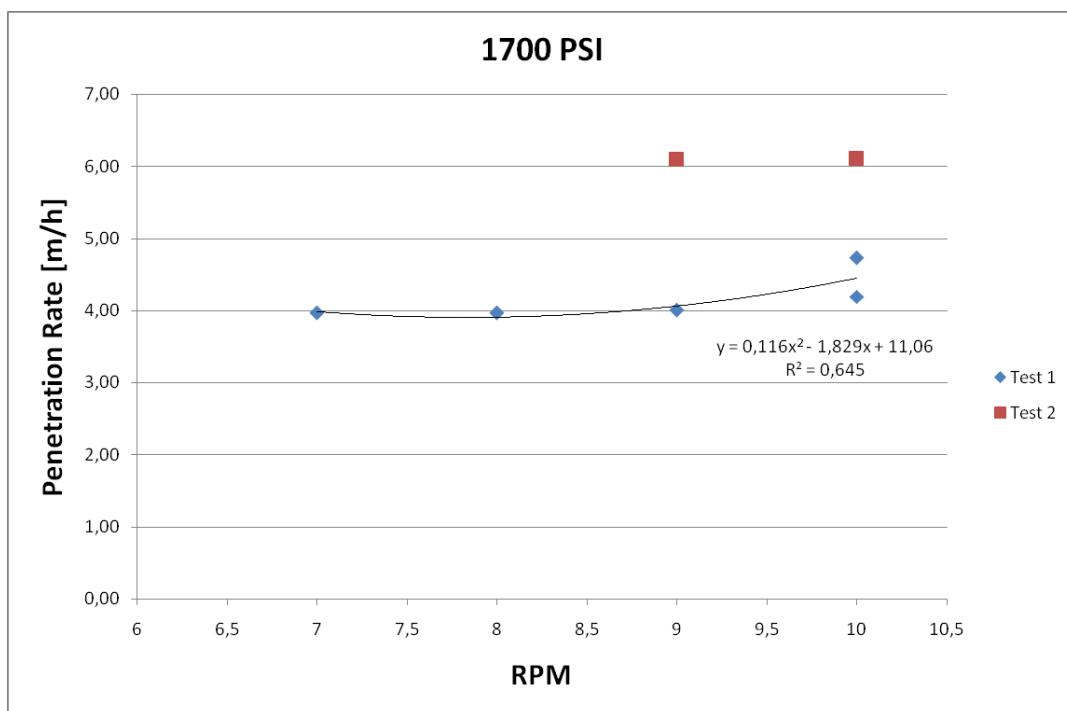
Figure 5.41: Penetration rate for the two RPM trials performed at 1700 PSI
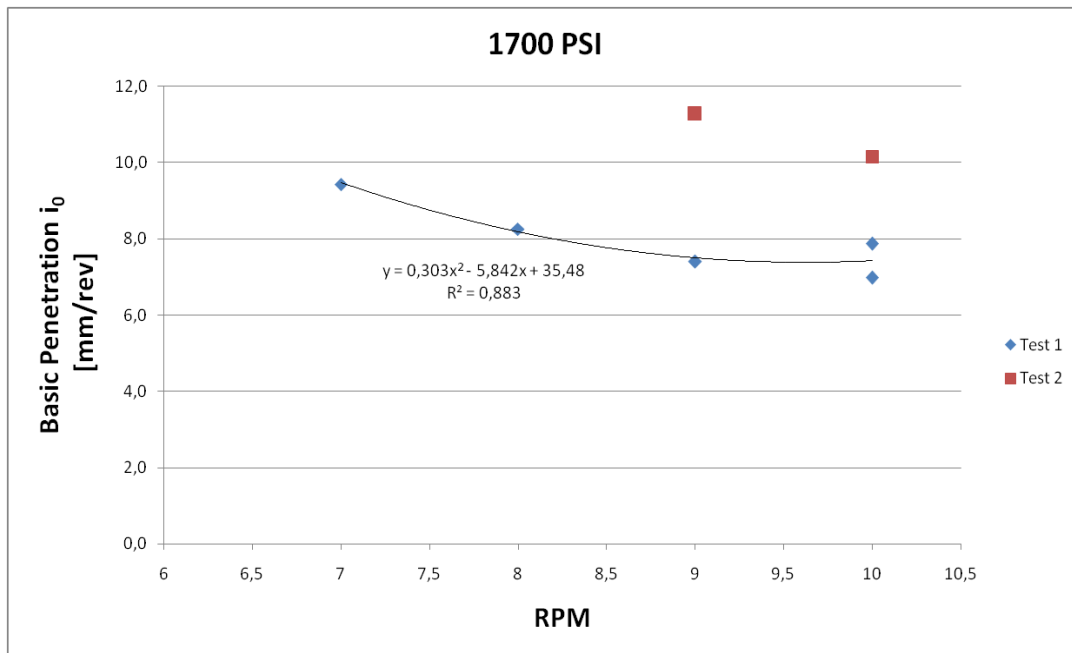
Figure 5.42: Basic penetration in mm/rev for the two RPM trials performed at 1700 PSI

As in the test with geological sampling it can be seen how the penetration rate stays fairly consistent with the varying RPM levels, while the basic penetration rate in mm/rev increases with decreasing RPM. The reason for this should be that since the penetration rate in highly fractured rock like this is being limited by the muck removal capacity of the TBM conveyor and not by the thrust force, one should expect the penetration rate to stay the same no matter which RPM is utilized. Thusly a reduction in RPM will also give an increase in penetration per revolution of the cutterhead.

1400 PSI

This test was also conducted on the 17.03.2014. In this test the geological conditions changed very rapidly, and the operator struggled with keeping the thrust levels constant during the test. This test also represents the final attempt of conducting RPM trials in this field study.

The penetration rate in m/h for this test is shown in Figure 5.43 while the basic penetration rate in mm/rev is given in Figure 5.44.
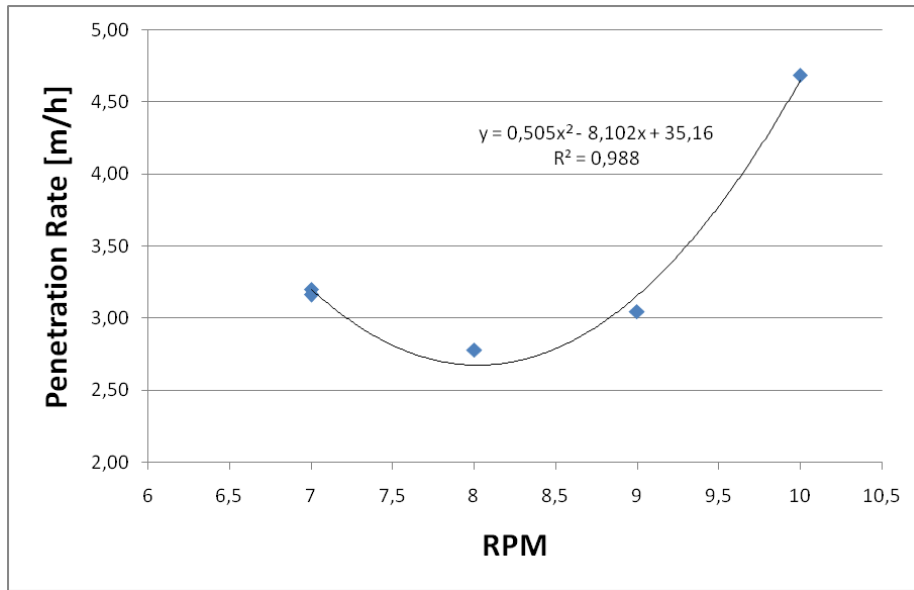
Figure 5.43: Penetration rate for the RPM trial performed at 1400 PSI
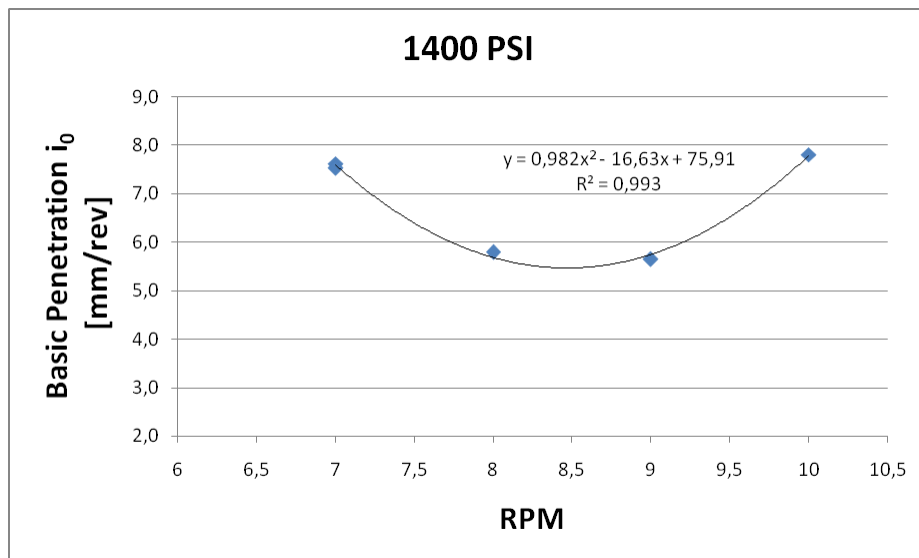
Figure 5.44: Basic penetration in mm/rev for the RPM trial performed at 1400 PSI

In this test the penetration rate increased greatly at the highest level of RPM, while for the three other RPM levels it stayed relatively consistent at around 3 m/h. The reason for the high increase at 10 RPM is most likely due to rapid changes in the geological conditions, and especially considering fracturing. The high value of penetration rate also gives a high value for the basic penetration rate in mm/rev for 10 RPM, while for the rest of the data points the basic penetration increases with decreasing RPM also for this test. The same arguments for the cause of this as given for the test at 1700 PSI applies here.

5.2.3. Cutter Life

Information regarding cutter life has also been collected and digitalized in an Excel spreadsheet. To assess the cutter life has not been a focus of the work in this thesis, but this information could be valuable in order to assess cutter consumption at a later stage should more work with the Stillwater Mine be done. The compiled data is given as a digital appendix to this thesis. A summary of the gathered data may also be seen in Appendix D and include the following information:

- Date of cutter change
- Position of cutters changed
- Chainage at cutter changes
- Machine hours at cutter changes
- Meters bored for cutters changed
- Amount of wear (mm)
- Reason for cutter change
- Serial numbers of cutters

Based on the information gathered it is possible to divide the bored tunnel into three sections and calculate a simplified cutter consumption after the procedures from Bruland (1998c).

Chainage [m]	H_f [m³/c]	H_h[h/c]	H_m[m/c]	Interval Length [m]	Cutters Changed	% of Cutters Changed
0-608	1444.5	6.6	60.8	608	10	30
608-1218	966.2	8.5	40.7	610	15	45
1218-1754	1157.7	9.1	48.7	536	11	33

Table 5.1: Cutter consumption for the TBM

No corrections have been done for TBM diameter in these calculations.

The calculated values for cutter life are high. The fact that actual cutter life is higher than predicted values in rocks with high CLI could indicate that the estimations of the NTNU model are too conservative when the Cutter Life Index is high.

In addition to the data presented regarding cutter life, four individual cutter ring halves from the last cutter change performed the 05.03.2014 and 06.03.2014 were collected and shipped back to the SINTEF Engineering Geology Laboratory in Trondheim. Theses samples may be used at a later time to analyze cutter wear in the TBM of the Blitz Project. The steel type of the cutter rings used in the TBM at the Blitz Project is a slightly modified H-13 steel.

5.3. Geological Investigation

The results of the geological investigation presented in chapter 4.4 are shown in this part of the report. The results include how the eight sections of tunnel were classified after the treatment of core logging data, the calculation of the average k_s value for each section and finally a correlation between the averaged k_s values and the TBM performance from each section based on the collected shift logs.

5.3.1. Calculated k_s and Fracture Classes for Each Tunnel Section

The results of the k_s calculation for each tunnel section is shown in Table 5.2. Detailed information about the calculations for each section can be found in the Excel spreadsheet which is given as a digital appendix to this thesis.

Tunnel section	Tunnel chainage represented [m]	Average k_s
1	372 - 594	1.74
2	594 - 818	2.08
3	818 - 1025	1.49
4	1025 - 1198	2.40
5	1198 - 1344	2.65
6	1344 - 1471	2.10
7	1471 - 1695	2.39
8	1695 - 1828	3.04

Table 5.2: Overview of the Calculated k_s for each Tunnel Section

These results indicate that the rock mass is highly fractured for most of the tunnel sections. A distribution of the fracture classes in each tunnel section, or core sample, can be seen in Figure 5.45-Figure 5.52. The average angle between the plane of weakness and the tunnel axis for each tunnel section is shown in Table 5.3. As no angles between the core and fracture structures were noted in the diamond drill log for tunnel section 1, it was assumed that this section had similar fracture angles as the start of tunnel section 2.

Tunnel section	1	2	3	4	5	6	7	8
Average angle [°]	46	34	32	51	57	34	35	43

Table 5.3: Average angle of weakness plane for each tunnel section

Figure 5.45: Distribution of fracture classes in tunnel section 1

Figure 5.46: Distribution of fracture classes in tunnel section 2
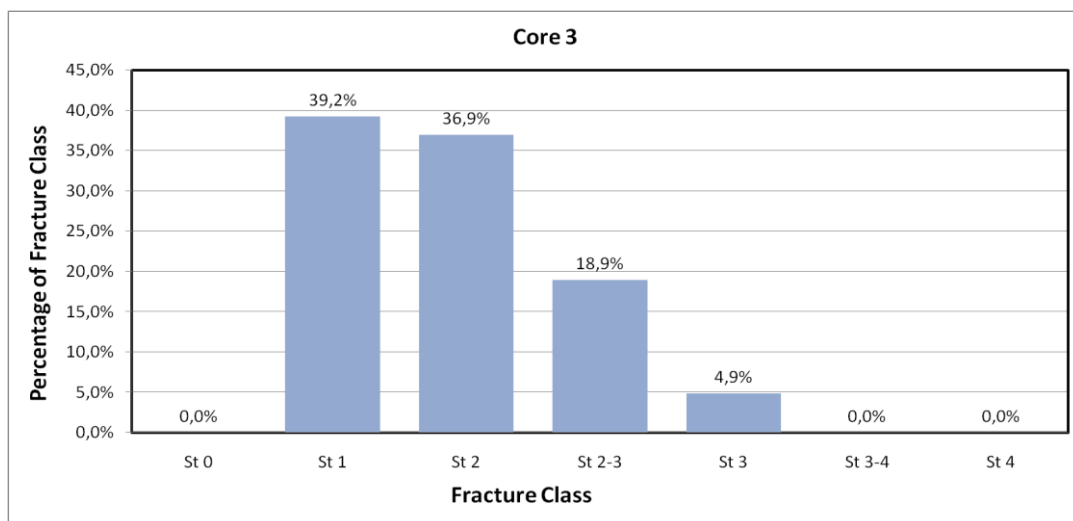
Figure 5.47: Distribution of fracture classes in tunnel section 3

88
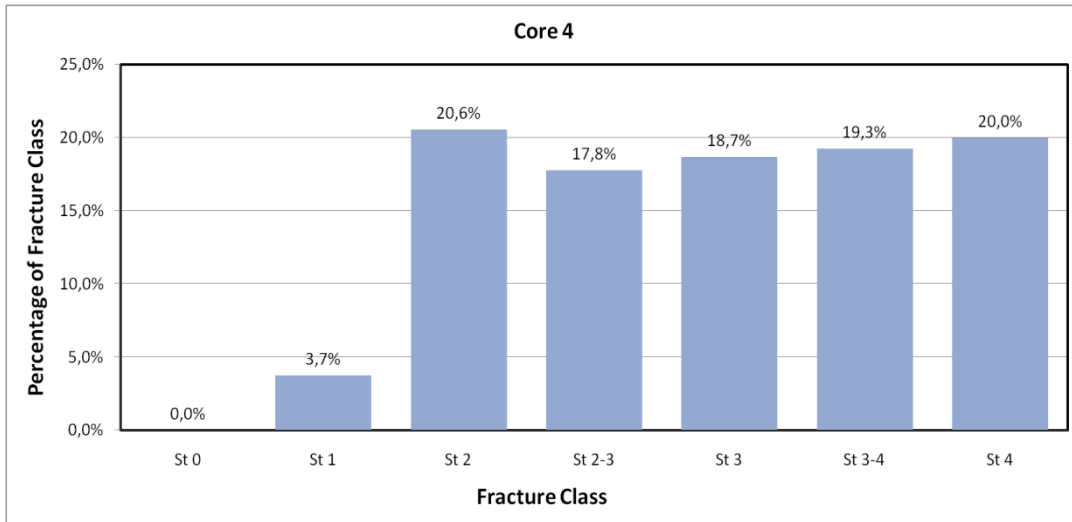
Figure 5.48: Distribution of fracture classes in tunnel section 4
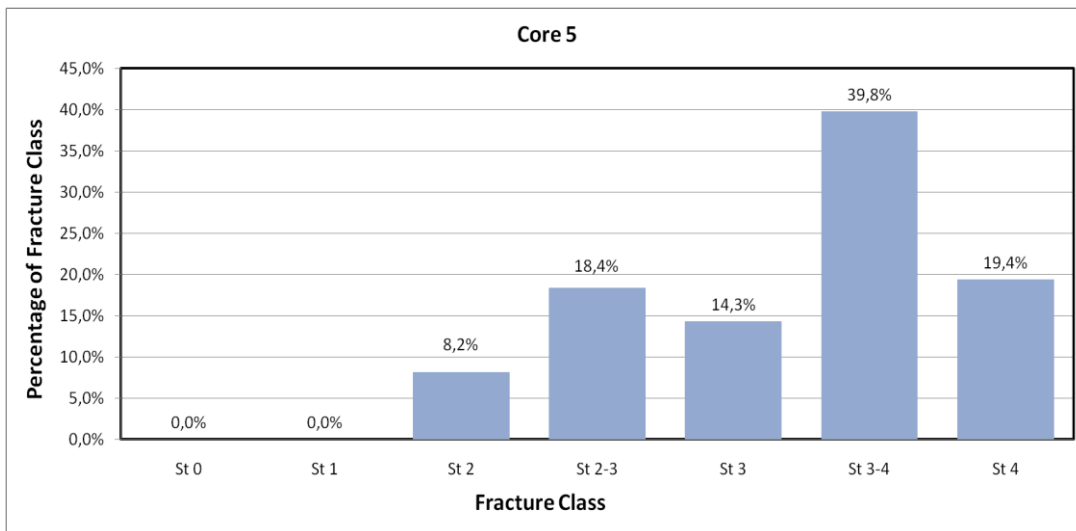
Figure 5.49: Distribution of fracture classes in tunnel section 5
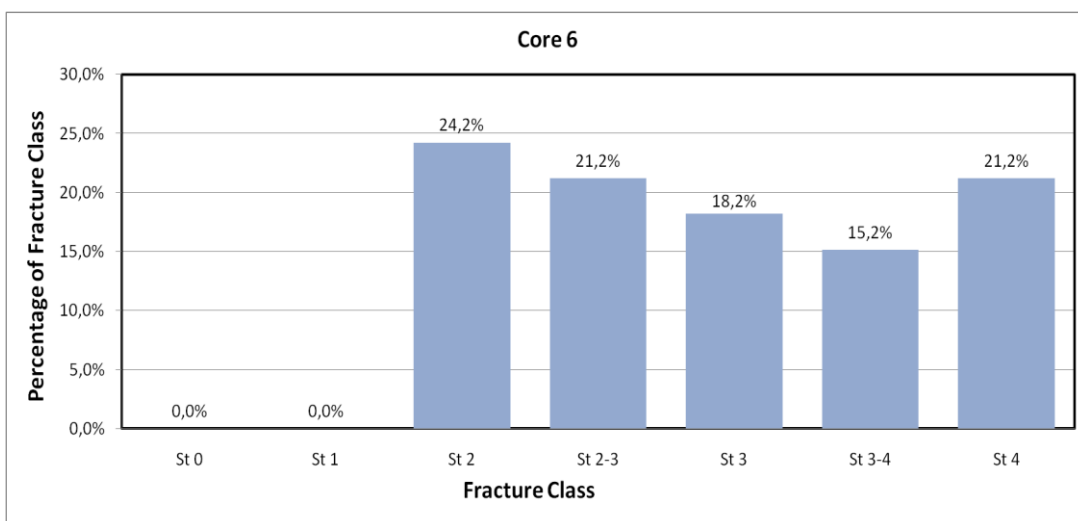
Figure 5.50: Distribution of fracture classes in tunnel section 6

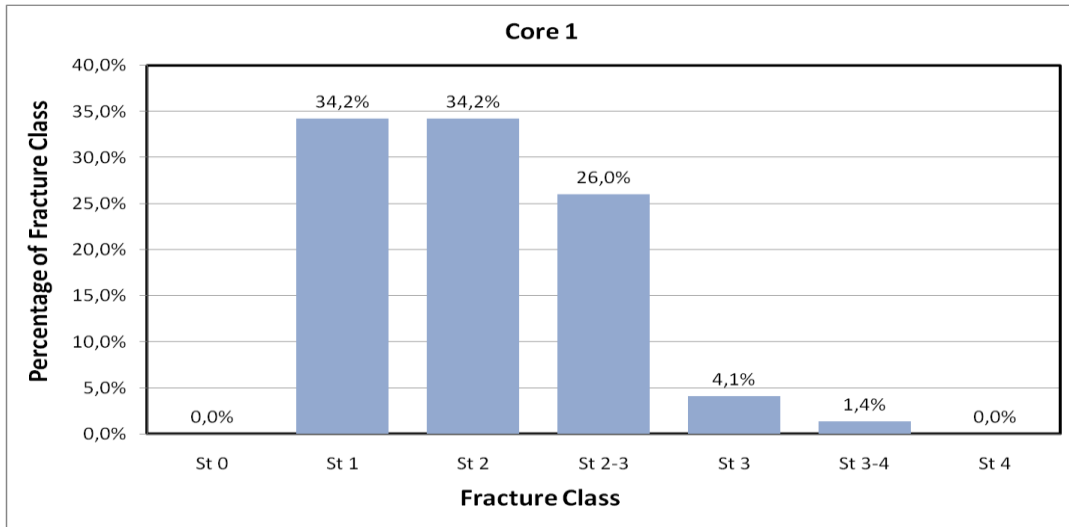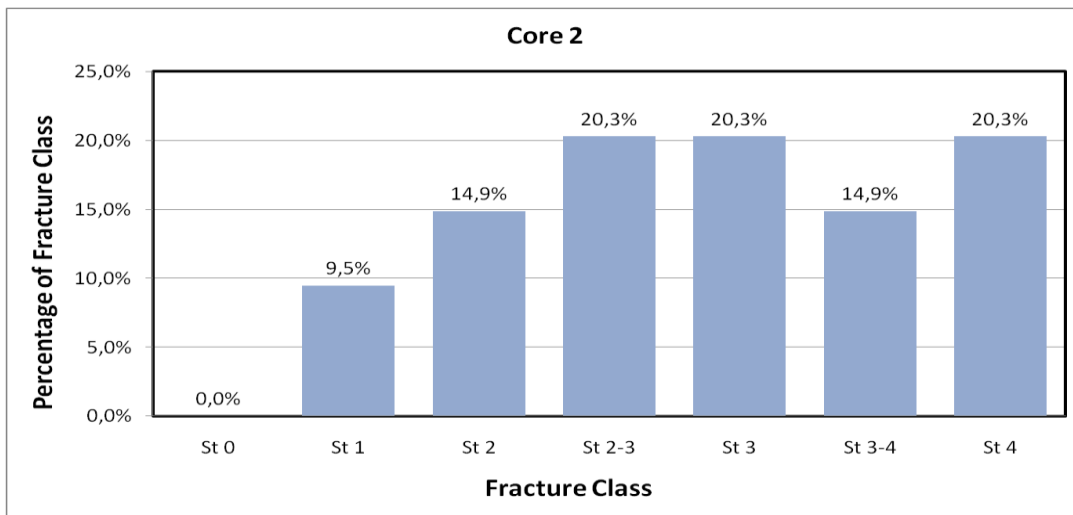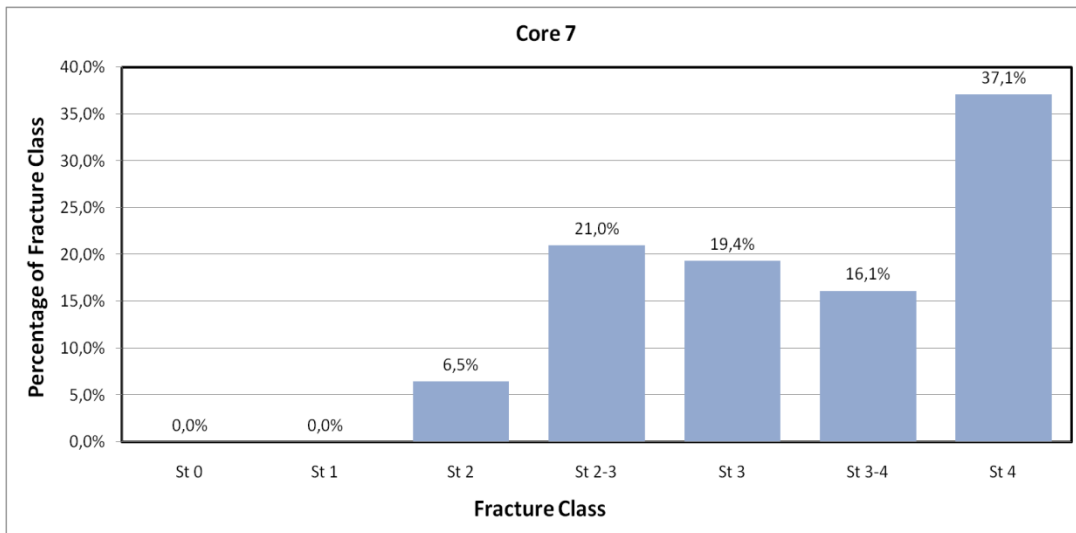Figure 5.51: Distribution of fracture classes in tunnel section 7
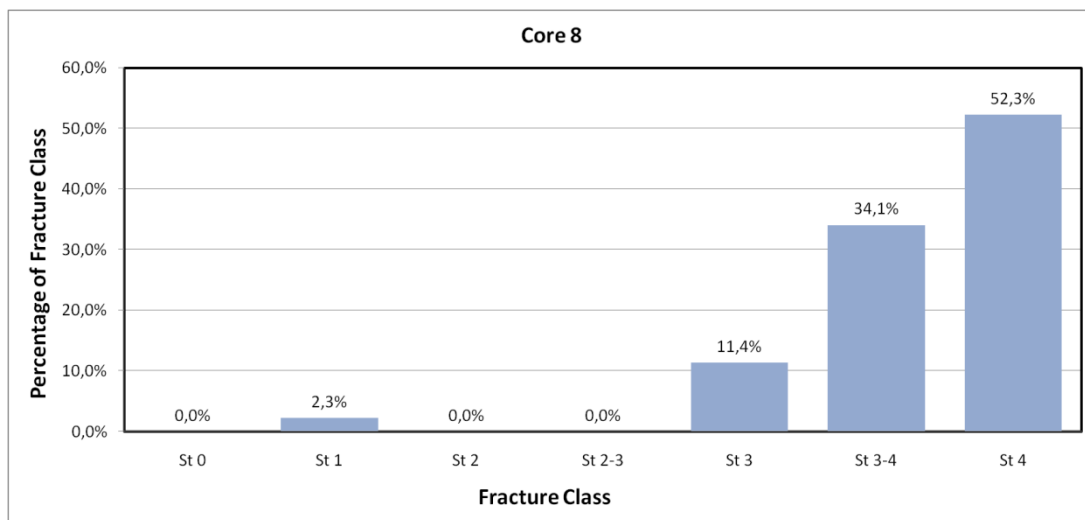
Figure 5.52: Distribution of fracture classes in tunnel section 8

The trend in distribution is that there is an increasing percentage of high fracture classes in the tunnel sections at the end. Especially tunnel section 8 has a high percentage of the highest fracturing classes, and this section also has the highest average k_s value.

5.3.2. Comparison Between Calculated k_s and Machine Performance

In the following part the comparison between the calculated k_s values and the performance of the TBM is presented.

Penetration rate versus k_s

Graphical comparison between calculated average penetration rate in m/h from the shift logs and the average k_s from the geological information available is shown in Figure 5.53.
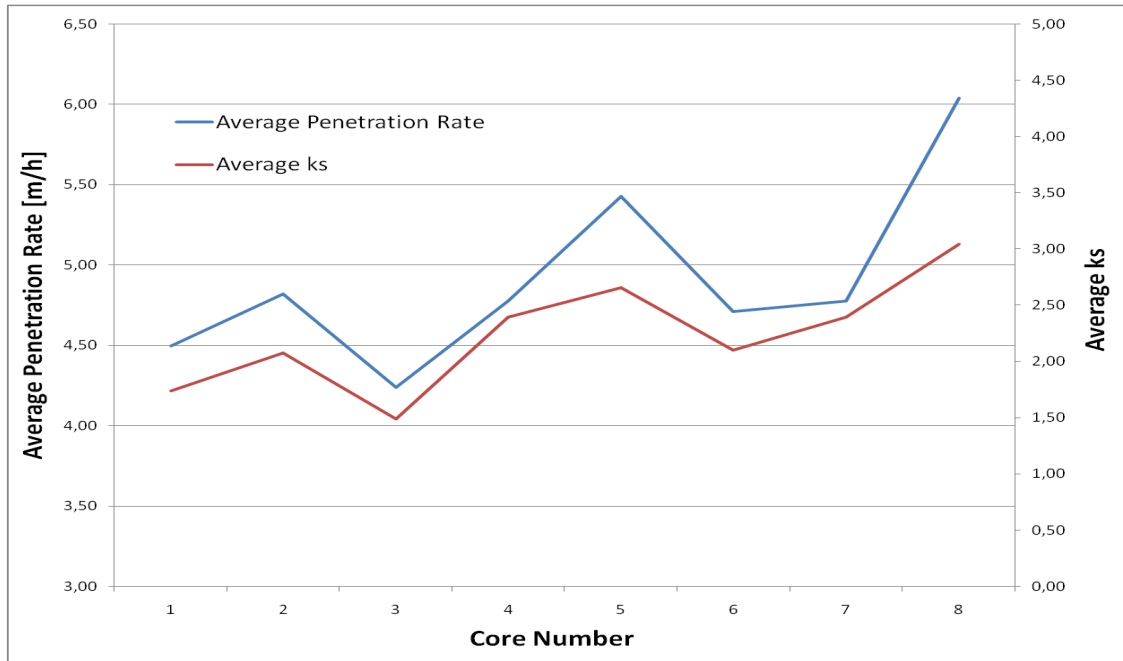
Figure 5.53: Correlation between average penetration rate and average k_s

One can see that the average penetration rate of the TBM has a good correlation with the calculated average k_s values for all of the tunnel sections. Even when considering that these k_s values are an average along every core length, the trend is relevant. The trend should also be the same even if investing more time into the work to get a more accurate estimate of the k_s.

It seems from these results that the NTNU model is very much correct in stating that the rock mass fracturing is by far the most important rock mass factor regarding the performance of the TBM. It would in this case have been interesting to section the tunnel into smaller sections, for example 20 meters, and then compare the new estimates of k_s with observed performance data from the shift logs of the TBM. A geological back mapping done in the tunnel would in this case give even more valuable information in order to assess the reliability and validity of this simplified calculation. Additional data from the core sampling regarding fracture sets and angles of these would naturally also be of help, as using only one fracture set in this estimation represents a big simplification.

91

Applied thrust force versus k_s

A comparison between the average applied thrust force and the k_s value for each tunnel section was done, and the result of this can be seen in Figure 5.54.
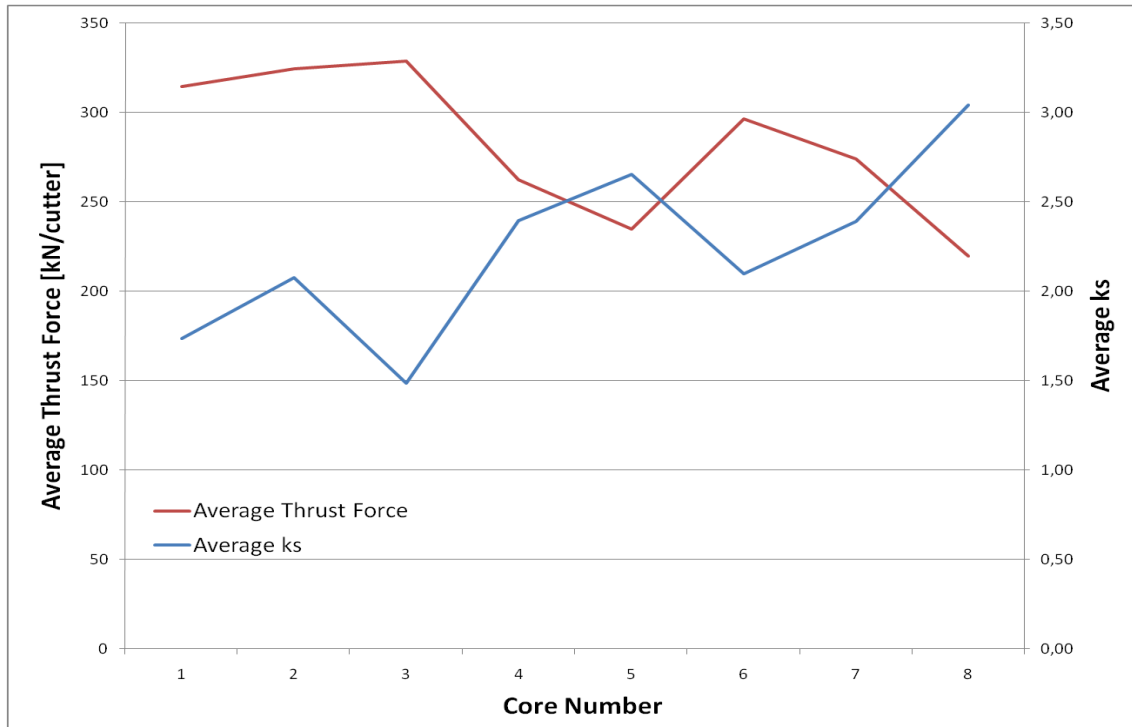
Figure 5.54: Applied thrust force versus k_s

This comparison shows that with increasing rock mass fracturing, the applied thrust force from the TBM decreases and vice versa. This can be explained by the fact that when the rock mass gets too highly fractured the TBM operator has to decrease the thrust force in order to not advance faster than the capacity of the TBM conveyor, and to not get excessive cutter wear or damage the TBM itself through high levels of vibration and high momentary cutter loads.

This result is of importance because most models used in estimating penetration rate, including the NTNU model, uses the applied cutter thrust as their main machine parameter. If it however turns out that the rock mass fracturing has a high effect on the applicable cutter thrust, this should have to be accounted for in the prediction models. This will cause the k_s to have an indirect effect on the performance of the TBM in addition to its effect on the rock mass boreability.

Machine utilization versus k_s

A comparison between the machine utilization and the k_s for each tunnel section was also done, and the result of this is shown in Figure 5.55. In this figure one can see that with increasing rock mass fracturing, the machine utilization goes down. The reason for this is most likely the same effect as was observed in the results from the TBM performance month by month given in chapter 5.1 of this report, which was that with higher penetration rates the utilization goes down since a higher percentage of the time is used for waiting for the train and performing additional rock support before further excavation can be done. And since the penetration rate is highly dependent on the rock mass fracturing, the utilization will likewise be dependent on the rock mass fracturing.

The correlation between machine utilization and the penetration rate for the eight tunnel sections used in this geological investigation is shown in Figure 5.56.
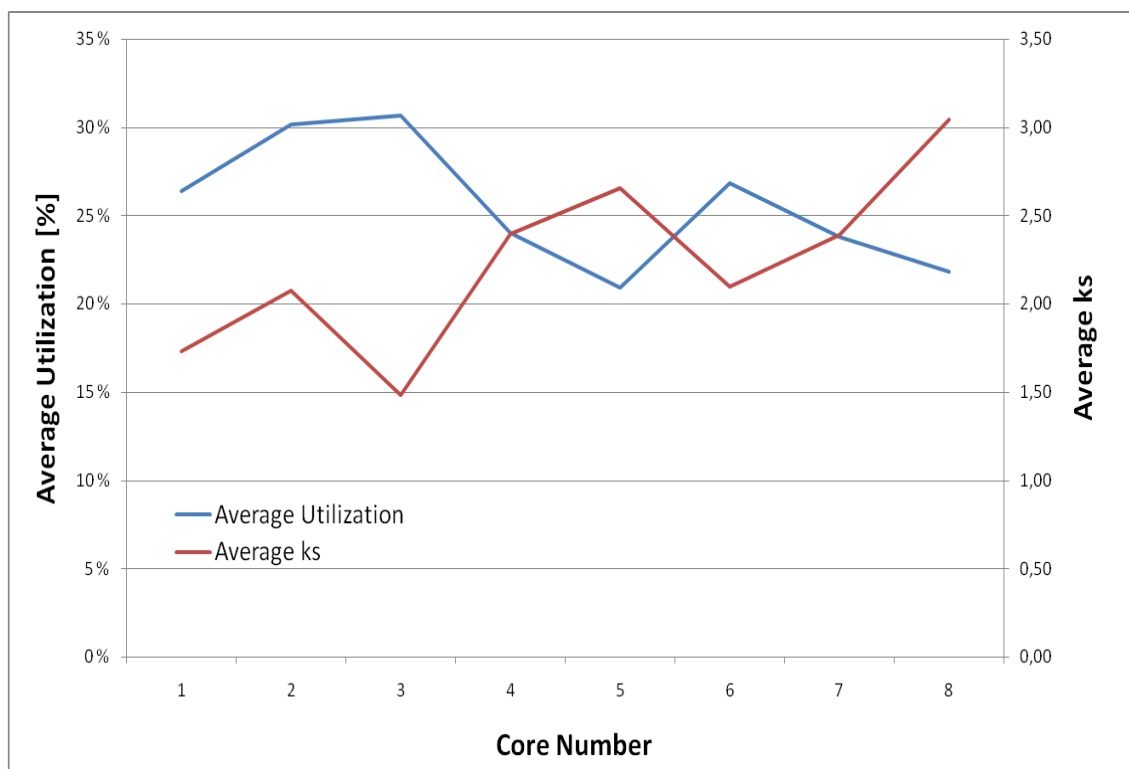
Figure 5.55: Machine utilization versus ks
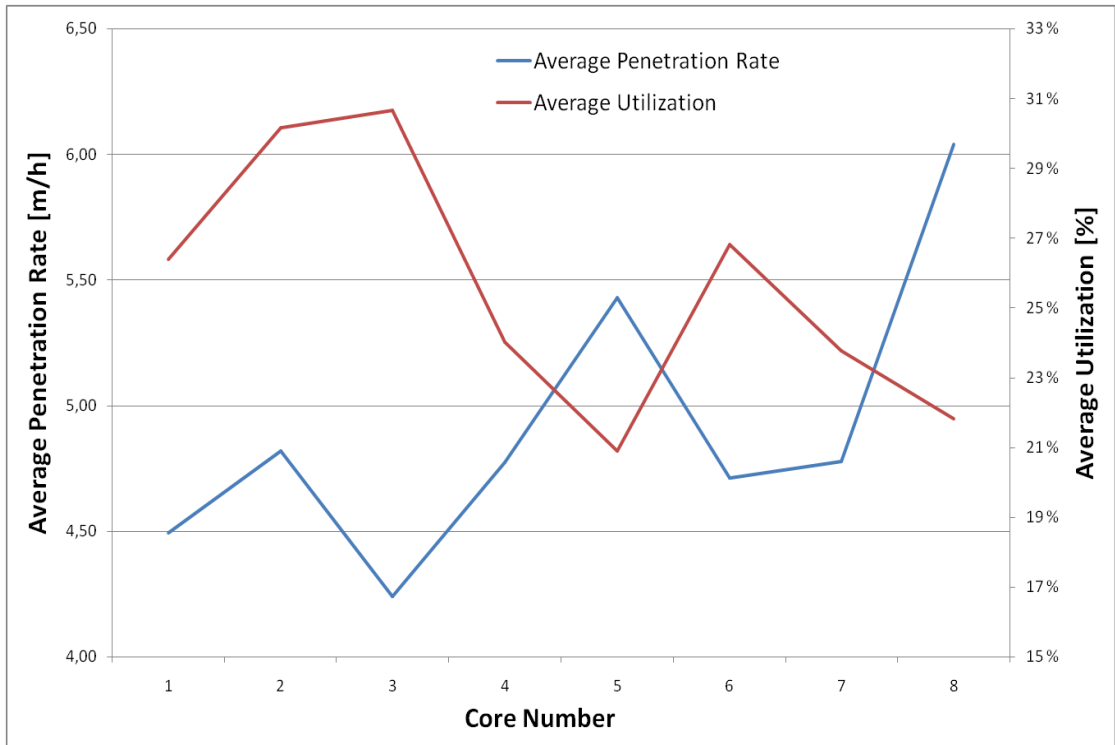
Figure 5.56: Machine utilization versus penetration rate

5.4. Laboratory Testing

This chapter presents the results of the laboratory testing performed at the SINTEF laboratory in Trondheim, Norway. This testing was performed in the time period between 23.04.2014 and 12.05.2014. Most test were performed by the author himself, under supervision from SINTEF personnel. The suggested test standard presented by Dahl (2003) has been followed in the drillability testing.

5.4.1. Summary

Three rock samples were selected from the project site visited, and shipped to the SINTEF laboratory in Trondheim for testing. The samples represent the following from the project:

Sample 1 - Rock chips from the RPM trial at 3300 PSI conducted the 12.02.2014
Sample 2 - Core samples from probe stop number 7 that correspond to the chips in sample 1
Sample 3 - Core samples from probe stop number 8 as presented in this report

The probe stops 7 and 8 correspond respectively to the diamond drill holes number 37591 and 37682 according to the notation of the Stillwater Mining Company. The tunnel chainage in which the rock chips from Sample 1 was picked was approximately 1645 meters. Pictures of the samples can be seen in the Figure 5.57-Figure 5.60.

Figure 5.57: Sample 1 to the left, Sample 2 in the middle and Sample 3 to the right

Figure 5.58: Example of rock material from Sample 1

Figure 5.59: Example of rock material from Sample 2

Figure 5.60: Example of rock material from Sample 3

A visual inspection of the rock samples show that there are some difference in mineralogical composition between Sample 1 and Sample 2, despite the fact that Sample 2 was believed to be core sample taken parallel to the tunnel position where Sample 1 was picked. This difference was confirmed by the mineralogical analysis which is presented in chapter 5.4.9.

A summary of the test results from the drillability testing is shown in Table 5.5. Other test results include the Point Load Index and the Vickers Hardness Number Rock (VHNR). The results of these tests were as shown in Table 5.4. The porosity for the rock samples was not tested for, as the information provided by the Stillwater Mining Company stated the rock type norite which was tested is of poor porosity.

	Point Load Index , I_{s50} [MPa]	VHNR [kg/mm^2]
Sample 1	5.0	712
Sample 2	5.0	674
Sample 3	5.1	Not calculated

Table 5.4: Test results for the Point Load Index and the VHNR

Sample No.	1	2	3
Rock type (given by the Client)	Norite	Norite	Norite
Brittleness Value (S_{20})	59.5 High	54.8 High	48.3 Medium
Sievers' J-Value (SJ)	99.8 Extremely low surface hardness	29.6 Low surface hardness	10.7 Medium surface hardness
Abrasion Value Cutter Steel (AVS)	19.5 Medium	7.0 Low	17.0 Medium
Drilling Rate Index™ (DRI™)	71 Very high	60 High	49 Medium
Cutter Life Index™ (CLI™)	25.9 High	24.1 High	11.6 Medium
Quartz content (DTA) (Weight %)	< 1	< 1	< 1
Cerchar Abrasion Index (CAI	5.1 High	3.9 High	5.9 High

Table 5.5: Executive summary of drillability test results

Each individual test result is presented in the following subchapters. In addition to this the results of a performed sieve curve and a chip analysis is presented, as well as the mineralogical analysis of Sample 1 and 2.

5.4.2. Brittleness Test

The Brittleness Test was performed the 30.04.2012 and done according to the procedures given in chapter 4.5.1. Each test sample was composed as shown in Table 5.6-Table 5.8.

Sample 1	Distribution [%]	Component [g]
Mass from rectangular sieve 11.2 mm [g]:	43.3	233
Mass from rectangular sieve 8.0 mm [g]:	45.4	244
Mass from quadratic sieve 11.2 mm [g]:	11.3	61
Sum:	100.0	**538**

Table 5.6: Composition of Sample 1 for the Brittleness Test

Sample 2	Distribution [%]	Component [g]
Mass from rectangular sieve 11.2 mm [g]:	36.8	185
Mass from rectangular sieve 8.0 mm [g]:	49.1	247
Mass from quadratic sieve 11.2 mm [g]:	14.1	71
Sum:	100.0	**504**

Table 5.7: Composition of Sample 2 for the Brittleness Test

Sample 3	Distribution [%]	Component [g]
Mass from rectangular sieve 11.2 mm [g]:	41.3	227
Mass from rectangular sieve 8.0 mm [g]:	49.5	273
Mass from quadratic sieve 11.2 mm [g]:	9.2	51
Sum:	100.0	**551**

Table 5.8: Composition of Sample 3 for the Brittleness Test

The test results and corresponding classification can be seen in Figure 5.61. As can be seen Sample 1 and 2 are classified with high brittleness while sample 3 with medium brittleness. The compaction index of all the samples was given a value of 2 after testing, which means that the material came loose from the testing jar with a small manually applied force.
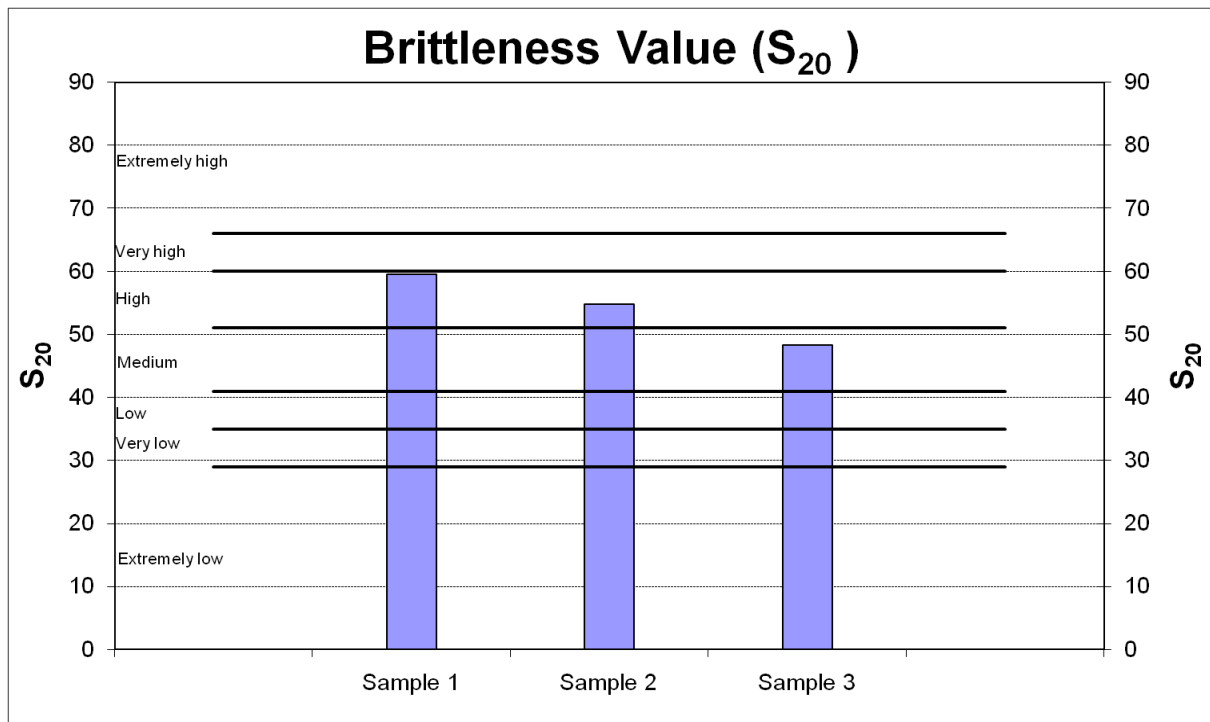
Figure 5.61: Brittleness Test results and classifications

99

5.4.3. Sievers' J (SJ)

The Sievers' J testing was performed the 28.04.2014 and the 29.04.2014. The test pieces used was chosen and cut to pieces to fit the test apparatus by SINTEF personnel. The test results and corresponding classification are shown in Figure 5.62. As can be seen, Sample 1 is classified with extremely low surface hardness, Sample 2 with very low surface hardness, and finally Sample 3 with medium surface hardness.
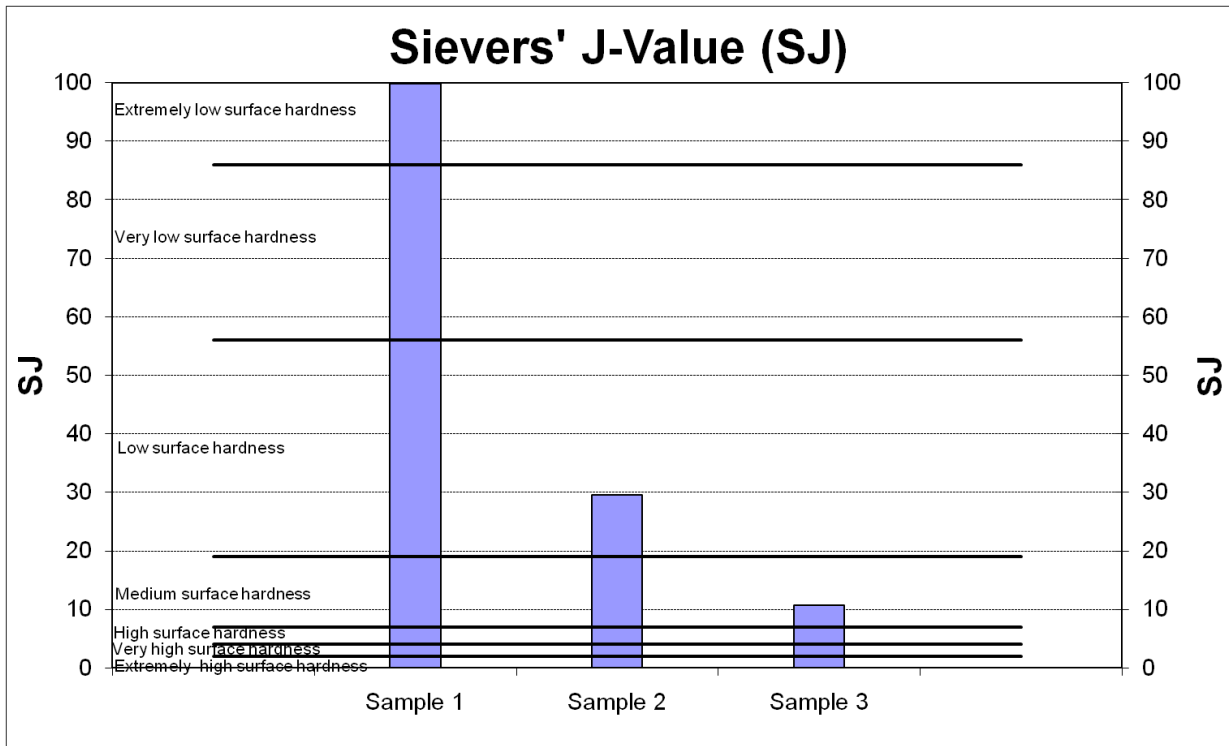
Figure 5.62: Sievers' J test results and classification

The difference between Sample 1 and 2 is surprisingly high as this was supposed to be samples of the same rock material, but one as broken rock chips from the TBM and one as core samples. The first drillings of Sample 2 was done on a core sample which by visual inspection was found to contain a greater amount of light mineral believed to be plagioclase. A second core part from Sample 2 with more similar appearance to the chips in Sample 1 was thusly chosen to do additional drillings, but the test results remained within the same area as the first time. The test result for Sample 2 includes the average of all drillings that was performed for this sample.

Visual inspection of the test piece from the rock chips in Sample 1 showed several fractures in the rock material that might have been caused by the rock breaking process in the TBM. The drill holes in the test piece was also found to contain a high amount of powder after testing.

Results from all drillings for each sample as well as pictures of test pieces are shown in the Figure 5.63-Figure 5.68
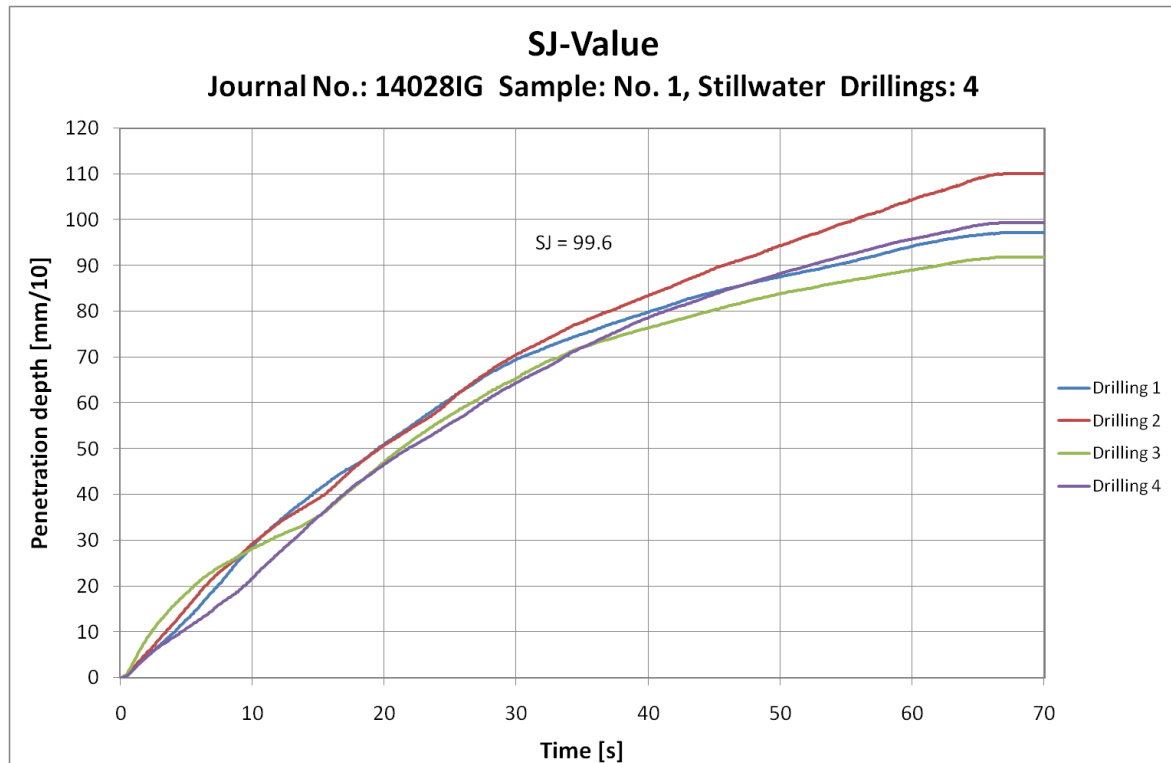
Figure 5.63: Sievers' J drillings for Sample 1
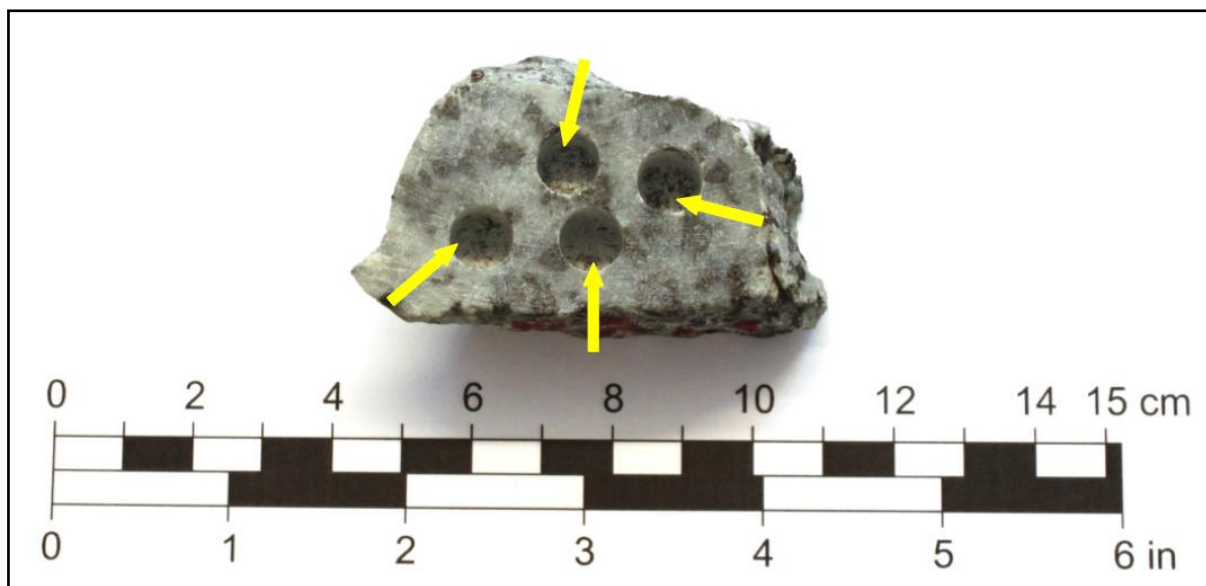
Figure 5.64: Test piece from Sample 1 after drilling
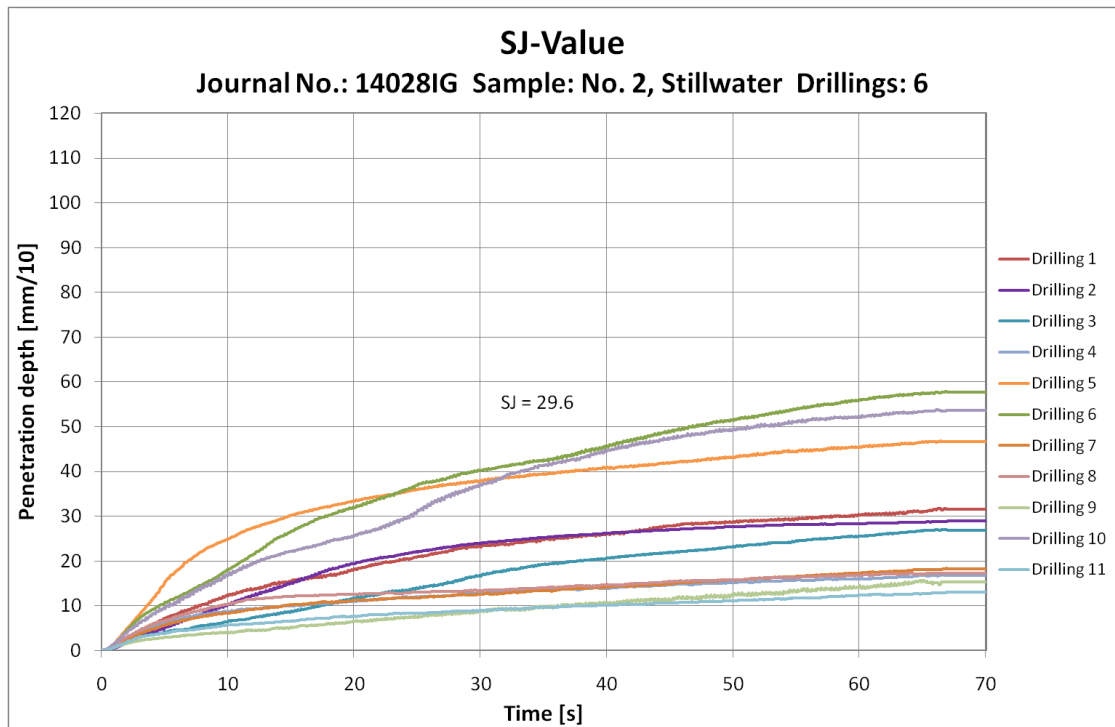
Figure 5.65: Sievers' J drillings for Sample 2
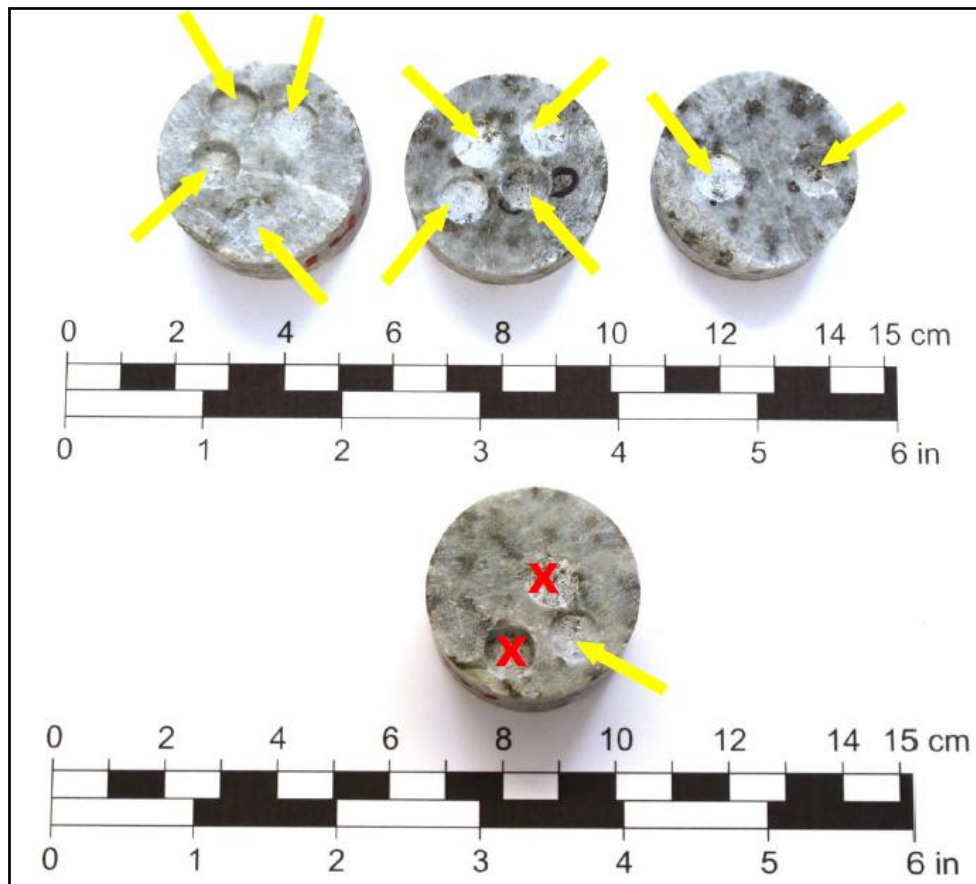
Figure 5.66: Test pieces from Sample 2 after driling. Drillings were performed on both sides of two individual core pieces. Red crosses marks invalid drillings due to machine error
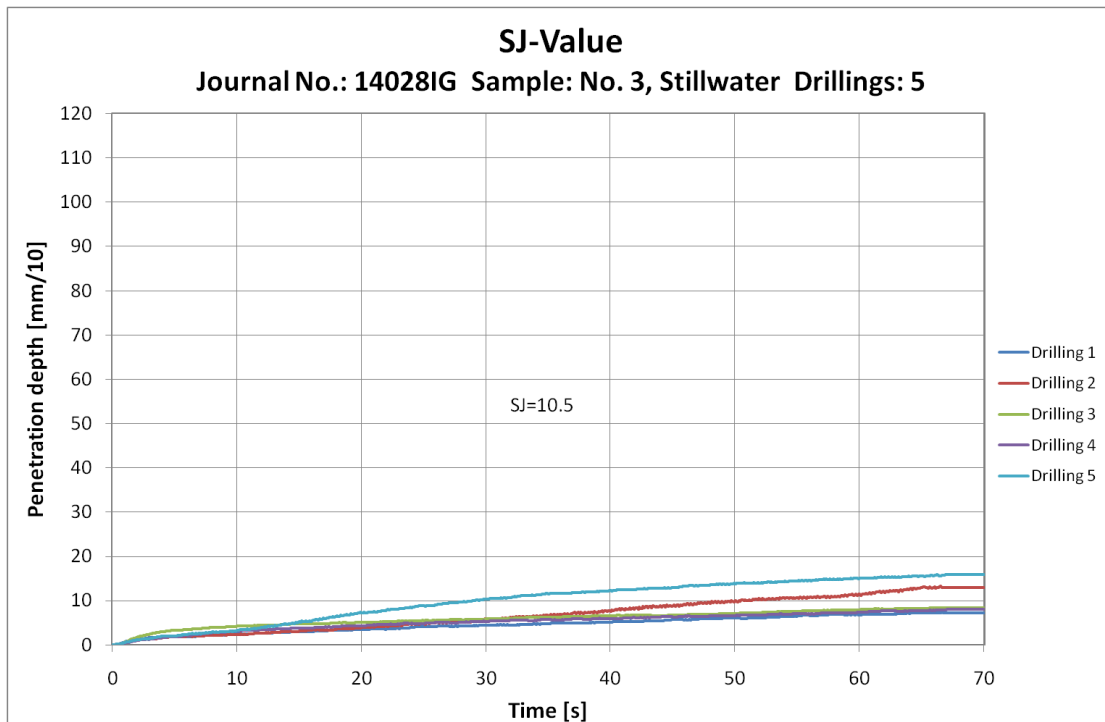
Figure 5.67: Sievers' J drillings for Sample 3
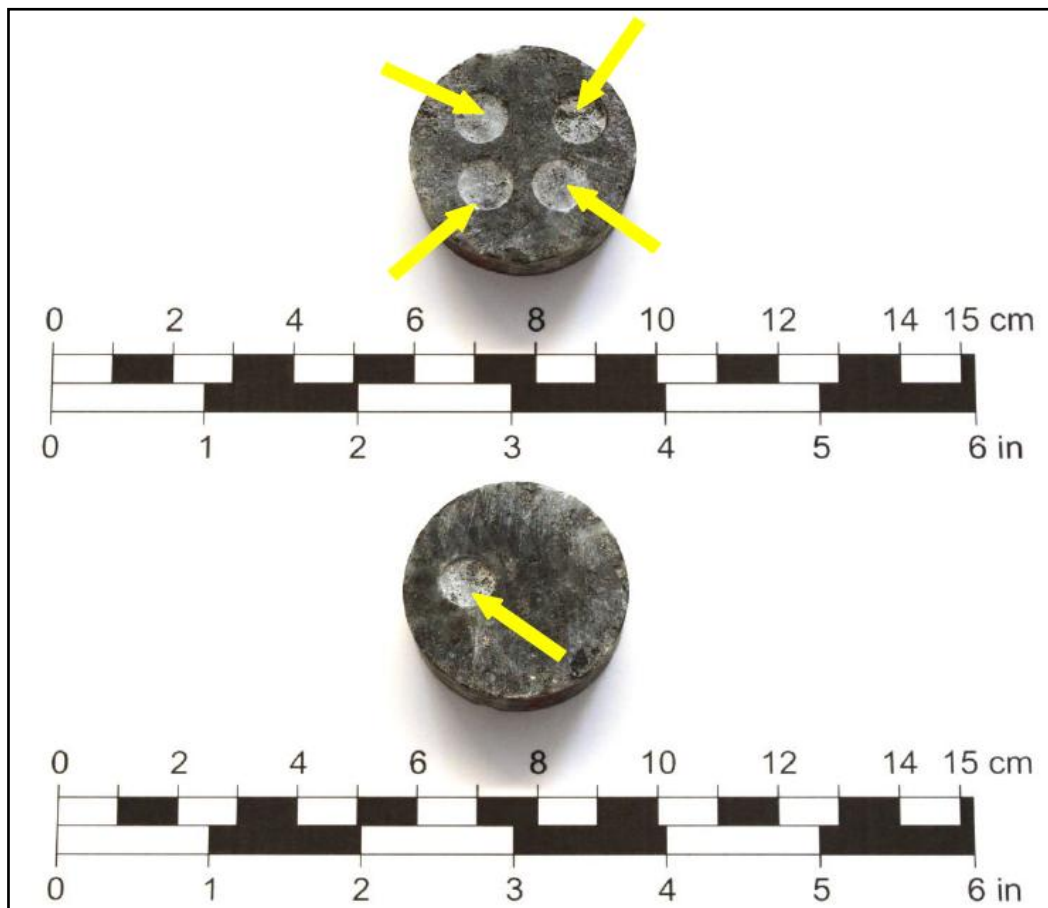
Figure 5.68: Test piece from Sample 3 after drilling. Drillings done on both sides of core piece

5.4.4. Sievers' J Interception Point (SJIP)

Based on the Sievers' J test results the Sievers' J Interception Point was also calculated, and the results are shown in Figure 5.69-Figure 5.71.
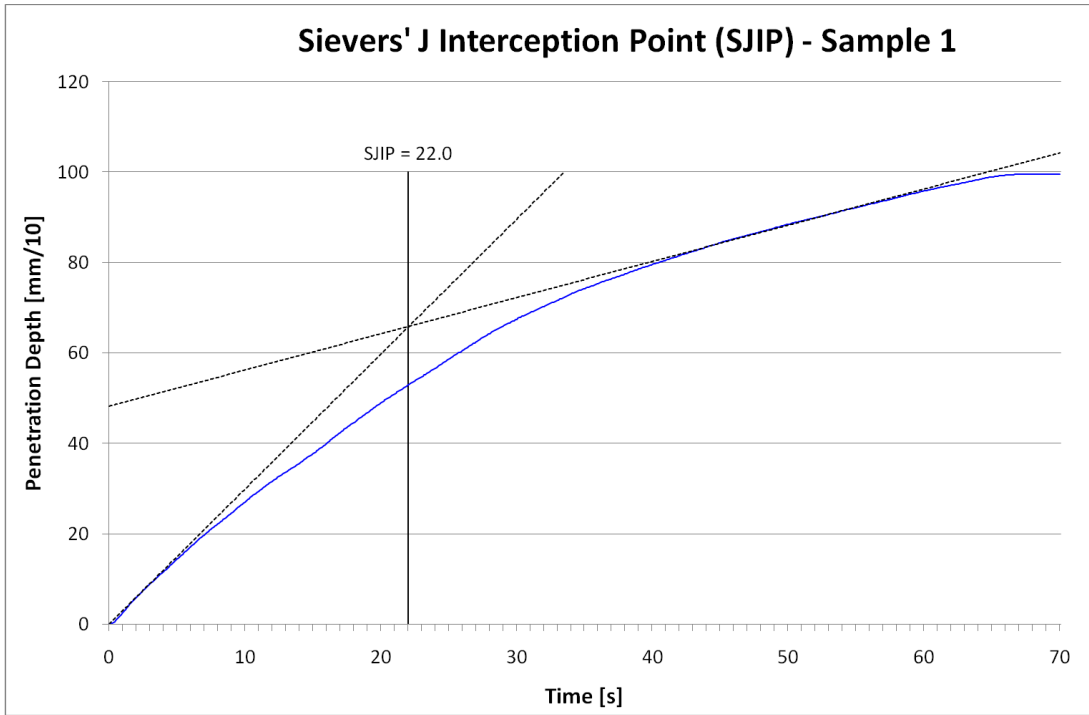
Figure 5.69: Sievers' J Interception Point for Sample 1
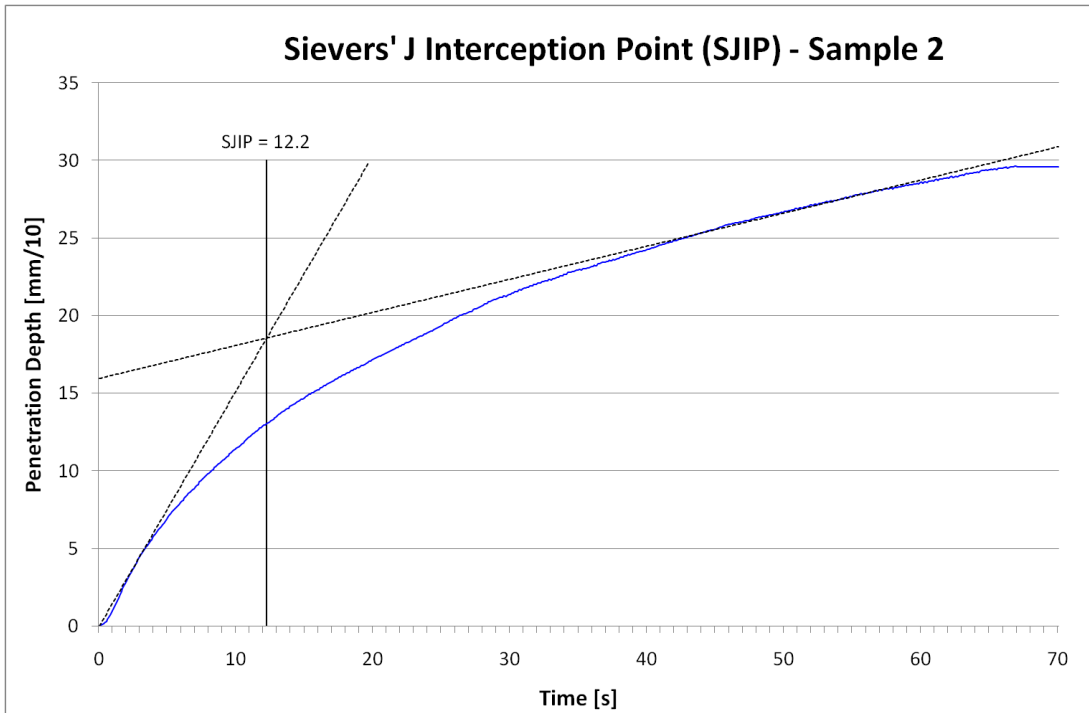
Figure 5.70: Sievers' J Interception Point For Sample 2
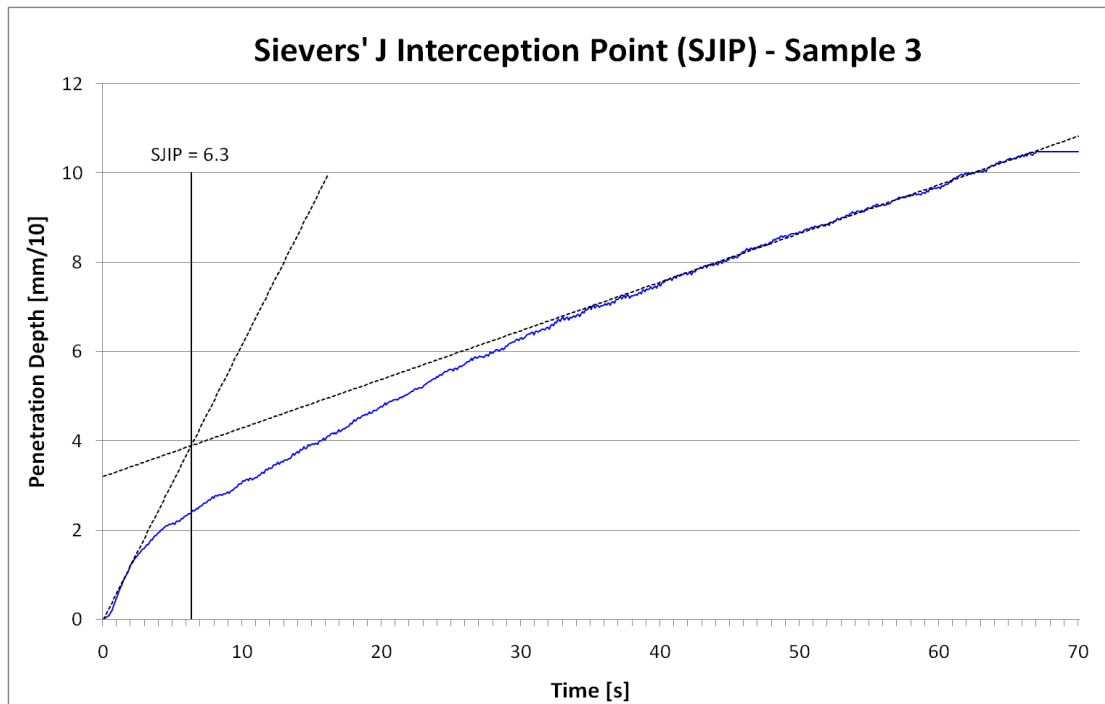
Figure 5.71: Sievers' J Interception Point for Sample 3

By the classification shown in chapter 4.5.3 the samples get the following cutter life classification:

- Sample 1 - Extremely high
- Sample 2 - High
- Sample 3 - Medium

5.4.5. AVS

The AVS testing was performed on the 30.04.2014 and the 02.05.2014 and was done by the procedures presented in chapter 4.5.4. The rock material was crushed in several operations, starting at 5 mm size, then 1 mm before several times at 0.5 mm was done. The method of setting the opening size for the crushing apparatus was done by manually adjusting the opening, which was hard to perform in the same manner for each test sample.

The test results and correlating classifications is shown in Figure 5.72. As can be seen, Sample 1 and 3 are classified as medium abrasive while Sample 2 is classified as low. A possible explanation of the low value of Sample 2 could be mineralogical differences which influence the result. Errors in the procedure to crush down the material could also be a factor as the crushing apparatus had to be manually set, which could cause the opening to be less than the planned 0.5 mm in the final crushing.
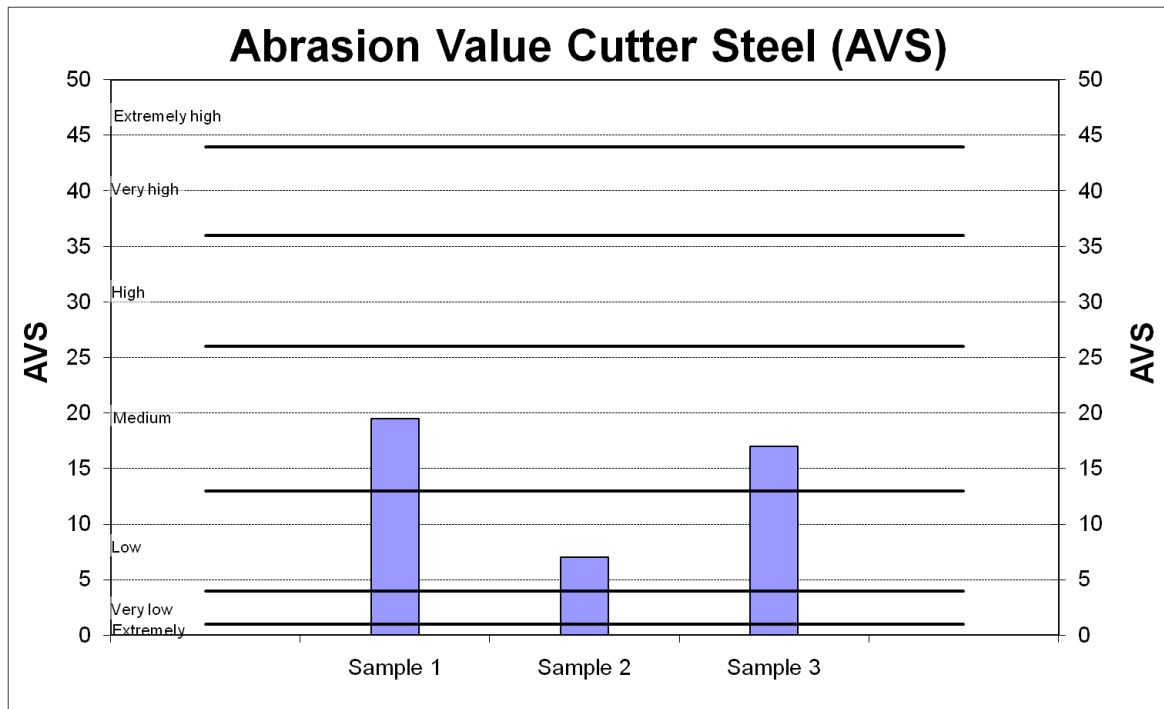
Figure 5.72: AVS test results and classification

5.4.6. The Drillability Indices

Based on the individual test results which have been presented, the Drilling Rate Index™ and the Cutter Life Index™ was calculated. A summary of each test result is given in **Error! Reference source not found.** along with the flakiness number, compaction index, density and quartz content for each sample.

TEST RESULTS

Sample No.	1	2	3
Brittleness Value (S_{20}, 11.2 - 16.0 mm) [%]	59.5	54.8	48.3
Flakiness (f)	1.26	1.31	1.27
Compaction index	2	2	2
Density (ρ) [g/cm^3]	2.85	2.67	2.92
Sievers' J-Value (SJ) [mm/10]	99.8	29.6	10.7
Abrasion Value Cutter Steel (AVS) [mg]	19.5	7.0	17.0
Quartz content (DTA) [weight %]	< 1	< 1	< 1

Table 5.9: Summary of drillability testing

106

The flakiness number is within the same range for all samples, as is also the case for the compaction index which shows how well compacted the material was after the brittleness test. The densities differ somewhat, and is greatest for Sample 3. Sample 2 was the least dense of the samples.

To find the quartz content 40 grams of each AVS sample was crushed down to less than 20 μm and analyzed in a DTA. All of the samples were there found to contain traces of quartz, but less than 1 %.

The calculated drillability indices are shown in Table 5.10. The results of the DRI and corresponding classification is shown in Figure 5.73 while the same for CLI is shown in Figure 5.74. As can be seen Sample 1 and 2 have very high and high drillability and also give a high cutter life, while Sample 3 is classified as medium in both drillability and in cutter life.

CALCULATED INDICES

Drilling Rate Index™ (DRI™)	71	60	49
Cutter Life Index™ (CLI™)	25.9	24.1	11.6

Table 5.10: Calculated drillability indices
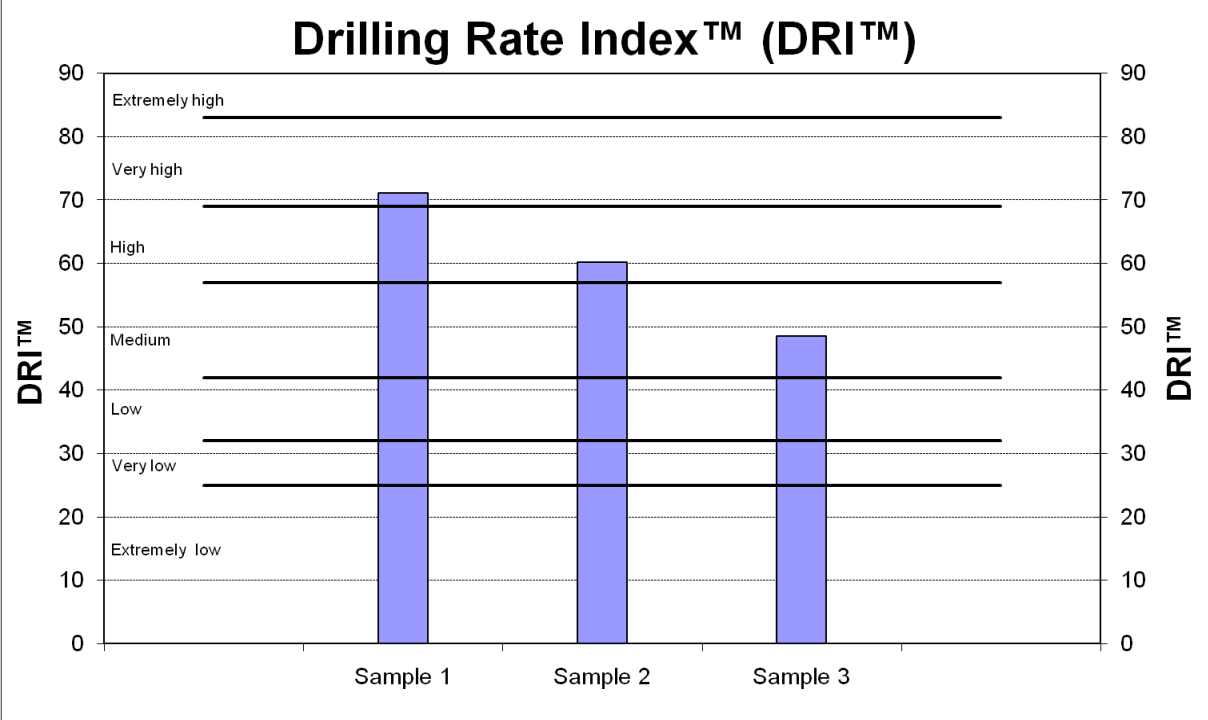
Figure 5.73: Calculated drilling rate index and classifications
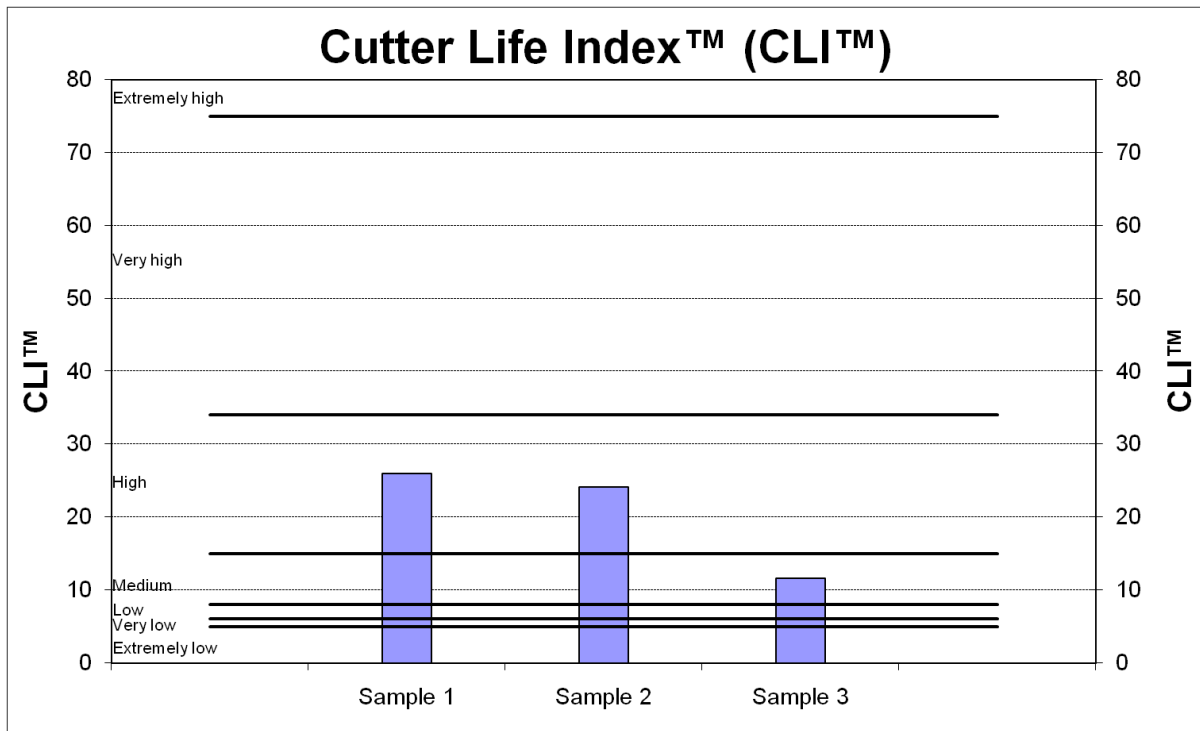
Figure 5.74: Calculated cutter life index and classifications

These results seem to fit the performance of the TBM at the Stillwater Mine well, where both high penetration rates and high cutter life has been observed through the field study. The difference in DRI between Sample 1 and 2 is interesting as both these samples should represent the same rock material. This may be explained by mineralogical differences between the samples or that the rock breaking process in the TBM has caused the test pieces in Sample 1 to get highly fractures with micro cracks and thusly influencing the Sievers' J drill test significantly. The drillability test report is given in Appendix G.

5.4.7. Cerchar Abrasivity Index (CAI)

The Cerchar Abrasivity Index testing was performed on the 13.05.2014. The testing was performed according to the method presented in 4.5.6 with the exception of the execution time. Due to a misunderstanding the time used to pull the pin across the samples was increased from 10 seconds to approximately 60 seconds. The effect of this error is uncertain, but according to Dahl (2014) the test results should not deviate by too much compared with if the test had been performed with the correct execution time.

The test results and the corresponding classification for the three samples is shown in Figure 5.75. A picture of the sample after the testing is seen in Figure 5.76, where the red arrows indicate the direction the pin was pulled in and the direction of which the test progressed.
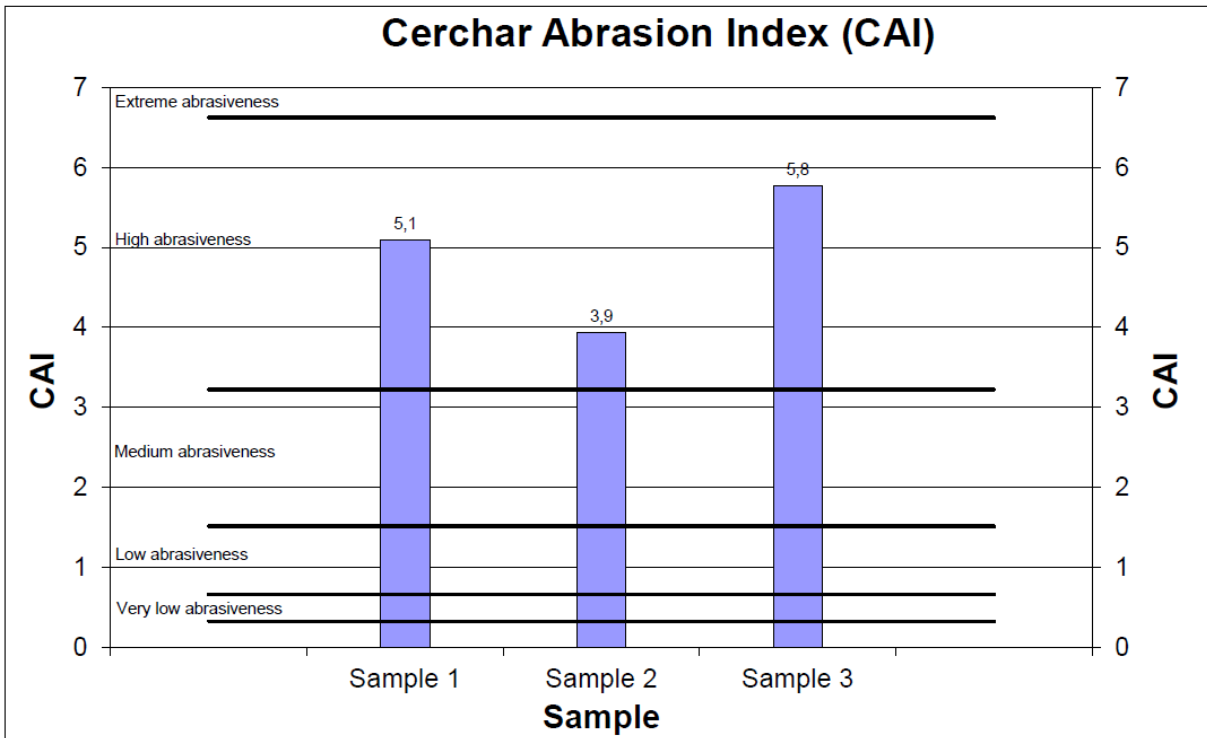
Figure 5.75: Test results for the Cerchar Abrasivity Index testing

Figure 5.76: Picture of the Cerchar Abrasivity Index samples after testing

All three test samples are classified as highly abrasive after the Cerchar Abrasivity Test. By comparing the value for CAI with the values for CLI and AVS, one can find that these results are within the correlation range presented by Dahl et al. (2011). Sample 2 is found to be the least abrasive in both the AVS and the CAI test.

5.4.8. Point Load Index

The Point Load Test was performed on the 28.04.2014. The test was conducted in cooperation with fellow student Andreas Krey Løkås.

Sample 1 consisted of pieces and lumps of material, while sample 2 and 3 were core samples. According to the methods presented in chapter 4.5.11 the dimensions of the pieces had to be converted to a equivalent core diameter before calculating the I_{s50}.

The results of the test can be seen in Table 5.11Table 5.11. All three of the samples are categorized as high strength after Bieniawski (1984). Calculations behind these results are shown in Appendix E. The indicated compressive strengths are within the range for the rock type norite given by the geologists at the Stillwater Mining Company as shown in chapter 3.4 of this report.

	Sample 1	Sample 2	Sample 3
Normalised Index, I_{s50} [MPa]:	5.0	5.0	5.1
Indicated Compressive Strength, σ_c [Mpa]:	80.3	80.5	81.6
Indicated Tensile Strength, σ_t [Mpa]:	4.0	4.0	4.1

Table 5.11: Point Load Index test results

5.4.9. Mineralogical Analysis - XRD

To better be able to explain the differences in test results between Sample 1 and 2, it was chosen to perform a mineralogical analysis of the two samples. The leftover material from the DTA was therefore sent to analysis at the SINTEF lab.

The results of this analysis can be seen in Table 5.12. As can be seen, the main mineral for both samples is plagioclase which represent about two thirds the minerals. The other main mineral for Sample 1 is pyroxene which constitutes the final third of the minerals. This mineral is however just 9 percent of Sample 2. Sample 2 contains a great variety of minerals, including chlorite, alkali feldspar, quartz, calcite and mica. The complete analysis is given in Appendix F.

Sample No.	1	2
Plagioclase	64 %	67 %
Pyroxene	33 %	9 %
Chlorite	3 %	8 %
Alkali Feldspar	< 1 %	3 %
Zeolite	< 1 %	2 %
Quartz		4 %
Calcite		3 %
Mica		4 %
Amphibole		< 1 %

Table 5.12: Results from the Mineralogical Analysis

According to Dahl (2014) the reason why this analysis gives a higher content of quartz for Sample 2 than what was found in the DTA is that the quartz has to be in a structured crystal form to be detected by the DTA. Quartz may however be present bound to other minerals, which is most likely the case here.

The difference in mineralogy for the two samples can explain many of the differences between Sample 1 and 2 that were observed during testing. The many different minerals found in Sample 2 could act as a coating agent for more abrasive minerals in the AVS test which therefore lower the abrasiveness (Dahl, 2014).

The different minerals could most likely also be some of the explanation as to why the Sievers' J drilling gave such a big difference between Sample 1 and 2, but perhaps not account for all of the difference, which was as high as by a factor of 3.

5.4.10. Vickers Hardness Number Rock (VHNR)

Based on the mineralogical analysis presented the Vickers Hardness Number Rock is calculated for both of the samples. The results of this calculation is shown in Table 5.13 and Table 5.14. These numbers can then be used in the NTNU model for estimation of performance and cutter life.

Sample 1	Percentage	VHN [kg/mm^2]	Portion of total hardness
Plagioclase	64 %	800	512
Pyroxene	33 %	600	198
Chlorite	3 %	50	2
Total hardness VHNR			712

Table 5.13: Calculated VHNR for Sample 1

Sample 2	Percentage	VHN [kg/mm^2]	Portion of total hardness
Plagioclase	67 %	800	536
Pyroxene	9 %	600	54
Chlorite	8 %	50	4
Alkali Feldspar	3 %	730	22
Zeolite	2 %	400	8
Quartz	4 %	1060	42
Calcite	3 %	125	4
Mica	4 %	110	4
Total hardness VHNR			674

Table 5.14: Calculated VHNR for Sample 2

It is in this calculation assumed that the pyroxene minerals belong to the orthopyroxene mineral hyperstehene. Zeolite and alkali feldspar is neglected for sample 1, as is amphibole for sample 2, since these minerals constitute less than 1 % of the samples. Mica is given the value of biotite which is a mineral within the mica group. The VHN value for the mineral zeolite was found by consultation of Prof. Amund Bruland the 4th of June 2014.

5.4.11. Sieve Curve

A muck sample was collected the 19.02.2014. The sample was taken directly from the transport conveyor during an emergency stop that was caused by the need for extensive bolting before the TBM could continue boring. Approximately 25 liters of muck was collected. The machine parameters in the moments before the emergency stop was as following:

- 2700 PSI propel pressure which equals to a gross cutter thrust of approximately 280 kN/cutter
- Cutterhead rotation speed of 8 RPM
- Average penetration rate during the stroke at 4.3 m/h

The sample was sieved at the SINTEF Engineering Geology Lab in Trondheim according to the procedure presented in chapter 4.5.5. It was chosen to sieve a quarter of the total muck sample to not exceed the capacity of the sieve apparatus. As the muck sample had been graded during transport a representative sample for sieving was composed based on best personal judgment. The resulting grain size distribution of the muck can be seen in Figure 5.77.
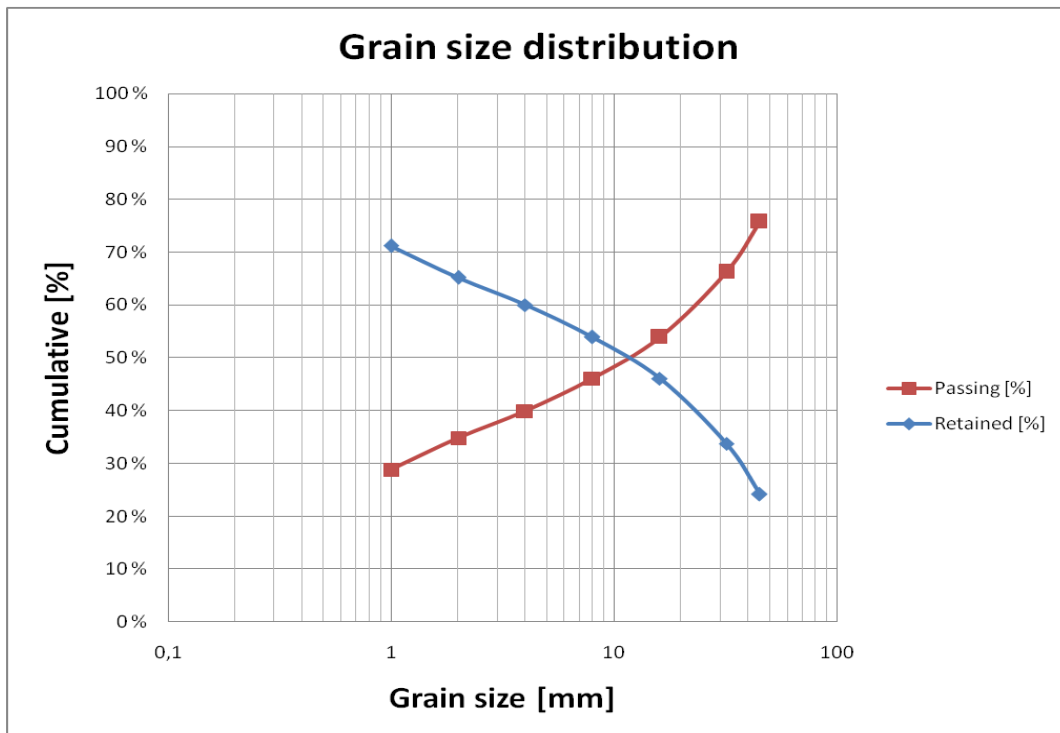
Figure 5.77: Grain size distribution of collected muck sample

As can be seen in the figure half of the muck passes through the sieve at 11.5 mm. This is a fairly high percentage of smaller rock fragments. This can be explained by the fact that during the period of boring where the muck was collected the rock mass was highly fractured, and few sizeable chips were present.

It is normally expected that a lower percentage of larger rock fragments indicates a less efficient rock breaking process, but it is unclear if this is the case. Collection of muck should in this case also have been done in a geological area of less fractured rock in able to better assess the rock breaking efficiency.

5.4.12. Chip Analysis

As a part of investigating the rock breaking process in the TBM one of the rock chips from Sample 1 was chosen to be cut in half at the thickest part by a diamond saw and then checked for crack propagation. The cut chip can be seen in Figure 5.78.

Figure 5.78: Chip cut by diamond saw

The dimensions of the chosen chip were as follows:

- Length - 210 mm
- Width - 70 mm
- Thickness - 26 mm

The cut surfaces of the chip was then investigated visually, and the most prominent cracks that were seen was noted. The chip pieces were then sketched on a piece of paper in order to illustrate the findings. This can be seen in Figure 5.79.
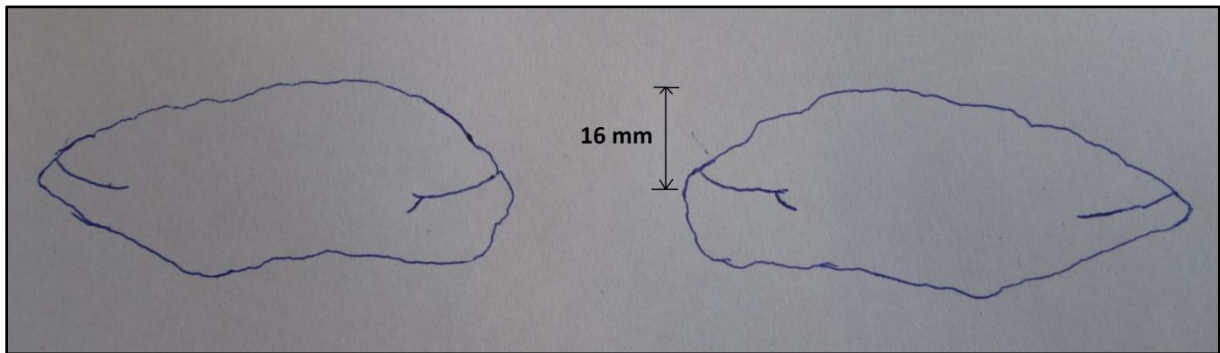
Figure 5.79: Sketched chip with crack formations

As can be seen there are two different cracks that have propagated from the kerf. It is not possible to say if these cracks have formed by one pass of the cutters alone or by several passes. The depth of the cutter edge at chipping is noted in the sketch, and was measured to 16 mm. Together with the chip thickness of 26 mm, one can calculate the kerf depth factor f_{kd} as mentioned in Bruland (1998d) as follows:

$$f_{kd} = \frac{16\ mm}{26\ mm} = 0.62$$

The crack propagation in this investigated case seems to indicate that the chip has been formed by tensile cracks originated at the cutter edge, in accordance with the interpretations given by Bruland (1998d). To further investigate the cracking the chip could have been cut in several slices to form a three dimensional picture of the crack formation. This was however not done in this case.

5.5. Performance Estimation by Using the NTNU Model

In order to get an estimation of performance of the TBM with the use of the NTNU model, the software Fullprof (NTNU, 2009) was used. Only the estimation of penetration rate is focused on in the scope of this work.

5.5.1. Assumptions and Preconditions

The following assumptions and preconditions apply for the estimate made in Fullprof:

- The tunnel length estimated is equal to the meters bored at the end of the field stay, which was 1828 meters.
- The tunnel is divided into 8 different zones corresponding with the zones from the geological investigation. Since the first 372 meters of tunnel was not probed, this part of the tunnel is combined with the first section of probe drilling.
- The drillability values of the geological sample number 2 from chapter 5.4 of this report are chosen to apply for all of the tunnel length.
- The k_s value calculated for each zone in chapter 5.3 is inserted directly into the geological parameters of the estimation.
- The applicable cutter thrust in the estimation is set to 290 kN/cutter, which is the weighted average over the tunnel.
- Working hours of 40 hours per week as explained in chapter 5.1 of this report.
- TBM data as given in chapter 3.3 of this report.
- Other preconditions are kept as given by the software.

This gives the following zones used in the estimation:

Zone number	Length [m]	DRI™	CLI™	Total k_s	Quartz Content
1	594	60	24.1	1.74	< 1 %
2	224	60	24.1	2.08	< 1 %
3	207	60	24.1	1.49	< 1 %
4	173	60	24.1	2.40	< 1 %
5	146	60	24.1	2.65	< 1 %
6	127	60	24.1	2.10	< 1 %
7	224	60	24.1	2.39	< 1 %
8	133	60	24.1	3.04	< 1 %

Table 5.15: Geological zones used in Fullprof estimation

5.5.2. Estimated Performance

The result for the penetration rate given by Fullprof over the entire tunnel length with these assumptions and preconditions was 5.11 m/h with a machine utilization of 36.3 %. These values are both somewhat higher than the actual observed performance, which was 4.8 m/h and 26 %. Especially the utilization differs, but this is also expected as Fullproof is based on civil tunneling projects while the observed tunnel is constructed at a mine.

The biggest uncertainties in this estimation are the geological conditions. Using the same drillability values for all of the tunnel is a great simplification and the calculated k_s values used are also highly uncertain. In addition to this the results would have been different if a different applicable cutter thrust had been chosen. The reason for choosing the weighted average over the tunnel is based on the finding of Macias et al. (2014a).

During the recording of performance data from the TBM, high values of cutter thrust was observed. These values are not corrected for friction or drag, nor for the towing of the backup system. To use an applicable cutter thrust that is equal to the weighted average over the entire tunnel will probably give a somewhat higher value than what is the real cutter load.

5.5.3. Estimated Penetration Rate versus Actual Penetration Rate

The estimated penetration rate for each zone/core number is shown in Figure 5.80 along with the average k_s values and the actual penetration rate for each zone calculated from the shift logs of the TBM.
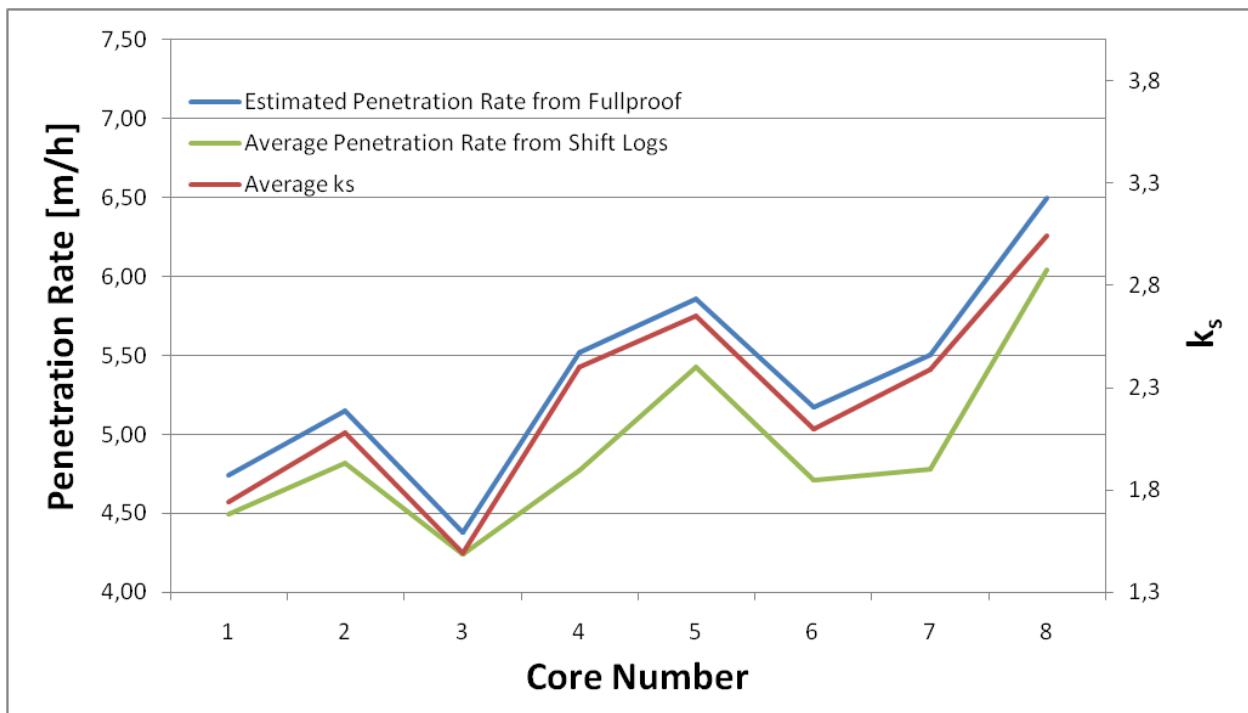
Figure 5.80: Average k_s for each zone compared to estimated and actual penetration rate

One can see that the estimated penetration rate and the actual penetration rate have a good correlation, but that the estimated values are systematically a bit higher than the actual. This could be due to a false input in the estimation, for example if the actual applicable thrust force in the TBM has been lower than what was assumed in Fullprof.

Since the rock mass fracturing factor is said to be the most important factor of penetration rate in the NTNU model it is natural that the estimated penetration rate and the k_s is so closely correlated. Seeing that the actual observed penetration rate follows the same trend as the estimated values, one could argue that the effect of the k_s is correctly understood in the NTNU model.

6.   Discussion

The results of the work done in this thesis and the methods used to obtain them are in this chapter discussed. The main uncertainties can be divided into three categories:

- *Geological uncertainties*
- *Uncertainties in methods used to collect data*
- *Uncertainties in the methods used to process data*

Especially the uncertainties regarding the geological investigation is of importance to the scientific value of these results.

6.1.   Literature Study

Through the literature study conducted it has been found that there are several complicated parameters and factors influencing the rock breaking process in a TBM drive. The indentation seems to be of high importance, as it determines how efficiently energy is transmitted from the cutterhead to the rock, and thereby how efficient the rock chipping will be. This in its turn will influence the penetration rate of the TBM.

It seems that there is an agreement between a multitude of researchers that the chipping mechanism in a TBM is caused by a tensile mode of failure, and not by shear failure as has been believed by some. The processes of indentation, chipping and penetration are highly influenced by several geological and machine factors, which have been recognized in the literature reviewed. Regarding the geological conditions it seems obvious that the degree of fracturing is of special importance alongside the drillability of the rock.

These main findings from the literature study are supported by the results of the field study and laboratory testing performed in this thesis.

6.2.   Field Testing

Both the penetration tests and the RPM trials done at the Stillwater Mine have given the results that were expected. With increasing thrust force the penetration rate of the TBM increases exponentially, and with a decreasing RPM the basic penetration rate goes up. There are however several uncertainties regarding this testing that have to be considered.

.

As there was no computer logger on the TBM at the Blitz Project, all performance data during the tests was noted by the author of the thesis. The TBM operator could not be used to log data as a sensor for the TBM conveyer was broke, which made it hard for the operator to focus on other things than making sure that the belt was not overloaded and clogging up the cutter head. This logging of data by the author is a possible source of error for the testing. Values had to be averaged by best personal judgment. In addition to this, the fact that geological sampling of rock chips had to be performed at the muck carts of the train instead of from the TBM conveyor represents a big uncertainty for the results achieved. Since rock was picked from the top of full muck carts, the material was most likely graded to some extent.

The fact that the penetration tests and RPM trials had to be done over several strokes, makes the geological influence harder to control. For a RPM test with 5 different RPM levels a total length of 9 meters is bored. The rock mass properties will most likely change during this length of tunnel.

It should also be mentioned that testing done after 19.02.2014 is in curve with radius 610 meters. The effect of this on the test results is however believed to be of small importance. .

6.3. TBM Performance Data

Through the performance data collected from the TBM it is found that the average penetration rate of the TBM after 1828 meters bored is 4.8 meters per hours, which is a relatively high value. The high value is most likely due to beneficial geological conditions with a high degree of fracturing throughout the tunnel drive. This is to some extent confirmed by the limited geological investigation done in the thesis.

The average utilization of 26 % is not very high, but one must keep in mind that this tunnel is part of a mine and not a civil tunneling project which is often used for comparison. Also the utilization should have been adjusted to exclude the time used to install additional rock support in areas where this has been needed. If this had been done, the utilization would have gone up.

The gross average cutter thrust found by processing the shift logs can be said to be high, as the highest value found was 349 kN/cutter. The maximum recommended load from the producer of the cutters is 311 kN/cutter. The reason for these high values is most likely from the fact that no correction for friction, drag or towing of the TBM backup has been done. Had this been considered the values of cutter thrust levels would most likely have been within the maximum recommended.

Luxner (2014) states that the use of the TBM at the Stillwater Mine has been a great success so far, as it has been 46 % cheaper and 5.1 times faster than constructing a similar drive by the use of conventional methods at the mine. One must keep in mind that this comparison is done based on experience data from this specific mine. Nevertheless this supports the findings in the literature study that when the geological conditions are suitable the advantage of using a TBM instead of conventional Drill & Blast Tunneling can be substantial (Macias and Bruland, 2014; Maidl et al., 2008).

The biggest uncertainties in the work of processing the shift logs used to assess the TBM performance are as follows:

- Values noted by the machine operator does not necessarily represent the true averaged value over the shift
- The value of machine hours noted by the operator seems in many cases to have been rounded up or down to the nearest whole hour. The error this represent is mineralized by averaging values over longer tunnel lengths in the calculations
- Where values for machine hour are missing, these values have had to be estimated by the author of this report.
- As no tunnel chainage is systematically noted by the operator, an accumulated tunnel chainage based on meters bored for each shift has been noted by the author

6.4.   The Influence of RPM on Performance

One of the main goals of this thesis has been to investigate the influence of RPM on TBM performance. The amount of field testing conducted has not been satisfactory, but the few results obtained are interesting. The most promising results are shown in Figure 6.1 and Figure 6.2. In these figures one can see that there is a trend for the basic penetration rate in mm/rev to be increasing with reduced RPM. The reason for this is most likely because of a more beneficial loading rate between the cutters and the rock.

The tests shown in these figures are a mix of tests with geological sampling and tests without geological sampling which have more uncertainties related to them. The most valuable test in this regard is in the authors opinion the RPM trial done at 3300 PSI (345 kN/cutter). In this test the geological conditions kept stable, and five levels of RPM was tested. This test shows a clear trend of increased basic penetration with decreasing RPM, with a optimum at 8 RPM.

Regarding the penetration rate in meters per hour, this is less influenced by the RPM, but it can be found that a lower RPM gives a lower penetration rate. When considering a operational perspective this helps to understand why the TBM at the Stillwater Mine has been driven mostly at the highest levels of RPM. One must however keep in mind that increased RPM gives a higher rolling velocity of the cutters and higher peak loads on the cutters. This will in its turn affects the cutter consumption of the TBM. Considering that these test show a lower basic penetration per cutterhead revolution for the higher RPMs, this will also have an effect on cutter life as the distance rolled by the cutters will be longer.
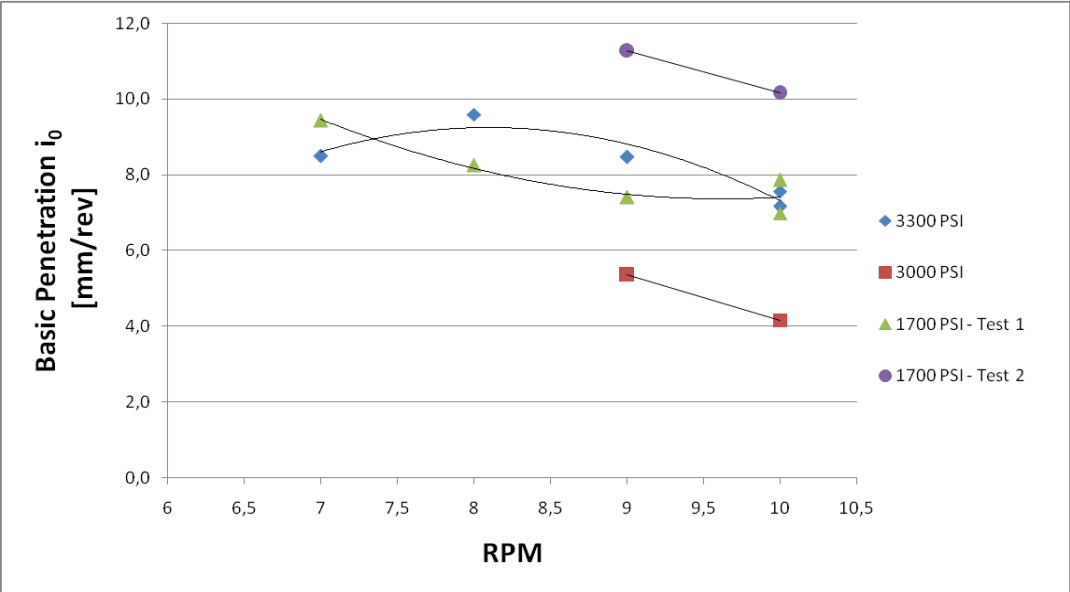
Figure 6.1: Summary of RPM trials with respect to basic penetration
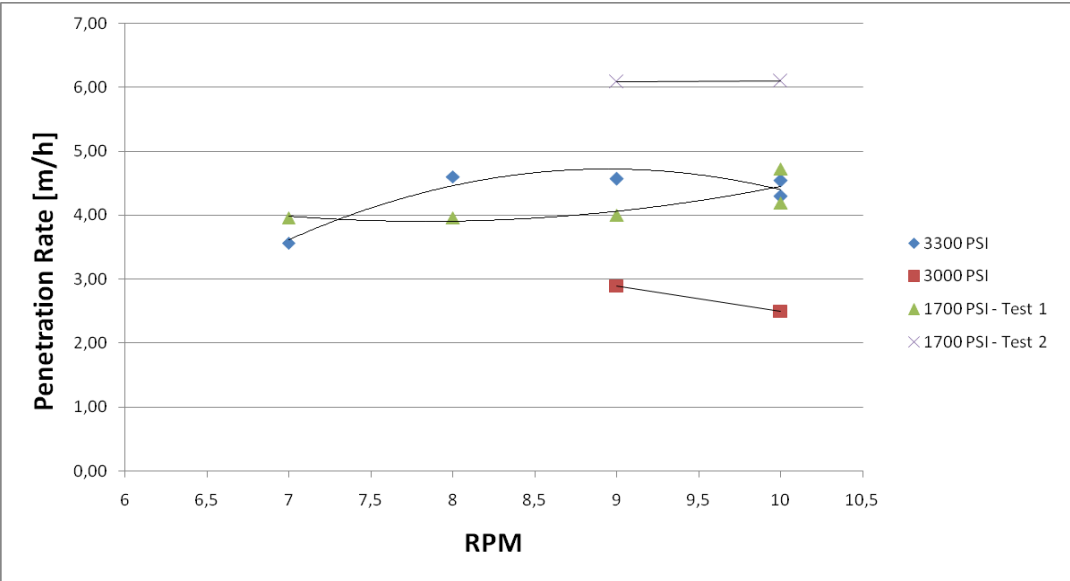
6.2: Summary of RPM trials with respect to penetration rate

122

In addition to the RPM trials conducted, the RPMs effect on TBM performance was also investigated by the use of the available data from shift logs. This data is shown again in Figure 6.3.
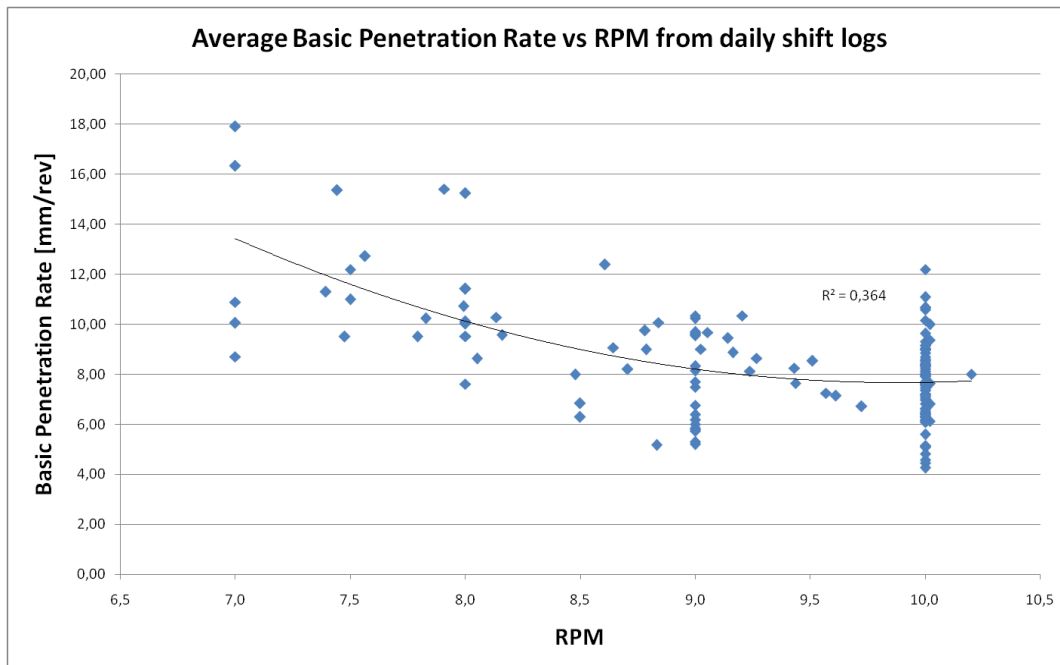
Figure 6.3: RPM versus basic penetration rate from shift logs

From these data it is also possible to see a trend that when the cutterhead RPM is lowered, the basic penetration of the TBM goes up.

It was noted during the field stay that the main limitations of the penetration rate in areas of high degree of fracturing has been the ability to remove the muck quickly enough to avoid burying the cutterhead. When this case is most dominant in the tunnel, it is natural that the basic penetration will increase with decreasing RPM. This is because the penetration rate would be the same no matter the RPM as long as the advance is limited by the capacity of the conveyor system.

However some of the geological testing performed was done in areas where the rock was of such high competency that the conveyor no longer was the limiting factor. Also in this case it is clear that the basic penetration is influenced by the RPM of the cutterhead. The amount of testing performed under these conditions is far from sufficient to be able to draw any conclusions. It is however clear that the RPM's effect cannot be disregarded, and further research should be performed on this matter, and a correction factor for cutterhead RPM included in the NTNU prediction model.

123

6.5.   Cutter Life

Based on the very limited assessment of cutter consumption based on the cutter change logs provided, it can be found that the cutter life in the TBM used in the Blitz Project is high. This is also supported by the laboratory results regarding cutter life for the geological samples chosen. The cutter ring samples sent to the SINTEF laboratory in Trondheim show only normal abrasive wear, no of chipping or mushrooming. These cutter ring samples, along with the cutter change logs gathered could be used to further assess the cutter consumption of the Blitz Project in the future. The cutter ring samples collected are marked with serial numbers, which makes it possible to find the position the ring had on the cutter head through the use of the cutter change log.

The low wear is most likely due to favorable geological conditions. However there are some very important operational factors that contribute to this too. The TBM at the Stillwater Mine is being driven with a fairly stiff cutterhead, as the side and roof support is high during boring. This reduces the vibration of the cutterhead, and thereby the cutter wear. The fact that cutters are changed before reaching a high amount of wear and that several cutters are changed at the same time, keeps the cutterhead as uniform as possible and thusly reducing high momentary cutter loads.

6.6.   Geological Investigation

The geological investigation performed in the work of this thesis through the analysis of core samples has given some interesting findings. The effect of k_s on both penetration rate and on the applicable thrust force seems clear, and coincide with the findings of Macias et al. (2014b). A thrust reduction was observed in areas of high rock mass fracturing which is believed to be an operational decision of the TBM operator in order to avoid machine damage and excessive cutter wear. The main results are presented again in Figure 6.4 and Figure 6.5.
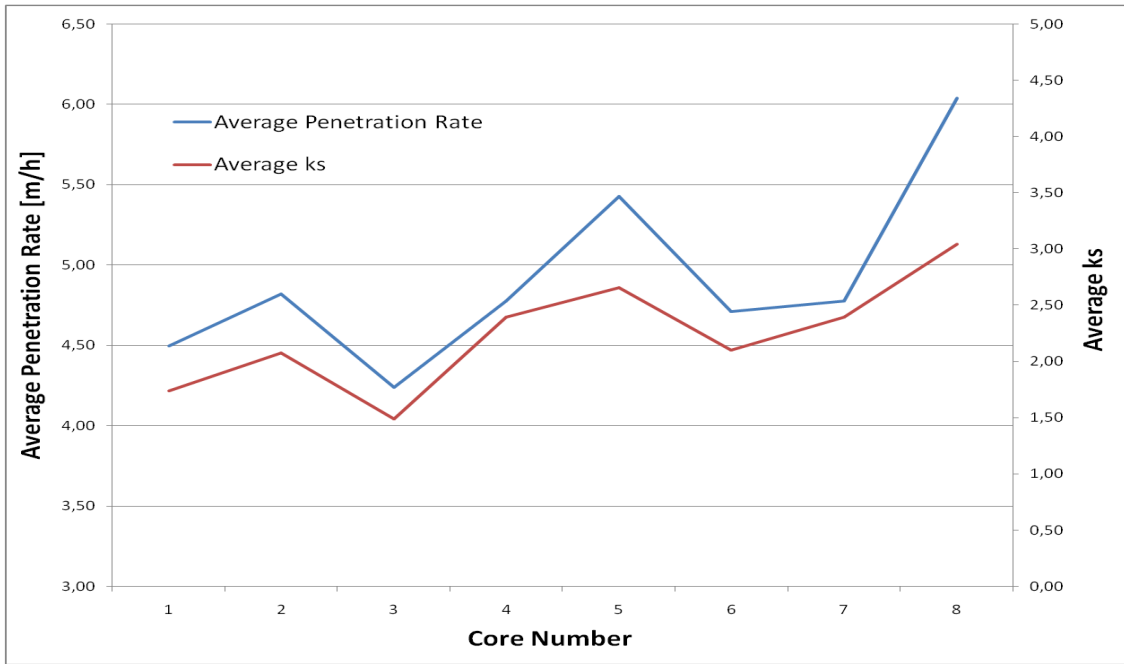
Figure 6.4: Correlation between average k_s and average penetration rate for each tunnel section
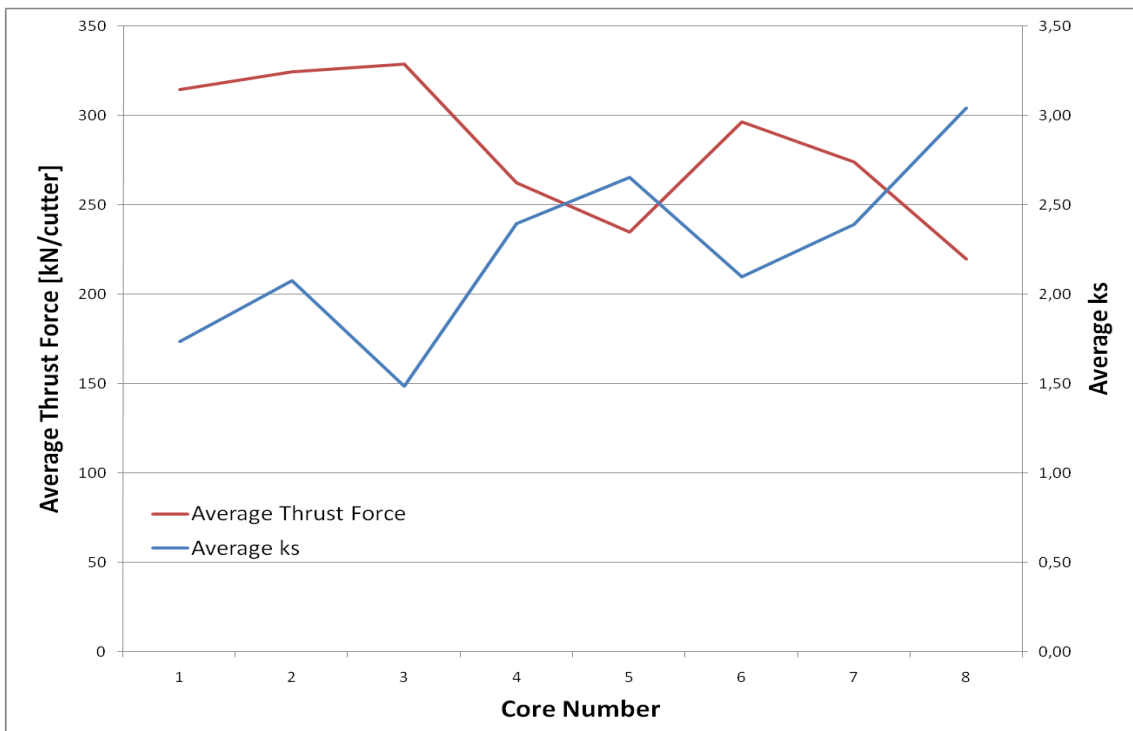
Figure 6.5: Correlation between average k_s and average thrust force applied for each tunnel section

The uncertainties related to the methods of estimating k_s are high. Due to limited geological information, many assumptions and simplifications has had to be made in order to perform the necessary calculations. The biggest of these uncertainties are listed as follows:

- The use of only one fracture set in estimating k_s
- The simplification of giving the fracture sets a dip of 70 degrees for the entire tunnel length
- The angles used for correlating geological data from core samples to a tunnel chainage are read off drill logs. Where values for longer tunnel sections are missing, the value of neighboring section is used
- The effect of Marked Single Joints is neglected
- The sectioning of the tunnel into eight parts based on the probe stops

The data collected and used in the estimation of an average k_s for each of the eight tunnel sections chosen should be treated more in depth at a later stage. The tunnel should be sectioned into much smaller intervals, and the k_s of these parts compared with performance data from the TBM shift logs from corresponding tunnel chainage. However the trends of this simplified and preliminary analysis of rock mass fracturing seem to support the findings of the literature study of this thesis, most notable by Macias et al. (2014a; 2014b).

The k_s has an significant impact on the penetration rate of the TBM, and also influences the applicable thrust force. This causes the k_s to have an indirect effect on the TBM performance. As described by Macias et al. (2014b), there will therefore be two different cases of what factors influence the penetration rate of the TBM the most. When the k_s is low the thrust force will be the main parameter in estimating the penetration rate, but when the k_s is high the thrust force can no longer be used as the most important input.

The core logging method of the Stillwater Mining Company also gives most of the information needed to calculate a traditional Q-value. Only information about water characteristics of the rock mass and stress conditions miss in order to do this. It would be interesting to see how a calculation of Q-value for the different tunnel sections would compare to the performed analysis of the rock mass fracturing factor.

6.7. Laboratory Testing

The summary of drillability testing performed results is shown again in Table 6.1.

Sample No.	1	2	3
Rock type (given by the Client)	Norite	Norite	Norite
Brittleness Value (S_{20})	59.5 High	54.8 High	48.3 Medium
Sievers' J-Value (SJ)	99.8 Extremely low surface hardness	29.6 Low surface hardness	10.7 Medium surface hardness
Abrasion Value Cutter Steel (AVS)	19.5 Medium	7.0 Low	17.0 Medium
Drilling Rate Index™ $(DRI™)$	71 Very high	60 High	49 Medium
Cutter Life Index™ $(CLI™)$	25.9 High	24.1 High	11.6 Medium
Quartz content (DTA) (Weight %)	< 1	< 1	< 1
Cerchar Abrasion Index (CAI	5.1 High	3.9 High	5.9 High

Table 6.1: Executive summary of drillability test results

One can from these results see that the range of DRI™ for the three samples tested is between medium and very high, while the range of the CLI™ for the same samples is medium to high. These results match the observed performance of the TBM with high penetration rates, and the cutter life calculated. The test results coincide well with the correlations between different test presented by Dahl et al. (2011).

Through the work with the laboratory testing it was found that the result in drillability testing for the two different samples which were believed to be rock chips from the TBM and corresponding core samples has given some surprising result. The difference in the Sievers' J value for these two test samples was as high as by a factor of 3, which gives rise to speculations that one cannot use rock chips as direct substitutes for core samples when testing for the drillability indices. Much of the difference observed in this case can however be explained by the mineralogical difference in the two samples. As the core samples from Sample 2 were picked from a depth of almost 200 meters in the core hole, the distance from the core to the tunnel at this point would have gotten big enough for the geological properties to change. The micro fractures observed in the chip samples used for testing indicates

nonetheless that there are factors that needs to be accounted for when using rock chips for drillability testing instead of core samples or other intact rock.

The limited analysis of a rock chip sample seems to support the findings in the literature study, namely that the chips break of the rock surface through a tensile mode of failure.

The biggest uncertainties in the laboratory testing is associated with how the tests were performed by the author For example how the apparatus for crushing down the material to be used in AVS testing was configured was something that was hard to do in the same manner for each test sample. If the material is crushed into a finer grade than what was intended, this will of course highly influence the test result.

6.8. Comparison of Estimated Performance and Actual Performance

The results of the comparison between estimated performance by using the NTNU model and the actual penetration rate found in the shift logs is shown again in Figure 6.6.
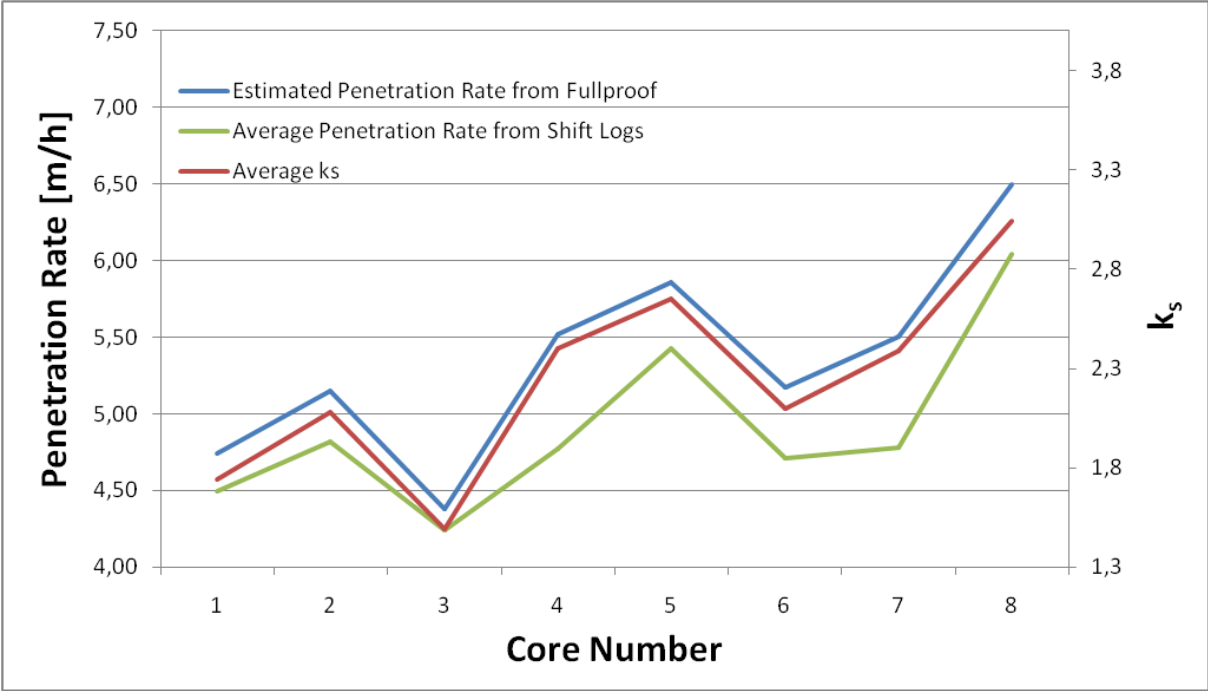
Figure 6.6: Comparison of estimated performance and actual performance

One can from this see that a there is a good correlation between the estimated penetration rate and the actual penetration rate. Also shown is the k_s value used in the estimation, which was calculated in the geological investigation for each of the probe stops, as presented earlier.

This result indicates that the NTNU model is a good tool to estimate the performance rate of a TBM. One can see that the estimated value is strongly correlated with the k_s, which is natural since this is the most important rock mass property used in the model.

The biggest uncertainties in this estimation can be listed as follows:

- Drillability results for Sample 2 tested in the laboratory was chosen to represent the entire tunnel length.
- The applicable thrust force used in the model was the averaged thrust applied found from the shift logs. The validity of this value is uncertain.

Even considering that this estimation is based on values which have been found through a long series of assumptions and simplifications, this is a good estimation from the NTNU model compared with the actual performance.

7.   Conclusive Remarks

The main objectives of this thesis were to document and assess the effect of RPM on the rock breaking and performance of a TBM, to assess the effect of rock mass fracturing on TBM performance, and to perform a complete geological testing of rock samples from the tunnel visited.

The limited results of the RPM trials performed show that the RPM in fact has an effect on the rock breaking. In all cases of testing a higher penetration per cutterhead revolution was observed, and analysis of the rock chip sizes showed that the rock broke off the tunnel face in a more efficient way.

The rock mass fracturing factor k_s is found to have a great influence on TBM performance. As expected a strong correlation between penetration rate and rock mass fracturing has been found. In addition to this a correlation between rock mass fracturing and applicable thrust force from the TBM has been found. This effect is of importance because most TBM prediction models use the cutter thrust as their most important machine factor when estimating penetration rate. When the rock mass is too highly fractured, it seems obvious that the applicable thrust used in the penetration models should have a correction factor consider this effect.

The laboratory research performed confirms that the established drillability testing at the NTNU/SINTEF laboratory provides valuable and correct input to be used in estimating TBM performance. The observed difference in Sievers' J drillability test between rock chips and core samples is interesting. Even if most of the difference in this case can be explained by mineralogical differences and micro fractures in the rock chips, more work should be done in assessing this difference.

In summary the Stillwater Mine is an excellent site for conducting research like this. The amount of information available is high, and geological conditions with a high degree of rock mass fracturing can be used to further assess the k_s value's effect on TBM performance. Especially a geological back mapping of the tunnel could easily be done, as the rock mass is exposed for the entire tunnel length.

8.   Further Work

A great amount of data has been collected during the work of this Master's Thesis which can easily be used for further research by the department. The Blitz Project at the Stillwater Mine is an excellent tunnel to use for research, as it runs through rock with geological conditions that makes it ideal to investigate the rock mass fracturing factors effect on performance.

In particular a full geological back mapping of the so far bored tunnel at the Blitz Project would provide highly valuable information. This information could be compared with collected shift log data, and even with the gathered geological information from probe drilling ahead of the TBM. The data of these probes could also be treated in much more detail than what has been done in the scope of this work. More time should be invested into sectioning the tunnel into smaller intervals and investigate if the rock mass fracturing still has a as good correlation with the performance data as was found in this report.

The work regarding assessing the RPMs effect on rock breaking and penetration rate should be continued, and a complete RPM trial should be tried completed in tunnel sections of more favorable geological conditions than what was encountered during this field stay. Should the trends found in the limited testing of this thesis be correct, a factor for cutterhead RPM should be added to a future update of the NTNU model.

The shift logs that were digitalized in the work of this thesis also contains information not utilized in the work of this thesis, which could be of interest at a later stage. Among other things is a systematical registration of rock support measures installed in addition to normal bolting patterns. Data to be used in research of cutter wear and wear mechanism has also been collected, even if not treated in detail in the work of this thesis. A complete cutter change log along with four individual face cutter samples which have been sent to the SINTEF lab in Trondheim could give valuable information.

When considering the laboratory tests performed in the work of this thesis, it is clear that the parameters influencing these are well understood by NTNU and SINTEF. However, work should be conducted in order to better understand the processes behind the Sievers' J testing. It is for now believed that one can use rock chips from the TBM and core samples from pre investigations alike, but this was not the case for the testing done here. The mineralogical influence is most likely a big explanation, but the difference was observed to be so high that micro fractures in the chips from the rock breaking process must have played a part in the results.

References

Bieniawski, Z.T. (1975). The Point-Load Test in Geotechnical Practice. *Engineering Geology,* 9(1): pp. 1-11.

Brook, N. (1985). The Equivalent Core Diameter Method of Size and Shape Correction in Point Load Testing. *International Journal of Rock Mechanics and Mining Sciences and Geomechanics,* Abstracts 22(2): pp. 61-70.

Bruland, A. (1998a). *Hard Rock Tunnel Boring Vol. 3: Advance Rate and Cutter Wear.* NTNU-Anleggsdrift: Project Report 1B-98, Trondheim.

Bruland, A. (1998b). *Hard Rock Tunnel Boring Vol. 5: Geology and Site Investigations.* NTNU-Anleggsdrift: Project Report 1D-98, Trondheim.

Bruland, A. (1998c). *Hard Rock Tunnel Boring Vol. 6: Performance Data and Back-mapping.* NTNU-Anleggsdrift: Project Report 1E-98, Trondheim.

Bruland, A. (1998d). *Hard Rock Tunnel Boring Vol. 7: The Boring Process.* NTNU-Anleggsdrift: Project Report 1F-98, Trondheim.

Bruland, A. (1998e). *Hard Rock Tunnel Boring Vol. 8: Drillability - Test Methods.* NTNU-Anleggsdrift: Project Report 13A-98, Trondheim.

Bruland, A. (2000). *Hard Rock Tunnel Boring Vol. 1: Background and Discussion.* Doctoral thesis at NTNU, Trondheim.

CSM - Colorado School of Mines (2008). *Computer Modeling for Mechanical Excavators.* Article online. Available at: http://emi.mines.edu/EMI-Hard-Rock-Tunnel-Boring-Machines *(Visited 05.12.13)*

Dahl, F. (2003). *The Suggested DRI™, BWI™, CLI™ Standard.* Available at: http://www.drillability.com (Visited 13.05.2014)

Dahl, F. (2013). *Interview with Filip Dahl, laboratory manager at SINTEF Geological Engineering Laboratory,* Trondheim (03.12.2013)

Dahl, F. (2014). *Interview with Filip Dahl, laboratory manager at SINTEF Geological Engineering Laboratory regarding Drillability Test Results,* Trondheim (21.05.2014)

Dahl, F., Bruland, A., Grøv, E. and Nilsen, B. (2010). *Trademarking the NTNU/SINTEF drillability test indices*, Tunnels & Tunnelling International: pp. 44-46

Dahl, F., Bruland, A., Jakobsen, P., Nilsen, B. and Grøv, E. (2011). Classifications of properties influencing the Drillability of rocks, based on the NTNU/SINTEF test method. *Tunnelling and Underground Space Technology,* 28(1): pp. 150-158. [Online] DOI: 10.1016/j.tust.2011.10.006

Dahl, F., Grøv, E. and Breivik. T. (2007). Development of a new direct test method for estimating cutter life, based on the Sievers' J miniature drill test. *Tunnelling and Underground Space Technology,* 22(1): pp. 106-116. [Online] DOI: 10.1016/j.tust.2006.03.001

Ewendt, G. (1989). *Erfassung der Gesteinsabrasivität und Prognose des Werkzeugverschleisses beim machinellen Tunnelvortrieb mit Diskenmeisseln.* Bochumer Geologische und Geotechnische Arbeiten, 33, Dissertation at the Ruhr University Bochum

Frenzel, C. (2010). *Verschleisskostenprognose für Schneidrollen bei maschinellen Tunnelvortrieben in Festgesteinen*, Doctoral thesis at the Technical University of Munich

Gaye, F. and Stephens, T.N. (1981). *A theory of disc cutting in medium and hard rocks.* Report, Transport and Road Research Laboratory, Crowthorne, UK.

Gehring, K. (1995). Leistungs- und Verschliessprognosen im maschinellen Tunnelbau, *Felsbau,* 13(6): pp. 439-448

Gong, Q.M., Zhao, J., Jiang, Y.S. (2006). In situ TBM penetration tests and rock mass boreability analysis in hard rock tunnels. *Tunnelling and Underground Space Technology,* 22(3): pp. 303-316 [Online] DOI: 10.1016/j.tust.2006.07.003

ISRM (1985). Suggested Method for Determining Point Load Strength, *International Journal of Rock Mechanics and Mining Sciences,* 22(2): pp. 53-60

Kahraman, S. (2001). Evaluation of simple methods for assessing the uniaxial compressive strength of rock. *International Journal of Rock Mechanics and Mining Sciences,* 38(7): pp. 981-994. [Online] DOI: 10.1016/S1365-1609(01)00039-9

Kutter, H.K., and Saino, H.P. (1982). *Comparative Study of Performance of New and Worn Disc Cutters on a Full-Face Tunnelling Machine*, Tunnelling '89 Institution of Mining and Metalurgy London, 2(1): pp.127-133

Lindqvist, P.A. and Hai-Hui, L. (1983). Behaviour of the Crushed Zone in Rock Indentation. Technical Note. *Rock Mechanics and Rock Engineering,* 16(3): pp.199-207.

Lindqvist, P.A. and Rånman, K.E (1980). *A tensile stress model describing side chipping between rock cutting discs.* Technical Note, Luleå University of Technology; No. 1980:59

Lindqvist, P.A., Hai-Hui, L. and Alm, O. (1984). Indentation Fracture Development in Rock Continuously Observed with a Scanning Electron Microscope. *International Journal of Rock Mechanics and Mining Sciences & Geomechanics Abstracts,* 21(4): pp. 165-182: [Online] DOI: 10.1016/0148-9062(84)90794-0

Log, S. (2013). Personal conversation 12.12.2013

Luxner, T. (2014*). Stillwater's Blitz TBM Project Update.* SME Annual Meeting, Feb. 23-26 2014, Salt Lake City, USA.

Macias, F. J., Bruland, A. (2014). *D&B versus TBM: Review of the parameters for a right choice of the excavation method.* The 2014 ISRM European Rock Mechanics Symposium (Eurock 2014), Vigo, Spain.

Macias, F. J., Jakobsen, P. D., Bruland, A., Log, S., Grøv, E. (2014a). *The NTNU Prediction Model: A Tool for Planning and Risk Management in Hard Rock TBM Tunnelling.* Proceedings of the World Tunnel Congress 2014 - Tunnels for a better Life, Foz do Iguazu, Brazil.

Macias, F. J., Jakobsen, P. D., Seo, Y., Bruland, A., Grøv, E. (2014b). *Rock Mass Influence on Hard Rock TBM Performance Prediction.* Proceedings of the World Tunnel Congress 2014 - Tunnels for a better Life, Foz do Iguazu, Brazil.

Maidl, B., Schmid, L., Ritz, W., and Herrenknecht, M. (2008). *Hard Rock Tunnel Boring Machines*. Ernst & Sohn Verlag, Berlin.

NTNU (2009). Fullprof software 2009. *Norwegian University of Science and Technology (NTNU), Trondheim, Norway*

Rostami, J., Ozdemir, L., Bruland, A. and Dahl, F. (2005). *Review of Issues Related to CERCHAR Abrasivity Testing and Their Implications on Geotechnical Investigations and Cutter Cost Estimates.* 17th Rapid Excavation and Tunneling Conference, Seattle, WA, USA

Saino, H.P. (1985). Prediction of Performance of Disc Cutters in Anisotropic Rock. *International Journal of Rock Mechanichs and Mining Sciences,* Abstract 22(3): pp. 153-161.

Schneider, E., Thuro, K., Galler, R. (2012). Forecasting penetration and wear for TBM drives in hard rock – Results from the ABROCK research project. *Geomechanics and Tunnelling,* 5(5): pp. 537-546. [Online] DOI: 10.1002/geot.201200040

SME (1992). *SME Mining Engineering Handbook*. Littleton, Colorado USA, Society for Mining, Metallurgy, and Exploration, Inc.

Stempkowski, R. (1996). *Kosten- und Leistungsanalysen im Maschinellen Tunnelbau.* Dissertation at the Technical University of Wien

Stillwater Mining Company (2010). Development Geology Best Practices

Stillwater Mining Company (2011). *Geotechnical Baseline Information Regarding the Footwall Drive Tunnels, Stillwater Mine Project.* Blitz Tunnel Construction, Exhibit C – Scope of Work (Received by e-mail 29.11.2013)

Stillwater Mining Company (n.d.) Available at: http://www.stillwatermining.com (Visited 27.05.14)

Suana, D. and Peters, T. (1981). The Cerchar Abrasivity Index and Its Relation to Rock Mineralogy and Petrography, *Rock Mechanics,* 15(1): pp. 1-7

The Research Council of Norway (n.d.) *Future Advanced Steel Technology for Tunneling - FAST-Tunn*. Available at: http://www.forskningsradet.no/servlet/Satellite?c=Prosjekt&cid=1253969229711&pagename=bia/Hovedsidemal&p=1226993636093 (Visited 19.05.2014)

The Robbins Company (2011), *Technical Proposal #032911-2O-T-REV 3 for the Supply of a Remanufactured 18'-0" (5.5 m) Hard Rock Open Gripper TBM, Back-up System and Auxiliary Equipment for the Footwall Drive Tunnels, Stillwater Mine Project* (Received by e-mail 29.11.2013).

The Robbins Company (n.d.) http://www.therobbinscompany.com/en/our-products/tunnel-boring-machines (Visited 01.06.2014)

Zare, S. and Bruland, A. (2012). Applications of NTNU/SINTEF Drillability Indices in Hard Rock Tunneling. *Rock Mechanics and Rock Engineering,* 46(1): pp. 179-187. [Online] DOI: 10.1007/s00603-012-0253-y

Appendices

A - Task Description

B - Example of Diamond Drill Log from the Stillwater Mining Company

C - Example of Tunnel Map Used in the Work

D - Data from Cutter Change Log

E - Point Load Index Calculations

F - X-Ray Diffraction Analysis (XRD)

G - Drillability Test Report from SINTEF

MASTER DEGREE THESIS
Spring 2014
for

Leon Nikolay Røren Eide

TBM Tunnelling at The Stillwater Mine

BACKGROUND

The NTNU estimation model for hard rock tunnel boring has long been a good tool for obtaining the needed TBM tunnelling estimations. The model must however be kept updated as the years pass in order to stay relevant. In particular the effect of several machine parameters have to be reassessed as the TBMs used are getting bigger and more powerful. The understanding of how geological conditions such as fracturing effects TBM performance should also be elevated. The laboratory tests used for assessing drillability of rock and cutter life must also be understood as well as possible, as these are important input in the prediction models made at the NTNU.

TASK DESCRIPTION

The task is meant to assess the effect different factors on the rock breaking process in a TBM, especially the factors RPM and Thrust Force. The thesis will consist of the following:

-Literature study on the topic of the rock breaking process [2 weeks]
-Field study of a TBM in use at the Stillwater Mines, Montana, USA [10 weeks]
-Laboratory research at the SINTEF/NTNU laboratory in Trondheim, Norway [4 weeks]
-Writing of the thesis [4 weeks]

The thesis will be done in cooperation with The Robbins Company.

Objective and purpose

The purpose of this Master's Thesis is to provide information and data to be used in the work of updating the NTNU model. In particular RPM and its effect on rock breaking and performance shall be investigated through field testing. Geological information with special respect to rock mass fracturing is also to be collected and presented. The purpose of this is to verify tunnelling performance against estimations and to increase knowledge about the tunneling operations. The TBM investigated is a main beam open gripper TBM used to construct a ventilation and haulage level at the Stillwater Mine in Montana, USA.
The laboratory tests used to obtain input for the NTNU model are also to be evaluated through testing of geological samples collected at the Stillwater Mine.

NTNU
Faculty of Engineering Science and Technology
Institute of Civil and Transport Engineering

General about content, work and presentation

The text for the master thesis is meant as a framework for the work of the candidate. Adjustments might be done as the work progresses. Tentative changes must be done in cooperation and agreement with the professor in charge at the Department.

In the evaluation thoroughness in the work will be emphasized, as will be documentation of independence in assessments and conclusions. Furthermore the presentation (report) should be well organized and edited; providing clear, precise and orderly descriptions without being unnecessary voluminous.

The report shall include:
➢ Standard report front page (from DAIM, http://daim.idi.ntnu.no/)
➢ Title page with abstract and keywords.(template on: http://www.ntnu.no/bat/skjemabank)
➢ Preface
➢ Summary and acknowledgement. The summary shall include the objectives of the work, explain how the work has been conducted, present the main results achieved and give the main conclusions of the work.
➢ The main text.
➢ Text of the Thesis (these pages) signed by professor in charge as Attachment 1.

The thesis can as an alternative be made as a scientific article for international publication, when this is agreed upon by the Professor in charge. Such a report will include the same points as given above, but where the main text includes both the scientific article and a process report.

Advice and guidelines for writing of the report is given in "Writing Reports" by Øivind Arntsen, and in the departments "Råd og retningslinjer for rapportskriving ved prosjekt og masteroppgave" (In Norwegian) located at http://www.ntnu.no/bat/studier/oppgaver.

Submission procedure
Procedures relating to the submission of the thesis are described in DAIM (http://daim.idi.ntnu.no/). Printing of the thesis is ordered through DAIM directly to Skipnes Printing delivering the printed paper to the department office 2-4 days later. The department will pay for 3 copies, of which the institute retains two copies. Additional copies must be paid for by the candidate / external partner.

On submission of the thesis the candidate shall submit a CD with the paper in digital form in pdf and Word version, the underlying material (such as data collection) in digital form (e.g. Excel). Students must submit the submission form (from DAIM) where both the Ark-Bibl in SBI and Public Services (Building Safety) of SB II has signed the form. The submission form including the appropriate signatures must be signed by the department office before the form is delivered Faculty Office.

Documentation collected during the work, with support from the Department, shall be handed in to the Department together with the report.

According to the current laws and regulations at NTNU, the report is the property of NTNU. The report and associated results can only be used following approval from NTNU (and external cooperation partner if applicable). The Department has the right to make use of the results from the work as if conducted by a Department employee, as long as other arrangements are not agreed upon beforehand.

NTNU

Faculty of Engineering Science and Technology
Institute of Civil and Transport Engineering

Tentative agreement on external supervision, work outside NTNU, economic support etc.
Separate description is to be developed, if and when applicable. See
http://www.ntnu.no/bat/skjemabank for agreement forms.

Health, environment and safety (HSE) http://www.ntnu.edu/hse
NTNU emphasizes the safety for the individual employee and student. The individual safety shall be in the forefront and no one shall take unnecessary chances in carrying out the work. In particular, if the student is to participate in field work, visits, field courses, excursions etc. during the Master Thesis work, he/she shall make himself/herself familiar with "Fieldwork HSE Guidelines". The document is found on the NTNU HMS-pages at http://www.ntnu.no/hms/retningslinjer/HMSR07E.pdf

The students do not have a full insurance coverage as a student at NTNU. If you as a student want the same insurance coverage as the employees at the university, you must take out individual travel and personal injury insurance.

Startup and submission deadlines
The work on the Master Thesis starts on January 20, 2014.

The thesis report as described above shall be submitted digitally in DAIM at the latest at **June 24, at 23:59:59.**

Professor in charge: Amund Bruland

Other supervisors: Sindre Log

Department of Civil and Transport Engineering, NTNU
Date: 13.01.2014, (revised: 22.06.2014)

_____
Professor in charge (signatur)

Stillwater Mining Company — Diamond Drill Log — Hole No. 37487

Northing 1,282.0
Easting 7,607.0
Evalation 5,027.0
Location 50E 7607

Incl. 3.0°
Azim. 73.0°

Started 13 Dec 2013
Completed 16 Dec 2013
Logged 18 Dec 2013
Total Depth 715.0'

Logged By Butak, Kevin

Sheet 8 of 12
Scale 1" = 10'

Core Size BQ

Assays

417.9 - 590.3' pbC Likely Norite
Zone 1

pbC

461.0 - 466.0'
serpentine moderate
70° to core axis wk
Bkn

Rating: ■ Comments: TBM Straight Ahead Probe, Crossed "A" Fault @ 417.9'

Report Date: 2 Apr 2014 11:53:37 AM

APPENDIX B - Example of Page from Diamond Drill Log used at The Stillwater Mine

APPENDIX C - Example of Tunnel Map Used in the Work

Cutter number out	Date	Footage when changed	Meters bored when changed	Machine hour when changed	Wear (mm)	Comment	Footage on cutter	Meters on cutter	Serial number new cutter
26	22.05.2013	1995	608	66	12		1995	608	12-010
27	22.05.2013	1995	608	66	10		1995	608	11-015
28	22.05.2013	1995	608	66	10	Small chips	1995	608	11-001
29	22.05.2013	1995	608	66	10		1995	608	11-008
30	22.05.2013	1995	608	66	11		1995	608	11-012
31	22.05.2013	1995	608	66	10		1995	608	11-010
32	22.05.2013	1995	608	66	11		1995	608	12-015
33	22.05.2013	1995	608	66	8		1995	608	12-021
1-3 quad	24.05.2013	1995	608	66	6" piece busted out of ring #1	Wear on rings minimal	1995	608	?
2-4 quad	24.05.2013	1995	608	66	4" piece busted out of ring #2	Wear on rings minimal	1995	608	?
1-3 quad	16.07.2013	2991.83	912	130	6" piece busted out of ring #1	Wear on rings minimal, top hub cap missing also	996	304	11-429 (94926)
26	17.09.2013	3379	1030	155	froze up	Stop sign shaped	1384	422	?
21	07.11.2013	3995	1218	194	15		3995	1218	old #32 11mm D3-8626
22	07.11.2013	3995	1218	194	18		3995	1218	old #31 11 mm 12-020
23	07.11.2013	3995	1218	194	18		3995	1218	old #33 6 mm 12-021
24	07.11.2013	3995	1218	194	21		3995	1218	12-019 23
25	07.11.2013	3995	1218	194	15		3995	1218	12-014 101
26	07.11.2013	3995	1218	194	14	Chipped disc	626	191	12-012 101
27	07.11.2013	3995	1218	194	15		2000	610	12-023 46
28	07.11.2013	3995	1218	194	13		2000	610	12-005 19
29	07.11.2013	3995	1218	194	13		2000	610	?
30	07.11.2013	3995	1218	194	13		2000	610	12-025 99
31	07.11.2013	3995	1218	194	11		2000	610	11-010
32	07.11.2013	3995	1218	194	11		2000	610	D3-8626
33	07.11.2013	3995	1218	194	6		2000	610	12-021
22	09.12.2013	4362	1330	215.3	12	Retainer ring gone, disc walked 2".	2357	718	12-011
5+7 quad	08.01.2014	4885	1489	246.5	12	Starting to look like a stop sign	4885	1489	?
19	03.02.2014	5232	1595	269	20	#5 disc, stop sign shaped	5232	1595	?
								0	
14	05.03.2014	5756	1754	294	17		5756	1754	11-012
15	05.03.2014	5756	1754	294	17		5756	1754	
16	05.03.2014	5756	1754	294	17		5756	1754	
17	05.03.2014	5756	1754	294	17		5756	1754	
18	06.03.2014	5756	1754	294	16		5756	1754	
20	06.03.2014	5756	1754	294	17		5756	1754	11-022
21	06.03.2014	5756	1754	294	17		1839	561	
23	06.03.2014	5756	1754	294	17		1839	561	

APPENDIX D - Data from Cutter Change Log

Results - Point Load Index

Basis: *ISRM Suggested Method for Determining Point Load Strength*

Journal nr.:   *14028IG*
Sample: *1*
Merknader: Normally or parallell with = ‖ / ⊥
Performed by: *Leon Eide and Andreas Løkås*
Date: *28.04.2014*

Test number:	Test type	Width [mm]	Height [mm]	D_e [mm]	Failure Load [N]	Point Load Index I_s [MPa]	Normalized Index I_{s50} [MPa]
1	Piece/lump	40.35	27	37.2	7520	5.4	4.7
2	Piece/lump	66.4	21.8	42.9	8650	4.7	4.4
3	Piece/lump	39	34.2	41.2	9250	5.4	5.0
4	Piece/lump	53.7	38	51.0	17488	6.7	6.8
5	Piece/lump	35.35	32.8	38.4	13050	8.8	7.9
6	Piece/lump	96.5	25.9	56.4	11490	3.6	3.8
7	Piece/lump	67.1	23.9	45.2	12710	6.2	5.9
8	Piece/lump	75	22.75	46.6	12530	5.8	5.6
9	Piece/lump	43.6	29.6	40.5	8370	5.1	4.6
10	Piece/lump	47.45	16.8	31.9	3700	3.6	3.0
11	Piece/lump	60	23.6	42.5	9350	5.2	4.8
Mean						**6.3**	**5.0**

Results indicate:		Compressive Strength	σ_c [MPa]	80.3
		Tensile Strength	σ_t [MPa]	4.0

- Equivalent diameter D_e is calculated by the following: $D_e = \sqrt{\frac{4}{\pi} * Width * Height}$

- Point Load Index I_s calculated by equivalent diameter D_e divided by Failure Load.

- Normalized Index I_{s50} calculated by the following: $I_{s50} = \frac{D_e}{50}^{0.45} * Point\ Load\ Index\ I_s$

- Compressive strength found by multiplying the Normalized Index with a factor of 16

APPENDIX E - Point Load Index Calculations

Results - Point Load Index

Basis: *ISRM Suggested Method for Determining Point Load Strength*

Journal nr.:   *14028IG*
Sample: *2*
Merknader: Normally or parallell with = ‖ / ⊥
Performed by: *Leon Eide and Andreas Løkås*
Date: *28.04.2014*

Test number:	Test type	Width [mm]	Height [mm]	D_e [mm]	Failure Load [N]	Point Load Index I_s [MPa]	Normalized Index I_{s50} [MPa]
1	Radially	-	-	36.1	9080	7.0	6.0
2	Radially	-	-	35.1	10370	8.4	7.2
3	Radially	-	-	36.5	9650	7.2	6.3
4	Radially	-	-	36.1	10920	8.4	7.2
5	Radially	-	-	36.0	1940	1.5	1.3
6	Radially	-	-	36.2	4350	3.3	2.9
7	Radially	-	-	36.2	940	0.7	0.6
8	Radially	-	-	35.5	14000	11.1	9.5
9	Radially	-	-	35.8	9750	7.6	6.5
10	Radially	-	-	36.2	1380	1.1	0.9
Mean						**5.8**	**5.0**

Results indicate:			
	Compressive Strength	σ_c [MPa]	80.5
	Tensile Strength	σ_t [MPa]	4.0

- Point Load Index I_s calculated by equivalent diameter D_e divided by Failure Load.

- Normalized Index I_{s50} calculated by the following: $I_{s50} = \frac{D_e}{50}^{0.45} * Point\ Load\ Index\ I_s$

- Compressive strength found by multiplying the Normalized Index with a factor of 16

154

Results - Point Load Index

Basis: *ISRM Suggested Method for Determining Point Load Strength*

Journal nr.: *14028IG*
Sample: *3*
Merknader: Normally or parallell with = ‖ / ⊥
Performed by: *Leon Eide and Andreas Løkås*
Date: *28.04.2014*

Test number:	Test type	Width [mm]	Height [mm]	D_e [mm]	Failure Load [N]	Point Load Index I_s [MPa]	Normalized Index I_{s50} [MPa]
1	Radially	-	-	35.8	8760	6.8	5.9
2	Radially	-	-	35.0	7450	6.1	5.2
3	Radially	-	-	36.2	5000	3.8	3.3
4	Radially	-	-	36.1	5740	4.4	3.8
5	Radially	-	-	36.1	7210	5.5	4.8
6	Radially	-	-	36.3	9290	7.1	6.1
7	Radially	-	-	36.2	13330	10.2	8.8
8	Radially	-	-	36.2	5510	4.2	3.6
9	Radially	-	-	36.0	7300	5.6	4.9
10	Radially	-	-	36.2	9540	7.3	6.3
Mean						**5.9**	**5.1**

Results indicate:			
	Compressive Strength	σ_c [MPa]	81.6
	Tensile Strength	σ_t [MPa]	4.1

- Point Load Index I_s calculated by equivalent diameter D_e divided by Failure Load.

- Normalized Index I_{s50} calculated by the following: $I_{s50} = \frac{D_e}{50}^{0.45} * Point\ Load\ Index\ I_s$

- Compressive strength found by multiplying the Normalized Index with a fa

155

APPENDIX E - Point Load Index Calculations

NTNU

Fakultet for ingeniørvitenskap og teknologi
Institutt for geologi og bergteknikk

Vår dato	Vår referanse
12.05.2014	LT / 14-060
Deres dato	Deres referanse

1 av 3

Leon Eide
IBAT
NTNU
7491 Trondheim
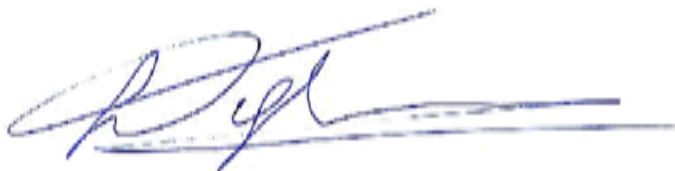
XRD-analyse av 2 prøver merket "Prøve 1" og "Prøve 2".

Analysene er utført på en Bruker D8 ADVANCE. DIFFRAC.SUITE.EVA programvare i kombinasjon med databasen PDF-4+ foreslår følgende mineralfaser.
Rietveld (Topas 4) er brukt til mineral-kvantifisering.

Prøve mrk.	Prøve 1	Prøve 2
J.nr.	140401	140402
Plagioklas	64 %	67 %
Pyroksen	33 %	9 %
Kloritt	3 %	8 %
Alkalifeltspat	< 1 %	3 %
Zeolitt	< 1 %	2 %
Kvarts		4 %
Kalsitt		3 %
Glimmer		4 %
Amfibol		< 1 %

Med hilsen

Laurentius Tijhuis
Overingeniør

Torill Sørløkk
Overingeniør

157

Norges teknisk-naturvitenskapelige universitet

Vår dato
12.05.2014

Vår referanse
LT / 14-060

140401: Prøve 1

Norges teknisk-naturvitenskapelige universitet

Vår dato
12.05.2014

Vår referanse
LT / 14-060

140402 Prøve 2

Calcite 3.23 %
Muscovite 2M1 4.03 %
Hornblende ferrotschermakite 0.34 %
Diopside 0.93 %
Chlorite IIb 7.72 %
Laumontite 2.04 %
Microcline intermediate2 2.52 %
Anorthite 67.93 %
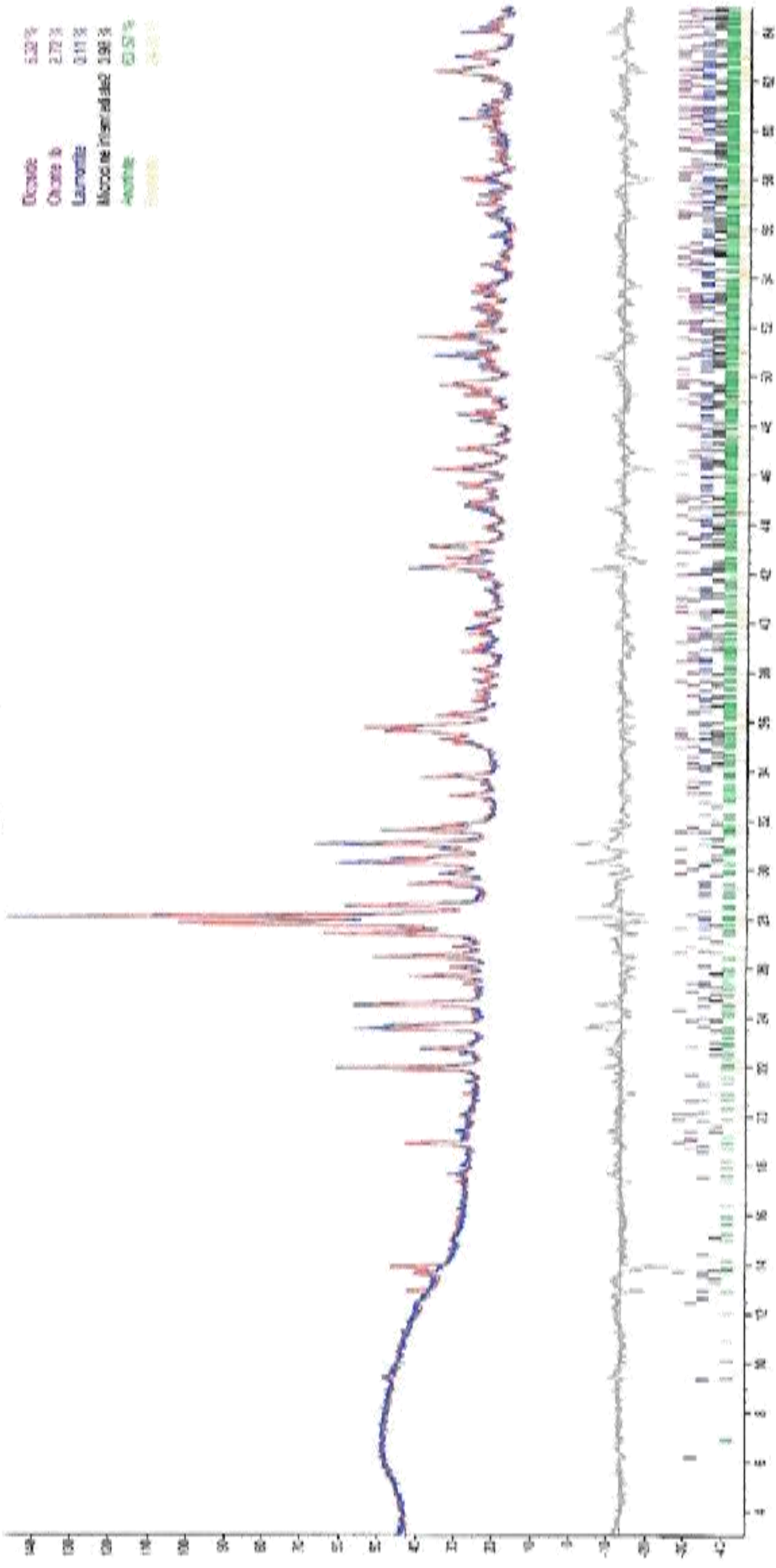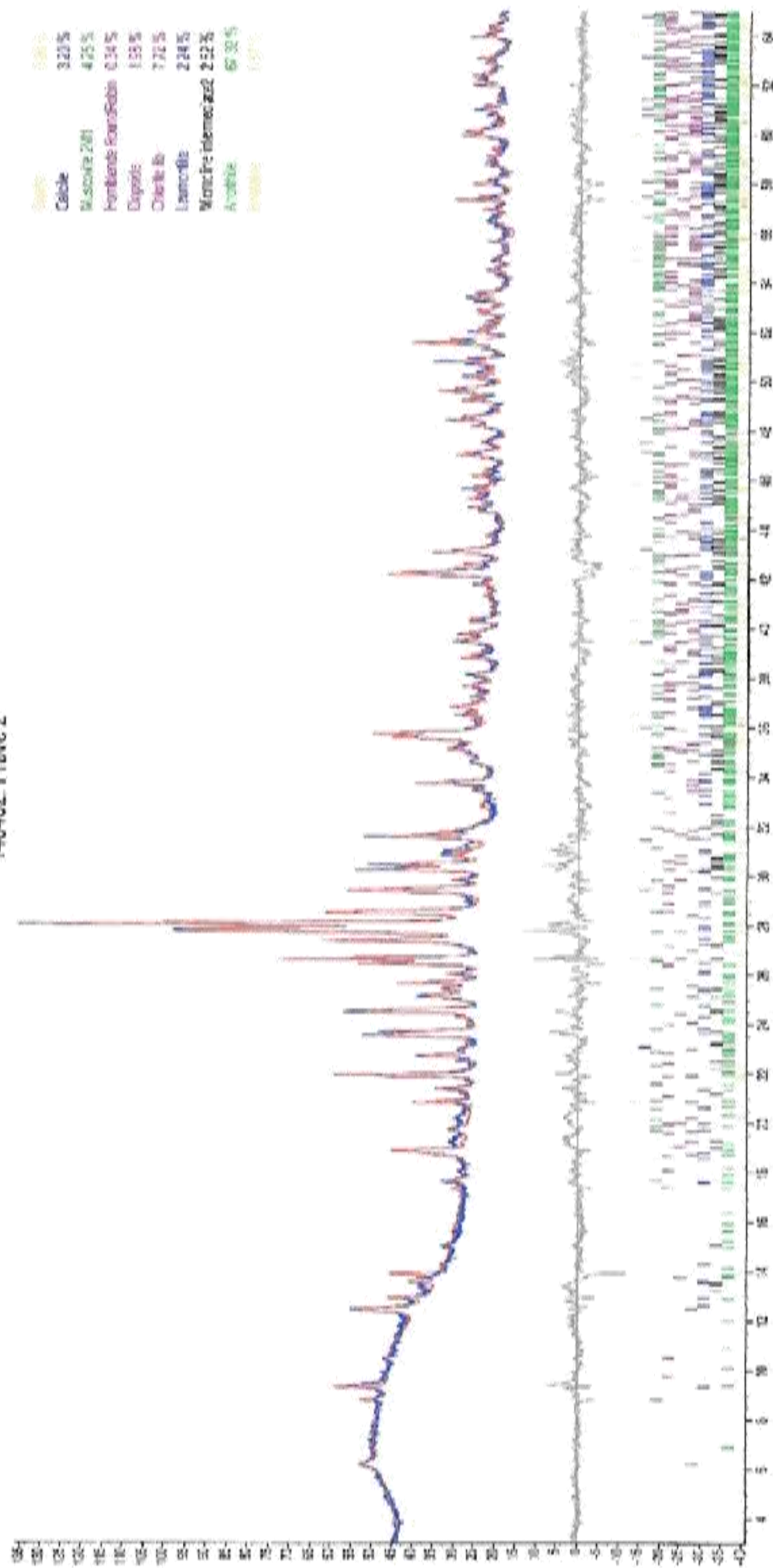
APPENDIX F - X-Ray Diffraction Analysis (XRD)

TEST RESULTS AND CALCULATED INDICES – LABORATORY TESTING OF ROCK CORE SAMPLES FROM STILLWATER, USA

1 Excecutive summary

Sample No.	1	2	3
Rock type (given by the Client)	Norite	Norite	Norite
Brittleness Value (S_{20})	59.5 High	54.8 High	48.3 Medium
Sievers' J-Value (SJ)	99.8 Extremely low surface hardness	29.6 Low surface hardness	10.7 Medium surface hardness
Abrasion Value Cutter Steel (AVS)	19.5 Medium	7.0 Low	17.0 Medium
Drilling Rate Index™ (DRI™)	71 Very high	60 High	49 Medium
Cutter Life Index™ (CLI™)	25.9 High	24.1 High	11.6 Medium
Quartz content (DTA) (Weight %)	< 1	< 1	< 1
Cerchar Abrasion Index (CAI	5.1 High	3.9 High	5.9 High

Classification of S_{20}, SJ, AV and AVS according to Dahl. F., et al. 2012. Classifications of properties influencing the drillability of rocks, based on the NTNU/SINTEF test method. Tunnelling and Underground Space Technology 28 (2012). 150-158.

Classification of DRI™, BWI™ and CLI™ according to Project Report "13A-98 Drillability Test Methods", published by the Department of Civil and Transport Engineering at the Norwegian University of Science and Technology.

Classification of CAI according to ASTM D7625-10 Standard Test Method for Laboratory Detremination of Abrasiveness of Rock Using the Cerchar Method.

2 Results Drilling Rate Index™ (DRI™), Cutter Life Index™ (CLI™) and Quartz content (DTA)

Basis: http://www.drillability.com, SINTEF/NTNU (2003), Suggested Methods for determining
DRI™, BWI™ and CLI™

TEST RESULTS

Sample No.	1	2	3
Brittleness Value (S_{20}, 11.2 - 16.0 mm)	59.5	54.8	48.3
[%] Flakiness (f)	1.26	1.31	1.27
Compaction index	2	2	2
Density (ρ) [g/cm^3]	2.85	2.67	2.92
Sievers' J-Value (SJ) [mm/10]	99.8	29.6	10.7
Abrasion Value Cutter Steel (AVS)	19.5	7.0	17.0
[mg] Quartz content (DTA) [weight	< 1	< 1	< 1

CALCULATED INDICES

Drilling Rate Index™ (DRI™)	71	60	49
Cutter Life Index™ (CLI™)	25.9	24.1	11.6

CLASSIFICIATION

Category	DRI	CLI™
Extremely Low	$\leq$	< 5
Very Low	25	5.0 - 5.9
Low	**33 -**	**6.0 - 7.9**
Medium	**42**	**8.0 - 14.9**
High	**43 -**	**15 - 34**
Very High	70 -	35 - 74
Extremely High	82	$\geq$ 75

3 Individual values from tests used to determine DRI™ and CLI™

Sample No.: 1

Test No	Brittleness Value S$_{20}$ [%]	Sievers' J-Value SJ [1/10 mm]	Abrasion Value Cutter Steel AVS [mg]
1	58.7	97.4	19
2	60.4	110.8	20
3	59.5	91.8	
4		99.3	
Mean	59.5	99.8	19.5
Stdev	0.84	8.00	0.71

Sample No.: 2

Test No.	Brittleness Value S$_{20}$ [%]	Sievers' J-Value SJ [1/10 mm]	Abrasion Value Cutter Steel AVS [mg]
1	58.7	31.6	7
2	52.0	28.9	7
3	53.8	26.8	
4		16.8	
5		46.7	
6		57.6	
7		18.3	
8		17.3	
9		15.4	
10		53.6	
11		13.0	
Mean	54.8	29.6	7.0
Stdev	3.50	16.09	0.00

Sample No.: 3

Test No.	Brittleness Value S$_{20}$ [%]	Sievers' J-Value SJ [1/10 mm]	Abrasion Value Cutter Steel AVS [mg]
1	49.4	7.5	17
2	45.7	14.3	17
3	49.7	8.1	
4		8.0	
5		15.5	
Mean	48.3	10.7	17.0
Stdev	2.21	3.89	0.00

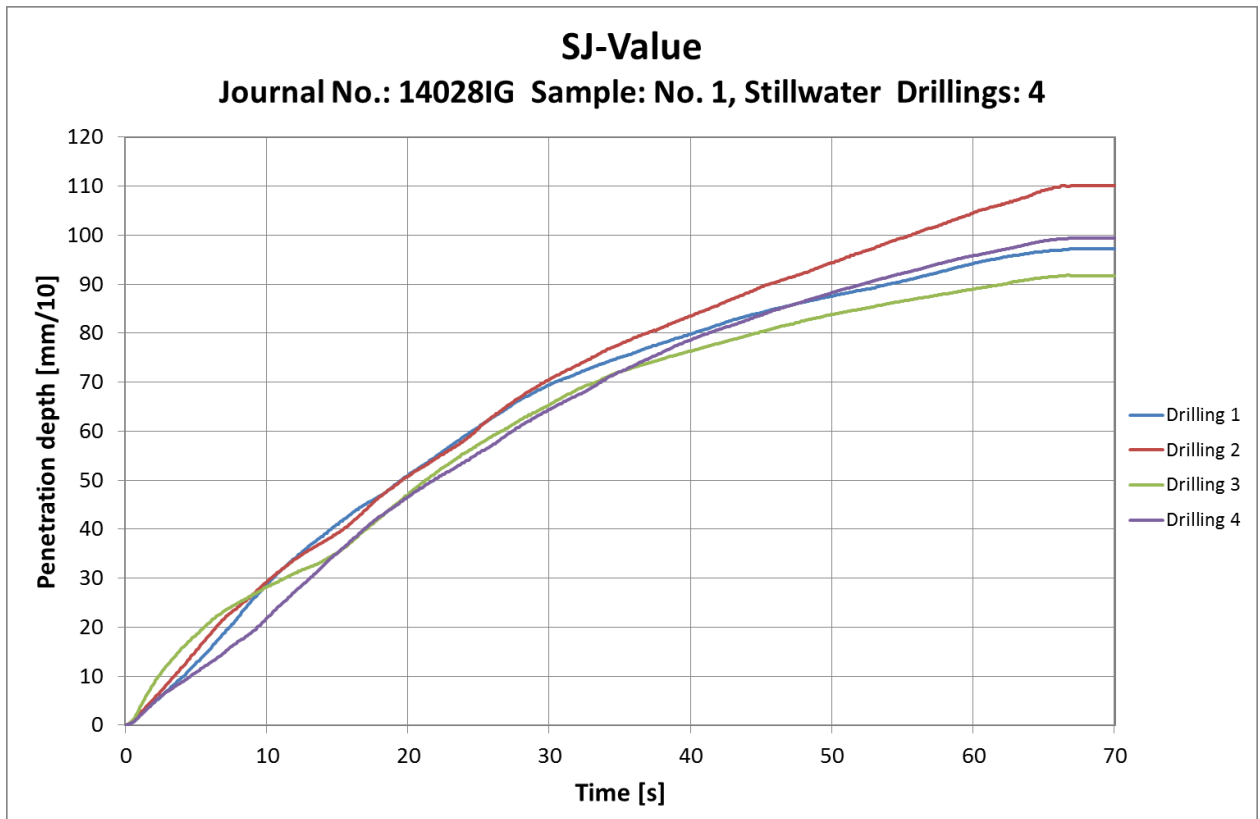## 4 Sievers' J-Value drillings presented as charts

Photo of the Sievers' J (SJ) specimen subsequent to completed testing. Yellow arrows indicate the position of the drillings.
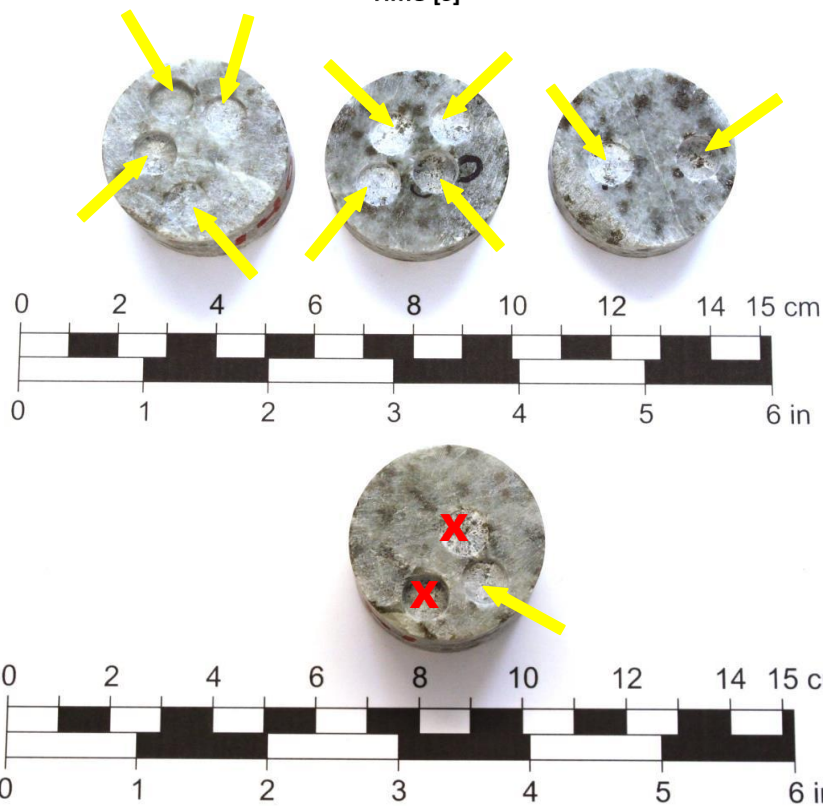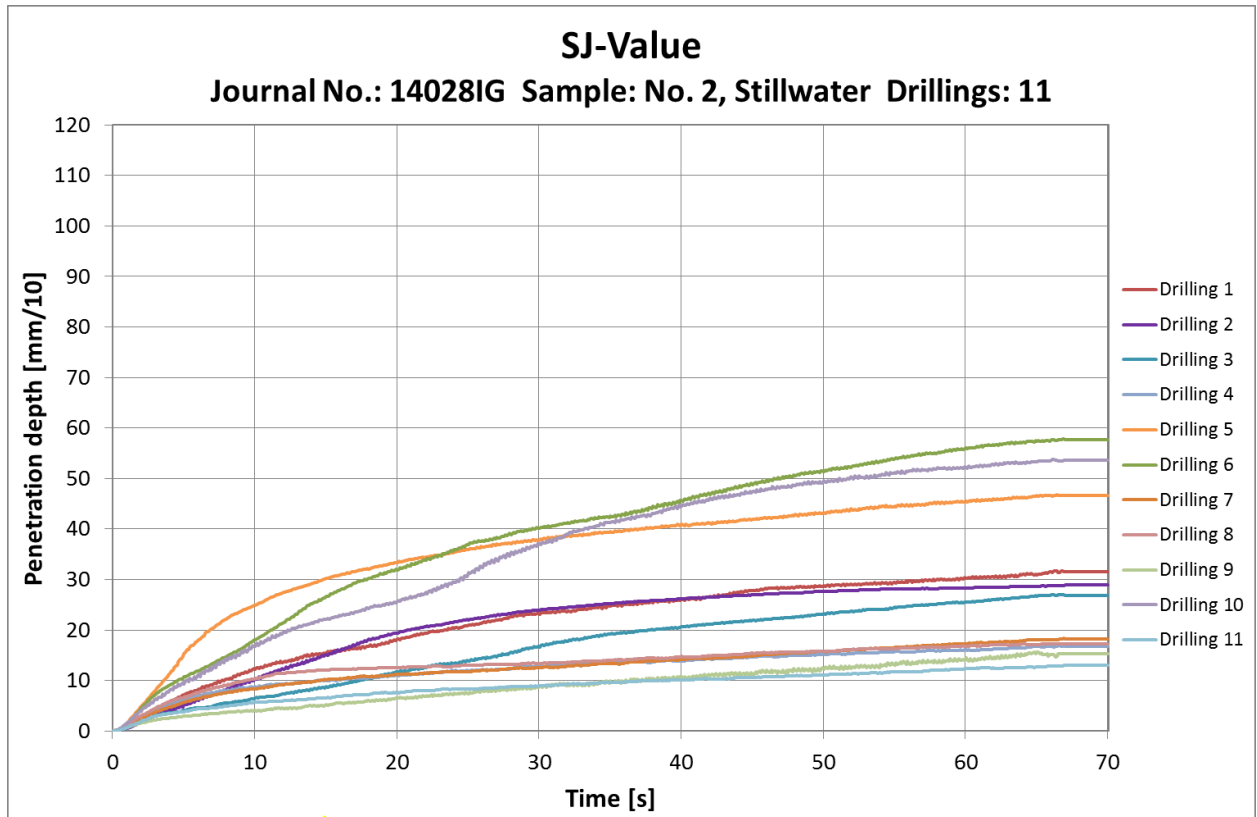
Photo of the Sievers' J (SJ) specimens subsequent to completed testing. Yellow arrows indicate the position of the drillings. Red X indicates an unsuccessful drilling which has not been used for calculation of the SV-Value.
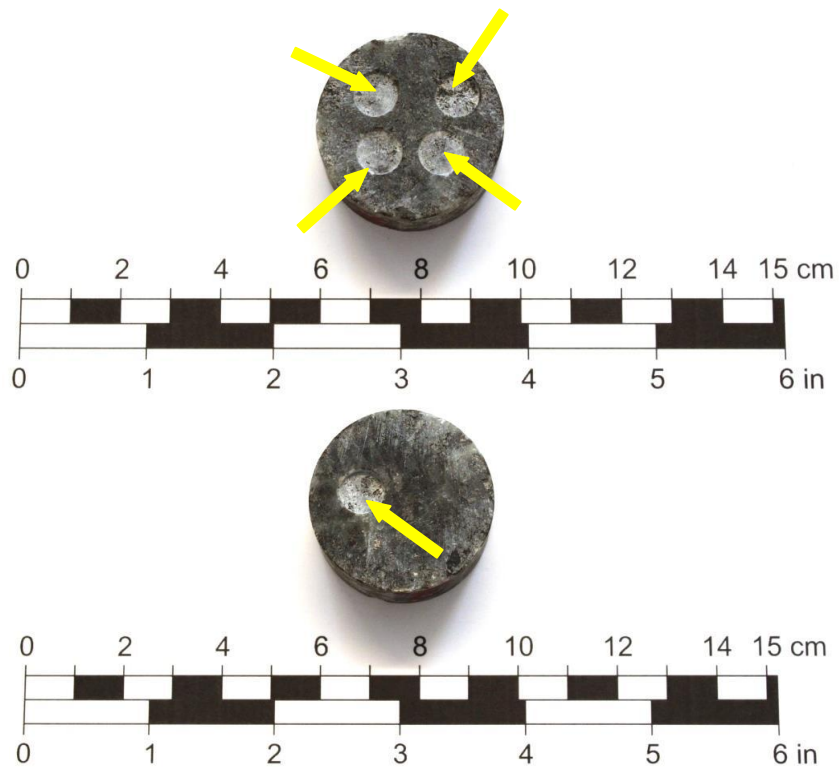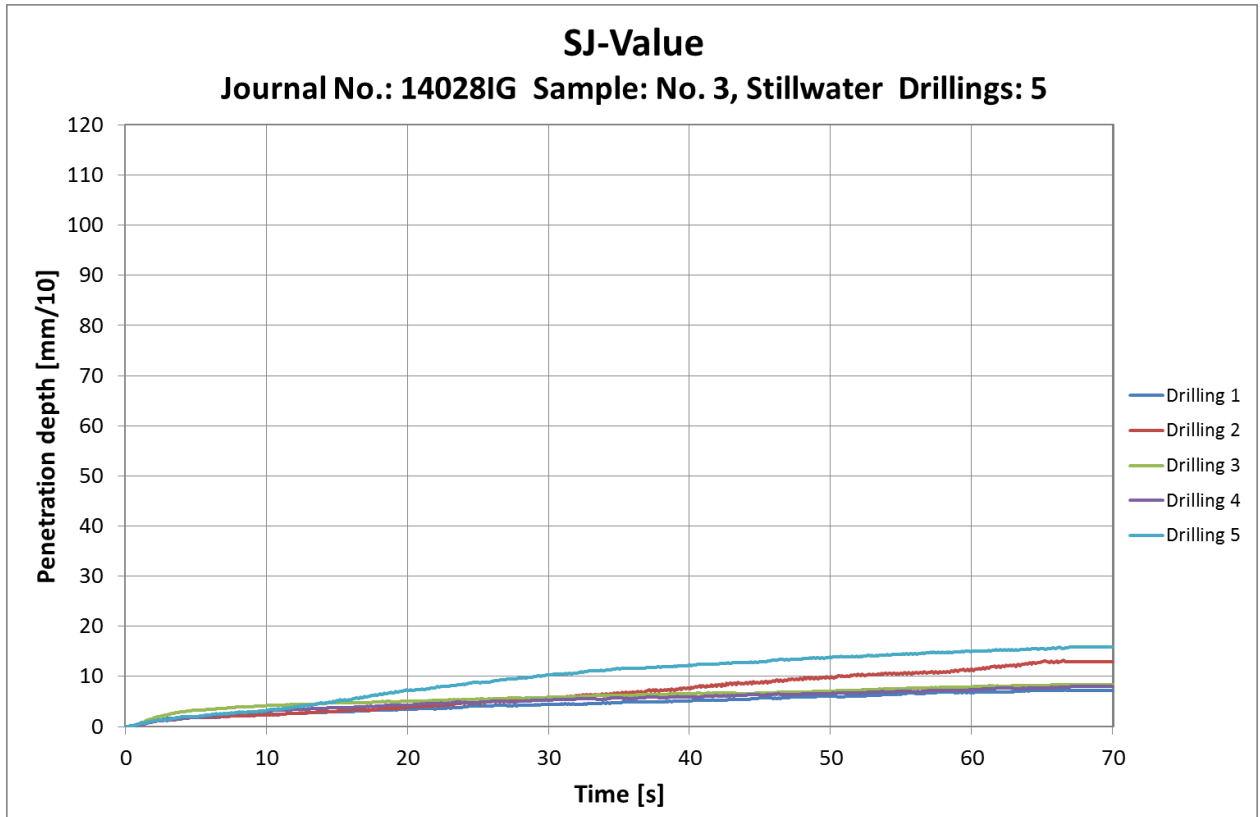
SJ-Value
Journal No.: 14028IG Sample: No. 3, Stillwater Drillings: 5

Photo of the Sievers' J (SJ) specimen subsequent to completed testing. Yellow arrows indicate the position of the drillings.

5 Results Cerchar Abrasivity Index (CAI)

Basis: ASTM D7625 – 10 Standard Test Method for Laboratory Determination of Abrasiveness of
Rock Using the Cerchar Method (2012).

All tests were performed by use of an Ergotech Cerchar testing machine equipped with pins of Rockwell Hardness 43 (specified by the supplier). The CAI is based on the mean value of 10 measurements of the wear flats of 5 pins (two perpendicular diameters on each pin). The tests were performed on a flat surface produced by slicing the specimen with a diamond saw (CAI_s).

CAI is calculated by CAI_s by use of the following equation:

$$CAI = 0.99 CAI_s + 0.48$$

Sample: No.: 1

Wear flat No.	Wear flat diameter [mm]	CAI_s	CAI
1a	0.48	4.8	5.2
1b	0.49	4.9	5.3
2a	0.45	4.5	4.9
2b	0.45	4.5	4.9
3a	0.50	5.0	5.4
3b	0.50	5.0	5.4
4a	0.45	4.5	4.9
4b	0.45	4.5	4.9
5a	0.47	4.7	5.1
5b	0.42	4.2	4.6
Mean		**4.7**	**5.1**
Stdev		0.26	0.26

Sample: No.: 2

Wear flat No.	Wear flat diameter [mm]	CAI_s	CAI
1a	0.35	3.5	3.9
1b	0.35	3.5	3.9
2a	0.34	3.4	3.8
2b	0.34	3.4	3.8
3a	0.27	2.7	3.2
3b	0.29	2.9	3.4
4a	0.36	3.6	4.0
4b	0.41	4.1	4.5
5a	0.38	3.8	4.2
5b	0.40	4.0	4.4
Mean		**3.5**	**3.9**
Stdev		0.44	0.43

Sample: No.: 3

Wear flat No.	Wear flat diameter [mm]	CAI_s	CAI
1a	0.54	5.4	5.8
1b	0.49	4.9	5.3
2a	0.69	6.9	7.3
2b	0.69	6.9	7.3
3a	0.40	4.0	4.4
3b	0.45	4.5	4.9
4a	0.46	4.6	5.0
4b	0.50	5.0	5.4
5a	0.58	5.8	6.2
5b	0.54	5.4	5.8
Mean		**5.3**	**5.8**
Stdev		0.97	0.96

CLASSIFICATION (ACCORDING TO ASTM)

Category	CAI (HRC = 55)	CAI (HRC = 40)
Very low abrasiveness	0.30 - 0.50	0.32 - 0.66
Low abrasiveness	0.50 - 1.00	0.66 - 1.51
Medium abrasiveness	1.00 - 2.00	1.51 - 3.22
High abrasiveness	2.00 - 4.00	3.22 - 6.62
Extreme abrasiveness	4.00 - 6.00	6.62 - 10.03
Quartzitic	6.00 - 7.00	N/A

6 TEST RESULTS AND CALCULATED INDICES PRESENTED AS BAR GRAPHS

Abrasion Value Cutter Steel (AVS)

Drilling Rate Index™ (DRI™)

Cutter Life Index™ (CLI™)

Cerchar Abrasion Index (CAI)